THE UNIVERSITY OF CHICAGO

HEPATITIS C VIRUS ENTRY IN THREE-DIMENSIONAL POLARIZED HEPATOMA ORGANOIDS

A DISSERTATION SUBMITTED TO

THE FACULTY OF THE DIVISION OF THE BIOLOGICAL SCIENCES

AND THE PRITZKER SCHOOL OF MEDICINE

IN CANDIDACY FOR THE DEGREE OF

DOCTOR OF PHILOSOPHY

COMMITTEE ON MICROBIOLOGY

BY

YASMINE MARGARET BAKTASH

CHICAGO, ILLINOIS

JUNE 2017

TABLE OF CONTENTS

LIST OF FIGURES

ACKNOWLEDGEMENTS

I would like to thank Kelly Coller-Metzinger for her help and advice. Anisha Madhav was also invaluable resource and helped construct both the EGFR and SR-BT plasmid sets. Special thanks to Matthew Evans as well for providing the CRISPR cell lines.

CHAPTER I

INTRODUCTION

Hepatitis C Virus

Hepatitis C virus (HCV) is a major health burden, with roughly 150 million chronically infected individuals across the globe (Baumert et al., 2017). Chronic infection, which occurs in 50-80% of patients, causes liver damage, progressing from hepatic fibrosis to cirrhosis and potentially hepatocellular carcinoma (HCC). HCC is the second highest cause of cancer-based mortality across the globe (Hoshida et al., 2014) and the leading indication for liver transplants (Gower et al., 2014; Mohd Hanafiah et al., 2013). Additionally, chronic HCV infection can lead to extra-hepatic manifestations, including non-Hodgkins lymphoma and diabetes mellitus, and can lead to increased risk of mortality due to stroke and heart attack (Negro et al., 2015; van der Meer et al., 2012). HCV is a blood borne pathogen, transmitted via exposure to contaminated blood; transmission is associated with medical procedures as well as intravenous drug use. In clinical settings, transmission often occurs with contaminated blood transfusions, needle reuse or injuries, and poorly sterilized medical equipment (Maheshwari and Thuluvath, 2010; Razavi et al., 2014). Due to the high prevalence of HCV, especially in underdeveloped countries, as well as difficulties in detecting the virus in its early stages, limited access to treatment, and re-infection, there has been a push to develop a vaccine. While there currently no available vaccines, there has been some progress towards development (Fauvelle et al., 2016). For many years, standard treatment for HCV was PEGylated interferon alpha and ribavirin (Liang and Ghany, 2013; Wilkins T, 2010). However, treatment showed variable success, with sustained virologic response (SVR) in roughly 50% of patients (Webster et al., 2015). SVR was also highly dependent on age, genotype of the

virus, and progression to cirrhosis (Ozaras and Tahan, 2009; Wilkins T, 2010). Furthermore, treatment often resulted in adverse side effects, often leading to patient discontinuation of therapy. A large breakthrough led to the development of several direct-acting antivirals (DAAs) targeting nonstructural proteins; combination therapy results in success rates above 90%, especially in the harder-to treat genotype 1 (Afdhal et al., 2014; Chung and Baumert, 2014).

HCV belongs to the positive-sense *Flaviviridae* family within the genus Hepacivirus, which has recently been expanded to include non-primate, bat, canine, and horse viruses (Burbelo et al., 2012; Kapoor et al., 2011; Kapoor et al., 2013; Lyons et al., 2012). HCV encompasses a highly heterogeneous set of viruses, with genotypes (and subtypes) whose genomes differ significantly from each other. Genotypes were found to differ by 30-33% at the nucleotide level; within a genotype, subtypes are roughly 20-25% different. Finally, isolates within a subtype show 10% nucleotide variability (Ohba K, 1995; Ohno O, 1997). Based on phylogenetic analysis of isolates, there are 6 main genotypes, with a potential seventh genotype identified in a Congolese immigrant (Shin-I et al., 2016).

The HCV virion is a small (~9.6 kb RNA genome), enveloped virus of roughly 45-80 nm in diameter, although cell culture-derived HCV (HCVcc) produces highly heterogeneous particles. The host cell-derived highly lipidated bilayer contains two viral glycoproteins, E1 and E2, and envelops a non-icosahedral nucleocapsid composed of multiple core subunits. HCVcc has also been found to have a much larger range of buoyant density than other viruses, ranging from roughly 1.03-1.25 g/mL (Lindenbach et al., 2005; Wakita et al., 2005; Zhong et al., 2005). However, intracellular particles display higher and less heterogeneous density (Gastaminza et al., 2006), suggesting association with cellular components during egress may alter the virion's buoyant density. Furthermore, such buoyant density is directly related to infectivity, with lower

buoyant density correlating with higher infectivity fractions (Hijikata et al., 1993). These observations, as well as studies co-immunoprecipitating HCV with antibodies to lipoproteins (Thomssen R, 1993), suggested the virions themselves associate with lipoproteins. The virions were termed lipoviroparticles (LVPs), both because of their associations with low-density lipoprotein (LDL) and very low-density lipoprotein (VLDL) as well as other apolipoproteins (Andre et al., 2002; Bartenschlager et al., 2011; Catanese et al., 2013; Gastaminza et al., 2010).

HCV has a very restricted tropism, only infecting the highly polarized hepatocytes of the liver. Initial contact is thought to take place at the basolateral face, where the hepatocyte comes into contact with the bloodstream. HCV has a highly complex entry process, first adhering to the cell via attachment factors, then engaging multiple host factors to enter the cell via endocytosis. Following endocytosis and uncoating, the positive-strand RNA genome serves as a template for internal ribosome entry site (IRES)-mediated translation (Honda et al., 1999; Niepmann, 2013). A single polyprotein is produced; co- and post-translation processing by cellular and viral proteases leads to production of three structural proteins (E1, E2, Core) and seven nonstructural proteins (p7, NS2, NS3, NS4A, NS4B, NS5A, and NS5B) (Moradpour and Penin, 2013). In concert with host factors, the nonstructural proteins form ER-derived replication complexes. Following replication of viral RNA, the RNA genome is thought to be trafficked to the lipid droplet, which are in close proximity to sites of viral replication, where nucleocapsids are assembled (Lindenbach, 2013). These capsids then bud into the ER lumen, obtaining its envelope containing the viral glycoproteins E1/E2. The virions then traffic through the Golgi (Coller et al., 2012) and egress in a manner resembling VLDL secretion (Lindenbach, 2013).

Viral Entry

Penetrating the host cell membrane to enter cells is a critical first step of the viral lifecycle. This entry process is driven by the interactions of viral particle with host factors. These associations control the multistep process involved in getting into the cells: viral attachment, internalization, trafficking, and genome release.

As a viral particle seeks a new host cell to infect, it must both protect its genome from damage as well as ensure this genome can be passed onto the next cell. In order to do this, the genome is packaged within a protein coat and often enveloped by the host membrane. When encountering the potential host cell, engagement by this exterior protective coat allows for interactions that lead to genome transfer into the cell. Thus, the viral particle must be stable enough to withstand external environmental threats while labile enough to allow for genome release. This metastable state can be triggered for conformational change and disassembly by cellular host factors and cues (Marsh and Helenius, 2006; Steven et al., 2005) such as receptor interaction, pH change, and covalent modifications (Grove and Marsh, 2011; Harrison, 2005; Hogle, 2002; Smith and Helenius, 2004). In general, there is significant feedback - engagement by the virus induces host cell signaling, and interactions with host proteins can lead to conformational changes of the virion.

Initial associations with the host cell are often nonspecific and serve to attach the virus to the cell surface, where it can then access its receptors. These interactions often occur with heparan sulfate as well as other glycolipid/glycoprotein attachment factors (de Haan et al., 2005; Marsh and Helenius, 2006; Vlasak et al., 2005). Unlike association with attachment factors, virus-receptor interactions directly promote entry via induction of conformational changes, signaling pathways, and/or internalization. Although a single virus-receptor interaction may have low affinity, binding

by multiple pairs results in a much higher avidity and leads to receptor clustering, potentially leading to activation of signaling cascades. Receptors (but not attachment factors) often help define the tropism of a virus.

Simple virus entry can involve a single receptor, as in CD155 for poliovirus (Mendelsohn et al., 1989) or LDLR by human rhinovirus 2 (Hofer et al., 1994). Others require coreceptors, as in the classic case of human immunodeficiency virus (HIV) (Berger et al., 1999). Briefly, following initial attachment via glycosylceramides and heparan sulfate, HIV binds to its primary receptor CD4 via its envelope protein (Dalgleish et al., 1984; Klatzmann et al., 1984). Conformational change of the envelope protein following its association with CD4 allows for interaction with either the CCR5 or CXCR4 coreceptor (Choe et al., 1996; Deng et al., 1996; Dragic et al., 1996; Feng et al., 1996). The use of multiple receptors increases avidity and ability to enter the cell. However, this comes at a cost – viral engagements with receptors are consequently temporally constrained, with the sequence of interactions essential to a successful entry process (Burckhardt et al., 2011; Lopez and Arias, 2004).

As mentioned, association with receptors leads to many virus- and cell-based changes. Although viral association with receptors can directly activate signaling, viruses can also induce signaling via clustering of proteins or lipids. Virally induced signaling via receptor association promotes a favorable environment for viral entry as well as to set the stage for later events in the lifecycle. The main goal of this signaling is to induce endocytosis. Oftentimes, however, the virus may require movement along the plasma membrane to amass or access entry factors. Coxsackievirus B requires signaling induced by its first receptor in order traffic to and access the second receptor. Polarized epithelial cells contain one receptor, decay-accelerating factor (DAF) on the apical surface; its second receptor, coxsackie and adenovirus receptor (CAR) is localized to

the basolateral/ tight junction and is therefore inaccessible to incoming viruses (Cohen et al., 2001). At the apical surface, the virus binds DAF; DAF clustering leads to an activation of Abl kinase and Rac-dependent actin relocalization to the tight junction, where the virus can associate with CAR (Coyne and Bergelson, 2006).

Uptake into the cell is key for viral entry. In some cases, the virus can induce local actin perturbations, allowing the virus to enter at the cell surface (Taylor et al., 2011; Wang et al., 2005; Yoder et al., 2008). For example, human cytomegalovirus association with EGFR and avβ3 integrin activates phosphoinositide 3-kinase and Src, leading to RhoA- and cofilin-based disruption of actin fibers and resulting viral capsid translocation (Wang et al., 2005). Some viruses (HIV, herpes simplex virus 1, Sendai) contain pH-independent fusion proteins; these viruses can consequently fuse at the plasma membrane (Marsh and Helenius, 2006). However, the majority viruses exploit cell-based endocytosis and vesicular trafficking/maturation to position themselves in the cytoplasm. Viruses can use cues, such as the changing pH, redox environment, and presence of particular proteins or lipids, to sense where they are in the cell in order to precisely and accurately position themselves after uncoating (Marsh and Helenius, 1989). Additionally, once endocytosed, the virus does not risk leaving components on the cell surface that could be detected by the immune system. The mode of internalization, oftentimes, is restricted by the size of the virus (Mercer et al., 2010b). Small viruses (<140 nm) usually internalize via small vesicles, frequently using clathrin-mediated endocytosis (CME), including Semliki forest virus, vesicular stomatitis virus, sindbis, human rhinovirus, and dengue virus (Glomb-Reinmund and Kielian, 1998; Helenius, 1980; Johannsdottir et al., 2009; Snyers et al., 2003; van der Schaar et al., 2008). Another small, vesicular mechanism of internalization is the caveolar/raft pathway. Caveolin is implicated in endocytosis of lipids/lipid rafts as well as their constituents. Internalization of

viruses, such as SV-40 (Pelkmans et al., 2002), leads to localization in pH-neutral caveosomes, often followed by vesicular trafficking to the ER via microtubules. Finally, larger viruses utilize macropinocytosis, a process by which cell membrane ruffles fold back in on themselves, taking up extracellular fluid in the newly-formed cavity. Unlike clathrin and caveolin, the size and shape are not dictated by proteins. But akin to these other endocytic mechanisms, once internalized, the vesicle can acidify, fuse, as well as integrate with the endosomal network (Hewlett, 1994; Racoosin, 1993). Vaccinia, Kaposi's sarcoma-associated herpesvirus, and ebolavirus all can internalize via macropinocytosis (Mercer and Helenius, 2008; Raghu et al., 2009; Saeed et al., 2010; Valiya Veettil et al., 2010). Although some viruses, like vaccinia and herpesvirus, are limited by size, macropinocytosis may provide an opportunity for other viruses to widen their host range.

HCV Entry

Entry of HCV into its host cell, the hepatocyte, is perhaps the most complex entry process known to date. This is known to require the virus's two envelope glycoproteins E1 and E2 as well as a range of host factors.

Early Discovery of Entry Factors

Initial studies aimed to identify entry factors via their ability to bind E2. After observations that soluble E2 could bind human, but not mouse, hepatoma cell lines, Pileri et al. transduced a cDNA library from those human cells that could bind E2 into nonbinding mouse cells. They found that the tetraspanin protein cluster of differentiation 81 (CD81) facilitated virion binding to cells and directly bound to E2 (Pileri et al., 1998). Studies then used HepG2 cells, which lack CD81, to

probe for additional entry factors. Crosslinking E2 to these cells revealed scavenger receptor class B member 1 (SR-BI) as another protein that directly bound to E2 (Scarselli et al., 2002). After it was found that viruses from human sera were associated with lipoproteins, studies found that low density lipoprotein receptor (LDLR) was involved in entry (Agnello et al., 1999). Other work suggested the presence of rLDLR allowed for HCV binding; the presence of HCV on the cell was correlated with the amount of rLDLR (Monazahian et al., 1999; Wunschmann et al., 2000).

Approaches then moved from work with purified E2 to surrogate HCV systems, or HCV-like particles (HCV-LPs), using cDNA of the HCV structural proteins to produce virus-like particles in insect cells (Baumert et al., 1998; Triyatni et al., 2002). These HCV-LPs were found to bind heparan sulfate proteoglycan (HSPG) (Barth et al., 2003). Work with virus-like particles then moved to the pseudoparticle system (HCVpp), which is composed of retroviral particles that randomly incorporate HCV envelope glycoproteins into their envelope. The pseudoparticles themselves contain a reporter construct that can be used to assay for entry of the particles (Bartosch and Cosset, 2009; Bartosch et al., 2003a; Hsu et al., 2003). These were used to confirm the roles of CD81 (Cormier et al., 2004; Zhang et al., 2004) and HSPG (Koutsoudakis et al., 2006) in HCV entry. The reporter construct within the HCVpp, in this case a drug resistance gene, also allowed for HCV entry screens. Using a cDNA library from the permissive Huh-7.5 line transduced into human kidney 293T cells in combination with this pseudoparticle screen, the tight junction protein claudin 1 (CLDN1) was identified as another entry factor (Evans et al., 2007). A similar screen, this time using non-permissive mouse embryonic fibroblasts (NIH3T3 cells), identified an additional tight junction protein occludin (OCLN) (Ploss et al., 2009).

However, the pseudoparticle system has drawbacks, namely that its maturation and egress pathway differs from HCV. HCVpp is a retroviral particle and is therefore assembled at the plasma

membrane (Freed, 2015); HCV envelopes at the ER and matures via the VLDL (very low density lipoprotein) pathway. As the HCV entry pathway seems to be intertwined with lipids/lipid components, HCVpp systems may miss some of the complexity of HCV entry. However, with the development of an infectious HCV clone, subsequent studies have been carried out with the full virus itself (HCVcc). Recent entry factors, such as epidermal growth factor receptor (EGFR), were discovered and validated with both HCVpp and HCVcc (Lupberger et al., 2011).

Lipoproteins and Lipoviroparticles

Analysis of HCV collected from patient serum has revealed a highly heterogeneous population, found to be a result of its association with LDL and VLDL (Bartenschlager et al., 2011; Catanese et al., 2013; Gastaminza et al., 2010; Gastaminza et al., 2006; Hijikata et al., 1993; Thomssen R, 1993). Lower density fractions, or those associated with LDL and VLDL, demonstrate higher infectivity (Hijikata et al., 1993; Lindenbach et al., 2006). Additionally, higher density (lower infectivity) fractions isolated from patients can be pulled down by antibodies against immunoglobulin G (IgG), suggesting the viruses are marked by antibodies; lower-density viruses displayed lower association with antibodies (Andre et al., 2002; Tao et al., 2009; Thomssen R, 1993). This suggests virion association with host lipoproteins serves multiple purposes – it aids entry into the hepatocyte via associations with host factors and shields the virus from detection by the immune system. Due to the virion's association with lipoproteins, they have been deemed lipoviroparticles, or LVPs.

This association with lipoproteins is intimately linked with the last stages of the viral lifecycle – HCV maturation and egress is thought to be linked to the VLDL biogenesis pathway

(Chang et al., 2007; Gastaminza et al., 2008; Gastaminza et al., 2006; Huang et al., 2007). Within the liver lipoproteins help mediate lipid homeostasis. They are produced in the ER, when Apolipoprotein B (ApoB) is co-translationally studded with lipids (Jamil et al., 1998; Shelness and Sellers, 2001). During its passage through the secretory pathway, it may be further lipidated by the addition of other apolipoproteins (ApoE and ApoC) as well as incorporation of lipid droplets (Wang et al., 2007). Further evidence that HCV matures along the VLDL pathway is that antibodies to apolipoproteins can be used to immunoprecipitate HCV particles (Andre et al., 2002; Chang et al., 2007).

ApoE is known to be required for HCV infectivity, but ApoB seems to be more dispensable (Gastaminza et al., 2008; Huang et al., 2007; Jiang and Luo, 2009; Maillard et al., 2006; Merz et al., 2011; Owen et al., 2009). ApoE is thought to aid in attachment, binding to heparan sulfate, LDLR, and SR-BI (Andre et al., 2002; Dao Thi et al., 2012; Hishiki et al., 2010; Jiang et al., 2012; Maillard et al., 2006; Owen et al., 2009). Additionally, soluble ApoE or ApoE antibodies can block viral attachment (Chang et al., 2007; Jiang et al., 2012; Owen et al., 2009).

HCV entry overview

HCV entry can be broken down into three step: (1) attachment, (2) internalization of the viral particle, and (3) fusion. Due the nature of the virus as a 'lipoviroparticle', its first contacts with the host cell are most likely mediated by these lipid components. Studies of HCV binding support this; HSPG (including Syndecan-1), LDLR, and SR-BI most likely contribute to initial attachment of the viral particle (Albecka et al., 2012; Catanese et al., 2010; Dao Thi et al., 2012; Koutsoudakis et al., 2006; Maillard et al., 2006; Shi et al., 2013). Virion-associated ApoE may

also aid in the low-affinity interactions with attachment factors (Jiang et al., 2012; Owen et al., 2009). It's hypothesized that initial attachment of the virus to SR-BI (potentially via its lipoproteins) allows for exposure of E2 (Catanese et al., 2010; Zeisel et al., 2007). SR-BI association with this glycoprotein via its hypervariable region 1 (Dao Thi et al., 2012; Scarselli et al., 2002) leads to another conformational change; this permits E2 binding of CD81 (Bankwitz et al., 2010). CD81, in turn, can associate with the tight junction protein CLDN1 (Harris et al., 2008; Krieger et al., 2010). OCLN is another late-acting protein in HCV entry; it may interact directly with HCV, potentially aiding in the internalization process (Sourisseau et al., 2013).

HCV was found to internalize in a clathrin-dependent manner (Blanchard et al., 2006; Codran et al., 2006; Coller et al., 2009; Meertens et al., 2006). Our group has demonstrated that the particle endocytoses with CD81 via clathrin-mediated endocytosis (Coller et al., 2009). Following internalization, HCV traffics through early endosomes (Coller et al., 2012; Meertens et al., 2006) and then undergoes low-pH dependent fusion (Blanchard et al., 2006; Haid et al., 2009; Hsu et al., 2003; Kobayashi et al., 2006; Koutsoudakis et al., 2006; Lavillette et al., 2006; Meertens et al., 2006; Tscherne et al., 2006). The HCV fusion protein is unknown. Both E1 and E2 contain putative fusion domains (Drummer et al., 2007; Lavillette et al., 2006); E2 was required for in vitro fusion with liposomes (Haid et al., 2009).

HCV Entry Factors – Attachment

In vivo, as HCV travels through sinusoid capillaries to reach hepatocytes, it encounters an environment rich in extra cellular matrix proteins (Perrault and Pecheur, 2009). Among these is the glycosaminoglycan (GAG) heparan sulfate. HCV binding to HSPG has been demonstrated

through HCV-LPs (Barth et al., 2003), HCVpp (Barth et al., 2006; Koutsoudakis et al., 2006), and HCVcc (Jiang et al., 2013), most likely through interactions with ApoE. Although HCV has been found to bind highly sulfated heparan sulfate (Barth et al., 2003; Barth et al., 2006), the base proteoglycan was unknown. Syndecan 1 and syndecan 4, of the syndecan HSPG family, were found to allow attachment of HCV (Lefevre et al., 2014; Shi et al., 2013); syndecan 1 is highly expressed in hepatocytes. This association is potentially mediated via ApoE (Jiang et al., 2013; Lefevre et al., 2014).

LDLR expression seems to be directly related to HCV attachment, seen in lymphocytes with increased LDLR expression (Agnello et al., 1999), and in cells with variable rLDLR expression (Monazahian et al., 1999; Wunschmann et al., 2000). Again, ApoE seems to be involved in interactions with this attachment factors (Owen et al., 2009).

SR-BI was first discovered based on its binding to E2 and hypothesized to be a receptor (Scarselli et al., 2002). Surprisingly, E2 binding is dispensable for HCV attachment; SR-BI instead relies on its association with lipoproteins (Dao Thi et al., 2012; Maillard et al., 2006). Further supporting this idea, the attachment function of SR-BI is not species dependent, as both mouse and human SR-BI display the same binding phenotypes (Dao Thi et al., 2012).

HCV Entry Factors – Receptors and "Core" Factors

Viral entry plays a large role in defining the tropism of any virus, but this is especially the case for HCV, as seen in the previously mentioned studies to identify entry factors. CD81 is a member of the tetraspanin family, which is characterized by four transmembrane domains and two extracellular loops. Tetraspanin proteins mediate signal transduction events, often involved in

development, cell growth, and motility/migration. As mentioned, CD81 was first identified through interactions with soluble E2 (Pileri et al., 1998); later evidence of its role in HCV was confirmed via HCVpp (Bartosch et al., 2003b; Cormier et al., 2004; Zhang et al., 2004) and HCVcc (Lindenbach et al., 2005; Wakita et al., 2005). HepG2 cells, upon expression of CD81, become susceptible to HCV infection (Lindenbach et al., 2005; McKeating et al., 2004; Zhang et al., 2004). Additionally, soluble CD81 and CD81 antibodies were shown to block HCV entry (Bartosch et al., 2003b; Brimacombe et al., 2011; Hsu et al., 2003; Wakita et al., 2005; Zhong et al., 2005). This interaction is specific to CD81, as other tetraspanins do not interact with E2 (Drummer et al., 2002; Petracca et al., 2000; Pileri et al., 1998).

Studies of HCV binding suggest E2 interacts with CD81 via its large extracellular loop (LEL) (Bertaux and Dragic, 2006; Drummer et al., 2002; Higginbottom et al., 2000; Petracca et al., 2000). Although soluble E2 has been demonstrated to bind CD81, mature viral particles cannot. This suggests a conformational change is required to expose CD81 binding sites (Bankwitz et al., 2010). This is further underscored by E1 and E2 mutations that allow binding to the mouse ortholog of CD81 (Bitzegeio et al., 2010). The data suggests such mutations induce a more open or labile conformation of the glycoprotein that would not initially be present, allowing for a previously unfavorable interaction. However, this comes at a cost of increased antibody neutralization; the virus may utilize this two-step process to protect the critical binding site with CD81.

CD81 has been shown to act at all stages of HCV entry. The CD81 LEL is also thought be important for its association with CLDN1 (Davis et al., 2012; Harris et al., 2008; Krieger et al., 2010). Furthermore, EGFR-based signaling controlling CD81 lateral diffusion and CLDN-CD81 association was found to be essential for HCV entry (Zona et al., 2013). HCV internalizes with

CD81 (Bertaux and Dragic, 2006; Coller et al., 2009) and seems to be required for the fusogenicity of the virus (Sharma et al., 2011).

SR-BI is highly expressed in hepatocytes, where it serves to mediate the uptake of cholesterol esters from HDLs, VLDLs, and oxidized LDL. It contains two transmembrane domains, a large extracellular loop, and an extended C-terminal cytoplasmic domain. SR-BI, like CD81, was first identified through its interactions with soluble E2 (Scarselli et al., 2002). Later work with HCVpp and HCVcc also demonstrated its requirement in HCV entry (Bartosch et al., 2003b; Catanese et al., 2010; Zahid et al., 2013; Zeisel et al., 2007). As mentioned, it is first thought to function as an attachment factor via ApoE. Following this, conformational changes in the virus allow for binding of the E2 glycoprotein (Catanese et al., 2010; Zeisel et al., 2007) via its hypervariable 1 (HVR1) sequence (Dao Thi et al., 2012; Scarselli et al., 2002). In support of this, deletion of HVRI reduces HCV infectivity due to viral dependency of SR-BI (Prentoe et al., 2014).

The extracellular loop of SR-BI is thought to influence HCV entry through its direct association with E2 and via a post-binding entry step that may require its lipid transfer function (Catanese et al., 2010; Dao Thi et al., 2012; Scarselli et al., 2002; Zahid et al., 2013). The latter requirement, however, may be indirect; perturbation of lipid transfer could alter cholesterol content and therefore affect signaling, microdomain association, and/or fusion. The C-terminal region of SR-BI has also been implicated in HCV entry, potentially involved in signaling process leading to HCV receptor complex trafficking (Dreux et al., 2009).

In line with SR-BI's role in cholesterol homeostasis, addition of various lipids can affect HCV entry. Studies have shown HDL-based enhancement of HCV infection; increase in infection is HVR1-dependent (Bartosch et al., 2005; Voisset et al., 2005). Oxidized LDL, however, inhibits HCV infection, again most likely dependent on SR-BI and the HVR1 region of E2 (von Hahn et

al., 2006; Westhaus et al., 2013). However, it is still unclear if and how the lipid transfer function of SR-BI is involved in HCV entry.

Claudin-1 is a member of the claudin family, a group of proteins that establishes the tight junctional integrity of the cell. Claudins, along with occludin, form the vast majority of tight junction proteins. Highly expressed in the liver, CLDN1 has four transmembrane domains, two extracellular loops, and a large C-terminal cytoplasmic domain. CLDN1, identified using a cDNA library to screen for susceptibility 293T cells, was the initial tight junction protein identified as an HCV entry factor (Evans et al., 2007). Recent evidence supports the possibility that the virus may interact with CLDN1. The E1/E2 complex, but not soluble E2 alone, was found to interact with the first extracellular loop of CLDN1 (Douam et al., 2014). Furthermore, HCV passaged with cells knocked out for CLDN1 shifted CLDN usage, from CLDN1 to CLDN6 (Hopcraft and Evans, 2015). When sequenced, adapted HCV exhibited a mutation in E1 that correlated with CLDN6 usage.

As seen with the alternative usage of CLDN6, HCV is capable of interacting with other members of the CLDN family. CLDN6 and CLDN9 can support entry (Meertens et al., 2008; Zheng et al., 2007), and can also associate with CD81 (Harris et al., 2010). However, due to the low expression of CLDN6 and CLDN9 in hepatocytes, it is unclear how relevant these associations are. Within CLDN1, the first extracellular loop may not only interact with E1/E2, it also seems to be required for its association with CD81 (Cukierman et al., 2009; Davis et al., 2012; Evans et al., 2007). The CD81-CLDN1 interaction is essential for HCV entry (Harris et al., 2010); CLDN1 antibodies that disrupt this association inhibit HCV entry (Krieger et al., 2010).

Occludin is a tight junction protein with four transmembrane domains, two extracellular loops, and extended N- and C-terminal domains. The two termini are responsible for maintaining

barrier function; the C-terminus also participates in signaling. Occludin's role, unlike CLDN1, is not well known. It seems to be required for HCV entry – knockdown of OCLN inhibits HCVpp entry (Liu et al., 2009); expression of OCLN confers permissibility to mouse hepatoma cell lines (Ploss et al., 2009). Although to date, there is no direct binding evidence, OCLN usage (with OCLN-directed blocking antibodies) showed isolate specificity, suggesting that the virus directly interacts with OCLN (Sourisseau et al., 2013). In addition, a mouse model of HCV infection required expression of human CD81 and OCLN for successful infection (Dorner et al., 2011). HCV requires both the first and second extracellular loops for entry (Ploss et al., 2009; Sourisseau et al., 2013).

HCV Entry Factors – Potential Entry Factors/Accessory Proteins

Further hypothesized receptors include Niemann-Pick C1-like 1 (Sainz et al., 2012), transferrin receptor (Martin and Uprichard, 2013), E-cadherin (Li et al., 2016), CD36 (Cheng et al., 2016), and ankyrin repeat domain 1 (Than et al., 2016); however these putative receptors have no direct binding evidence or any mechanistic evidence to suggest if/how they participate in the entry process.

Epidermal growth factor receptor (EGFR) and ephrin type-A receptor 2 (EphA2) are two receptor tyrosine kinases identified via an RNAi-based kinase screen (Lupberger et al., 2011). It was suggested that EGFR signaling led to CD81-CLDN1 association. Downstream signaling via HRas, of the MAPK (mitogen-activated protein kinase) pathway, is also required for entry (Zona et al., 2013). This group hypothesized that EGFR-based signaling led to CD81 lateral diffusion and subsequent CD81-CLDN association. Another study found EGFR activation required

association of the virus with CD81 but not CLDN. HCV binding to CD81 or antibody-mediated CD81 crosslinking led to activation of EGFR (Diao et al., 2012). Exogenous activation of EGFR could also enhance CD81 colocalization and virus internalization (Diao et al., 2012).

In addition to the receptor tyrosine kinases identified, protein kinase a (PKA) and phosphatidylinositol 4-kinase type III-alpha/beta (PI4KIIIα/β) have been identified in the HCV entry process. PKA may be involved with CD81-CLDN interactions (Farquhar et al., 2012); the role of PI4KIIIα/β is not clear (Trotard et al., 2009).

Finally, the SR-BI interacting protein PDZ domain containing 1 (PDZK1) has also been implicated in HCV entry (Eyre et al., 2010). Its knockdown led to a decrease in HCV infection; cells expressing SR-BI mutants lacking the PDZK1-interacting domain also showed decreased HCV infection. PDZK1 is an interesting protein, as it can link proteins to the actin cytoskeleton (Fehon et al., 2010). Since HCV potentially requires actin for its receptor complex relocalization, PDZK1 could mediate this process. However, PDZK1 regulates SR-BI levels and localization (Kocher and Krieger, 2009); the findings in the study may be more due to mislocalization of SR-BI than requirements of PDZK1 itself.

Models of Entry

HCV is thought to encounter its "early" receptors SR-BI and CD81 on the basolateral face of the hepatocyte. However, the "late" receptors are both tight junction proteins. As these essential receptors have very different subcellular localizations, there have been several proposals as to how HCV can gain access to all of them. With the discovery of CLDN1, Evans et al. proposed a tight junction targeting model based on Coxsackievirus entry. As mentioned, following initial binding

of Coxsackievirus B to its first receptor DAF, it undergoes relocalization to the tight junction in order to access CAR, the second receptor (Coyne and Bergelson, 2005, 2006). Similarly, it was thought that HCV would first attach at the basolateral face, associate with SR-BI and CD81, then migrate to the tight junction. A second hypothesis suggested HCV-based disruption of the tight junction would allow the virus to access CLDN1 and OCLN at the basolateral face. In the third scenario, the virus may not need to directly interact with CLDN and OCLN and therefore does not require this long-distance relocalization.

Studies in HepG2 cells, which are partially polarized, supported the second model of HCV entry. They found greater association of CD81 with CLDN1 in nonjunctional regions, suggesting that perhaps that these extrajunctional pools of receptors functioned during entry (Mee et al., 2009). Furthermore, disrupting cell polarity boosted HCV infection, suggesting that an increase of tight junction proteins into the extrajunctional membrane spaces was conducive for HCV entry. Altogether, this suggested HCV might disrupt tight junction integrity so as to more readily access the tight junction proteins.

Our lab also studied the requirements of HCV entry. Single particle tracking of fluorescently labeled HCV showed colocalization with CLDN1, but not another standard marker of tight junctions, ZO-1 (zona occludens 1) (Coller et al., 2009). As Huh-7.5 cells are highly unpolarized, CLDN1 was found on the majority of the plasma membrane rather than restricted to areas of cell-cell contact. When tracking HCV entry in concert with CD81-GFP, they found the virus entered without preference to cell junctional regions. This again might suggest support for the second model of extrajunctional entry. However, because Huh-7.5 and HepG2 cells are not (fully) polarized, localization of these receptors does not reflect the in vivo environment. Without an adequate system in which to test HCV entry, experiments studying receptor and signaling

requirements are inherently slanted towards extrajunctional entry. More relevant cell culture systems, such as organoids, may be able to recapitulate the complexity of the HCV entry process as it happens *in vivo*.

Organoid Cell Culture Systems

Organoids, loosely defined, are a scaled-down, simplified three-dimensional organ produced *in vitro* that demonstrate some of the functional capabilities of the entire organ. They are an invaluable middle ground between the standard 2D cell culture systems and *in vivo* animal/human studies. They have proven to be far more relevant than traditional cell culture systems and are not cost-prohibitive as with studies of whole organisms. Furthermore, as organoids are cell culture systems, they can easily be manipulated genetically or via drug and small molecule treatment.

Organoids grew out of experiments attempting to recreate organs *in vivo* via dissociation and reaggregation of embryonic chick organs (Weiss and Taylor, 1960). Such reassembly is hypothesized to occur via cell self-sorting and fate specification. Sorting/self-assembly may occur through segregation of cells into domains with matching adhesive properties, thus attaining a thermodynamically favorable state. This theory, known as Steinberg's differential adhesion hypothesis (Steinberg, 1964), is thought to occur via association of like cell surface adhesion proteins. These factors are much more prevalent in three-dimensional cultures, as was discovered when kidney (Montesano et al., 1991) and breast (Hagios et al., 1998) epithelial cells were seeded into extracellular matrix (ECM) hydrogels. These cells were able to develop tubules and ducts, as in their parental organs. This process has been optimized and standardized with the use of Matrigel

(Li et al., 1987), an ECM secreted by the Engelbreth-Holm-Swarm mouse sarcoma cell line. The ECM is rich in structural proteins such as laminin, collagen, and heparan sulfate, providing cells with a basement membrane on which to adhere and polarize.

As with other organ reaggregation studies, studies of the liver demonstrated that chick embryonic hepatic tissue is able to form liver-like units, including functional bile ducts (Weiss and Taylor, 1960). Researchers have since developed a Matrigel-based system to grow organoids with cells from adult mouse liver (Huch et al., 2013). These organoids, like those from the embryonic hepatic cells, differentiate to form functional hepatocytes. Additionally, when transplanted back into mice suffering from liver disease, these organoids can partially rescue mortality, further supporting their functionality. To this date, a full liver "organoid" model (with all the components of a liver) has not been established. Mixing three different cell populations (pluripotent stem cell-derived hepatic cells, mesenchymal stem cells, and endothelial cells) eliminates the need for differentiation (Takebe et al., 2013). This heterogeneous population, when seeded into Matrigel, stratifies and vascularizes, resulting in a liver bud-like organoid that can also be transplanted into mice.

The ability to generate cell culture systems that morphologically and physiologically resemble organs provides a massive breakthrough in both basic and translational research. Developmental biology has received a huge boost as a result of organoid technology; the field now has the ability to better study organogenesis *in vitro* (Ader and Tanaka, 2014; Greggio et al., 2013; Mondrinos et al., 2006). The ability to manipulate organogenesis has provided insight into aberrant development (Lancaster et al., 2013). Organoids are now commonly used in studies of organ function, how cells interact with each other within the organ, and how the organ interacts with its environment. Intestinal organoids, for example, are used to study nutrient uptake and secretion of

select hormones (Zietek et al., 2015). As manipulation has been used to study abnormal development, genetic manipulation can be used to induce disease states, including carcinogenesis (Drost et al., 2015). A new and exciting application involves transplantation of patient-derived cells into Matrigel; culturing these cells into organoids allows for *in vitro* approach to studying diseases that were previously difficult to model in animals. One key study found that organoids derived from autistic patients displayed an altered transcriptome profile (Mariani et al., 2015). Finally, organoids can be used to study host-microbe interactions. Studying colonization of the luminal epithelia of human gastric organoids by *H. pylori*, researchers found large physiological changes; noteworthy was a significant increase in proliferation due to an oncogenic protein (Bartfeld et al., 2015; Wroblewski et al., 2015).

As HCV infection occurs in the highly polarized environment of the hepatocyte, efforts have been made to more closely approach the *in vivo* architecture. HepG2 cells are somewhat polarized, more so than Huh-7.5 cells, and HepG2 cells expressing CD81 have been put forth as a model to study HCV infection in a 'polarized' system (Mee et al., 2009). However, the polarization is only partial; the system is further limited by reduced infection efficiency in HepG2 cells (Lindenbach et al., 2005; Mee et al., 2009; Narbus et al., 2011). An additional attempt was made to create three-dimensional polarized Huh-7 cells via bioreactors (Sainz et al., 2009). Although, unlike HepG2s, these cells produced somewhat comparable levels of virus as 2D Huh-7 cells, they were not demonstrably polarized. However, seeding Huh-7.5 cells into Matrigel produced organoid-like spheroids that could form functional bile canaliculi and contained cellular markers consistent with polarized hepatocytes (Molina-Jimenez et al., 2012). More importantly, the localization of the HCV entry factors CLDN1 and OCLN was now restricted to the tight junction, which is potentially critical for an accurate study of HCV entry.

Fluorescent labeling of viruses: DiD

As viral entry requires sequential interactions with various components of the cell, both for signaling and transport, visualizing such interactions is essential for elucidating the entry pathway. Immunofluorescence microscopy of viral entry allows for clear demonstration of association with entry factors via colocalization analysis, observance of heterogeneity in entry populations and processes, and delineating cytoskeletal factors important for entry via live cell analysis of viral particles' movement. Immunofluorescence of viral entry involves fluorescent labeling of both the virus and the desired cellular structures as well as a microscope sensitive enough to detect single particles.

The most essential factor in immunofluorescence of viral entry is labeling the virus itself. The virus must be labeled with sufficient fluorophors to allow detection. However, such labeling cannot interfere with the infectivity of the virus or its interactions with cellular factors, as can often occur with the insertion of fluorescent proteins. This can be circumvented by fluorescent dyes, which are less likely to affect the virion's entry process. However, for enveloped viruses, such dyes cannot be used to label internal components of the virus, such as the capsid or genome, after viral assembly and release.

The fluorogenic dye 1,1′-dioctadecyl-3,3,3′,3′-tetramethylindodicarbocyanine (DiD) overcomes many possible caveats. This lipophilic dye readily intercalates viral envelopes without compromising infectivity. Dyes often must compete with background fluorescence of the cell, leading to noisy signal, especially problematic in the case of small viral particles. Autofluorescence is reduced at longer excitation wavelengths; DiD usage therefore minimizes such noise. Depending on the concentration of DiD used, the surface density of the dye is often such that is self-quenches but is still enough for it to be detected via microscopy. Once the viral envelope fuses with cellular

membranes, the DiD dye is dequenched. This can be seen as an increase in fluorescent intensity or size of the puncta and is often used as a proxy for viral fusion.

One final caveat of all labeled viruses is specific infectivity (SI), or the ratio of particle to pfu (plaque forming unit). A SI of 1000, for example, means for every one infectious particle, there are 1000 that cannot infect the cell. When tracking association of a labeled viruses with cellular factors, quantitation should focus only on those particles that will lead to a productive infection. One option is to purify viral preps that contain highly infectious virus, and therefore low SI. Another option is to track these particles in real time and only focus on the subpopulation of viruses that undergo uncoating (via fluorescence dequenching), as uncoating indicates a successful transition to the next phase in the viral lifecycle.

DiD labeling of viruses was first developed for use with influenza (Lakadamyali et al., 2003) in hopes of elucidating how influenza is endocytosed. Live cell imaging of DiD-labeled particles allows for the division of influenza entry into three stages: slow, actin-dependent active transport in the cell periphery; rapid, dynein-dependent, unidirectional traffic towards the nucleus; and finally, intermittent, microtubule-based bidirectional movement in perinuclear area. Without single-particle tracking of the virus, these distinct steps would have been lost.

DiD was next adapted for another member of the *Flaviviridae*, dengue virus (van der Schaar et al., 2007). As mentioned, they found the virus to have a very high SI, or a much greater number of viral particles than were infectious (2600 to 72000). They found one potential source of the loss of infectivity – virions bound very inefficiently to the cell. Fusion of the virus with cellular membranes, assayed via dequenching, occurred in roughly 1 of 6 particles that bound. A follow-up paper traced dengue virus' entry via endocytosis (van der Schaar et al., 2008). Using DiD-labeled dengue virus and fluorescent cellular markers, they found that dengue virus

internalized via clathrin-mediated endocytosis, followed by traffic in Rab5- then Rab7-positive endosomes.

Our lab also utilized DiD labeling to study HCV entry in unpolarized hepatocytes. Labeling is facilitated by HCV's highly lipidated envelope. However, due to HCV's poor specific infectivity (only ~1 in 2000 virions is infectious), we could not be assured that associations with cellular factors would lead to productive infection. We overcame this limitation by taking advantage of the observation that infectious HCV is highly lipidated and has a different buoyant density than noninfectious HCV (Hijikata et al., 1993). In our protocol, several rounds of purification ensure specific labeling of highly infectious virus (Coller et al., 2009). Virus is first PEG-concentrated, then incubated with DiD. As previously mentioned, DiD has no effect on SI of the virus. The labeled virus separated on a gradient via ultracentrifugation to separate the virus based on its buoyant density. The gradient is fractionated and assayed for SI; the final SI of the now-purified virus is roughly 10.

Characterization of the purified DiD-HCV particles showed that >95% of them colocalize with the capsid and E2, DiD-HCV could be immuno-depleted with anti-E2 antibodies, and that DiD-HCV uncoating required the HCV receptor CD81 and acidic pH, as does *bona fide* HCV entry (Coller et al., 2009). The study used these DiD-labeled particles to examine the requirements of HCV entry, using live cell imaging to investigate DiD-HCV association with its receptors, actin, its internalization pathway, and subsequent endosomal trafficking.

Goal of this thesis

The goal of this thesis was to define the mechanism of HCV entry using three-dimensional hepatoma cells. Although *in vivo*, HCV infection takes place in the context of highly polarized hepatocytes, HCV research has, up until now, been performed in unpolarized cell systems. We therefore sought to examine HCV entry in a more relevant system, both to broadly define the entry pathway of HCV and to define the individual roles of its many entry factors. We first developed a system for single particle tracking of fluorescently labeled HCV in three dimensional organoids. These organoids display markers of polarity, hepatocyte function, and correct localization of HCV entry factors. We optimized this system for both live and fixed cell microscopy in order to capture interactions with cellular factors. We then used this system to follow labeled HCV during infection. We found HCV colocalizes with early factors SR-BI, CD81, and EGFR at the basolateral, then traffics to the tight junction in an actin-dependent manner. The receptor complex then colocalizes with CLDN1 and OCLN as well. These observations support the tight junction targeting model proposed by Evans et al. Although other groups proposed EGFR signaling mediated tight junctional relocalization, we find that in polarized cells, EGFR and its associated signaling are required for internalization. Finally, we explored the internalization pathway of the viral particle. In the polarized cell system, viruses are internalized via clathrin-mediated endocytosis, traffic through early endosomes, and undergo fusion in a pH-dependent fashion. EGFR is activated at the tight junction at time points associated with internalization. Residues on its cytoplasmic tail, potentially sites for components of the clathrin endocytic machinery, are also required for HCV infection. Finally, we demonstrate EGFR signaling is also required for recruitment of such adaptors to HCV.

CHAPTER II

DEVELOPMENT AND CHARACTERIZATION OF THREE-DIMENSIONAL ORGANOID SYSTEM FOR STUDYING HCV ENTRY

Abstract

Entry of Hepatitis C virus (HCV) into hepatocytes is made up of several complex stages, involving multiple host factors with specific localizations. Although many entry factors have been identified, their role and the much of the mechanism of HCV entry is unknown. As the virus requires two tight junction proteins, claudin1 (CLDN1) and occludin (OCLN), physiologically relevant cell culture systems are essential for studying HCV entry. However, the current cell culture systems show poor polarization and are therefore incompatible with studying a process that is based upon partitioning in cellular domains. In the current study, we have developed a system for studying HCV entry in three-dimensional polarized hepatoma organoids via live and fixed microscopy. Such organoids display both markers of hepatic polarization and functionality. Importantly, HCV entry factors now localize properly, with the tight junction entry factors CLDN1 and OCLN no longer available to the incoming virion, as would occur in hepatocytes *in vivo*. Such organoids are also infectable by HCV on levels comparable with their two-dimensional, unpolarized counterparts. We have also further characterized DiD labeling for HCV virions, demonstrating pure preps that specifically label highly infectious virions. This system allows us to follow interactions with host proteins in an environment that mimics the architecture of hepatocytes in the liver. Tracing DiD-labeled HCV entry in live cells, we found that the virus does not remain on the basolateral face, but seems to move towards the tight junction, suggesting the virus utilizes the tight junctional rather than extrajunctional entry route seen in unpolarized cells.

Introduction

Hepatitis C Virus (HCV), a member of the *Flaviviridae* family, is an enveloped, positive-sense RNA virus of approximately 9600 nucleotides. The HCV virion is frequently referred to as a lipoviroparticle, containing cellular apolipoproteins (Apos) and a lipid composition similar to very low density lipids (VLDL) (Bartenschlager et al., 2011). The virus has a highly restricted tropism, preferentially infecting hepatocytes, the uniquely polarized epithelial cells of the liver. Hepatocytes have disproportionately large basolateral surfaces that access the bloodstream via contact with sinusoidal capillaries; lateral association with adjacent hepatocytes form extended sheets (Perrault and Pecheur, 2009). The apical domains of adjacent hepatocytes, defined and maintained by tight junctions, form a network of bile canaliculi (Easter et al., 1983).

Unlike many viruses, which may require only one or two entry factors, studies have identified a large number of host factors utilized in the HCV entry process. After attachment, the virus is known to absolutely require scavenger receptor class B member 1 (SR-BI), cluster of differentiation 81 (CD81), CLDN1, and OCLN (Bartosch et al., 2003b; Evans et al., 2007; Liu et al., 2009; Pileri et al., 1998; Ploss et al., 2009; Scarselli et al., 2002; Zhang et al., 2004; Zheng et al., 2007). Additional proposed entry cofactors include EGFR (Lupberger et al., 2011), very-low-density lipoprotein receptor (Ujino et al., 2016), Niemann-Pick C1-like 1 (Sainz et al., 2012), transferrin receptor (Martin and Uprichard, 2013), serum response factor binding protein 1 (Gerold et al., 2015), E-cadherin (Li et al., 2016), CD36 (Cheng et al., 2016), and ankyrin repeat domain 1 (Than et al., 2016). While these factors, especially the core set of four entry factors, are thought to be required, their role in entry is unknown.

The entry factors CLDN1 and OCLN pose a potential hurdle for the virus. In hepatocytes, these proteins localize to the tight junction, away from the bloodstream and therefore inaccessible to the incoming virus. Based on the requirement for these factors, several models of HCV entry were proposed (Figure 1). Based on a pathway utilizing tight junctions in Coxsackie virus (Coyne and Bergelson, 2005, 2006; Coyne et al., 2007), it was hypothesized that HCV first associates with CD81 and SR-B1 on the basolateral face, then traffics to the tight junction (Evans et al., 2007). A second model proposed HCV could access CLDN1 and OCLN on the basolateral face via disruption of tight junctional integrity (Harris et al., 2008; Mee et al., 2009). A final model suggested that while HCV may require CLDN1 and OCLN in a signaling capacity, it may not need to directly associate with these proteins, eliminating the need for migration of the virus to the tight junction.

We previously developed single particle tracking of fluorescent HCV virions in order to investigate HCV entry (Coller et al., 2009). The study, which used a combination of RNA interference and immunofluorescence analysis, followed HCV entry in the standard unpolarized Huh-7.5 cell culture system (Coller et al., 2009). HCV was fluorescently labeled with the lipophilic dye DiD, which binds to the viral envelope, then purified for highly infectious virus via its buoyant density (Hijikata et al., 1993). Live cell imaging of DiD-HCV cotrafficking with CD81, CLDN1, and the entry cofactors identified in the screen was then performed. Perhaps surprisingly, HCV internalization occurred without preference for cell-cell junctions (Coller et al., 2009). Thus, either HCV entry does not occur at tight junctions, or unpolarized Huh-7.5 cells, lacking discrete tight junctions, are an insufficient model to study HCV entry. In order to distinguish between these two possibilities, entry must be studied in a polarized cell culture system.

In this study, we developed and optimized a more physiologically relevant system in which to study HCV entry, combining a three-dimensional polarized organoid system with DiD-HCV tracking of host-virus interactions. These hepatoma cells form spherical organoids with polarization that closely resembles hepatocyte architecture *in vivo.* Such organoids retain functionality of hepatocytes in the liver and can be readily infectable by HCV. More importantly, CLDN1 and OCLN localize exclusively to the inner, tight junctional region of the organoids, and are thus inaccessible without either trafficking or viral manipulation of the cell. Thus, this system allows for testing of various HCV entry hypotheses without the caveats and potential artifacts of an unpolarized cell culture system. Using live cell imaging in these polarized organoids, we found that DiD-HCV seems to migrate towards the tight junction, in support of the tight junctional relocalization model. This underscores the importance of using polarized cells to study viral trafficking.

Materials and Methods

Cell culture

Huh-7.5 cells (Blight et al., 2002) were maintained in Dulbecco's modified high glucose media (DMEM; Gibco) supplemented with 10% fetal bovine serum (FBS; Invitrogen), 0.1 mM nonessential amino acids (Gibco), and 1% penicillin-streptomycin (Gibco). Cells were grown at 37°C with 5% CO_2.

Pseudoparticle Transduction

To produce retroviral stocks, ~70% confluent p100 plates of 293T cells were transfected with 8 µg MMLV gag-pol, 4 µg vesicular stomatitis virus glycoprotein G, and 12 µg construct.

Plasmids were transfected using Lipofectamine 2000 (Life Technologies), as per manufacturer's guidelines. Supernatants were harvested 48 hours post-transfection, filtered through a 0.22 μM filter, then used to transduce cells. Huh-7.5 cells were incubated with pseudoparticles and 8 μg/mL polybrene for 5 hours. For live cell imaging, cells were transduced with CD81-GFP lentivirus (Coller et al., 2009).

Highly infectious virus preparation

Stocks of HCV genotype 2a RNA (infectious clone pJFHxJ6-CNS2C3) were generated as previously described (Berger et al., 2009; Coller et al., 2009; Coller et al., 2012; Mateu et al., 2008). Briefly, viral supernatants were collected for up to 5 passages after electroporation, then filtered through a 0.22 micron nitrocellulose filter and stored at 4°C protected from light. Viral titer was determined via limiting dilution and subsequent immunohistochemical staining with a monoclonal NS5A antibody (9E10, generous gift of Charles Rice, Rockefeller University) as described (Randall et al., 2006).

HCV Concentration and DiD Labeling

Viral stocks were concentrated via PEG (polyethylene glycol 8000; Fisher) precipitation (Blight et al., 2002; Coller et al., 2009). Viral supernatant was mixed with PEG (final concentration 8%) and incubated overnight at 4°C. Following centrifugation (20 minutes, 8000xg), pellet was resuspended in 15 mLs of the original supernatant; resuspended sample was spun down again (15 minutes, 8000xg) and pellet was resuspended in supernatant for a final concentration of 1/100 of the starting volume. 5 μL of DiD (Invitrogen), was added to 1 mL concentrated virus and incubated for 90 minutes with shaking, protected from light. Labeled virus was layered onto a 10–60%

weight/volume iodixanol gradient (OptiPrep, Sigma) in sterile water and centrifuged for 16.5 hours (34,000 RPMs at 4°C). The gradient was separated into 1 mL fractions; each fraction was subsequently analyzed for HCV RNA levels (following Trizol-LS extraction; Invitrogen, see HCV RNA quantitation) and infectious viral titer (Randall et al., 2006). Fractions with the best specific infectivity were added to Amicon Ultra 100k filters (Millipore) and spun for 20 minutes at 14000xg. Filters were then inverted in a new tube and spun for 2 minutes at 2000xg. The resulting supernatants were pooled for use in imaging studies.

Matrigel Polarization

To induce polarization, Huh-7.5 cells were embedded in Matrigel (Growth Factor Reduced, Phenol Red-free; BD Biosciences). Matrigel was first thawed on ice. Huh-7.5 cells were then trypsinized and diluted in DMEM + 10% FBS to a final concentration of 1 $x10^5$ cells/mL. Equal volumes of Matrigel and diluted cells were mixed and seeded into plates. The Matrigel solution was allowed to polymerize for 30 minutes at 37°C before adding DMEM + 10% FBS to cover. Cells were cultured for 6-8 days, changing media every other day.

Cell Recovery from Matrigel

Matrigel-polarized cells were harvested with Matrigel cell recovery media (BD Biosciences). Briefly, cells were shaken for 1 hour with 500 µL cell recovery media, then centrifuged at 300g for 5 minutes. Supernatant was removed, and the pellet was washed twice in PBS.

Electron Microscopy

Concentrated virus was labeled, gradient purified, and concentrated with Amicon filters as described above. Resulting supernatant was mixed with equal parts 4% paraformaldehyde. Samples were then prepared and processed at the electron microscopy facility using (12nm colloidal gold anti-human IgG, Jackson Immuno Research).

Fixed cell immunofluorescence microscopy of organoid cultures

Matrigel-cell mixtures were prepared as described above, and 75 µL of the solution was placed onto coverslips in 24-well plates. Cells were fixed in 3.6% paraformaldehyde (PFA) for 20 minutes at room temperature. Cells were permeabilized with room temperature 0.5% Triton x-100 in PBS for 10 minutes, and then rinsed with 0.1 M Glycine in PBS 3 times for 10 minutes each. Cells were incubated for 2 hours in blocking solution (0.1% BSA, 0.2% Triton x-100, 0.005% Tween-20, and 20% goat serum in PBS). Coverslips were incubated overnight at 4°C with primary antibodies diluted in blocking solution. (1:500 anti-ZO-1, Invitrogen; 1:1000 anti-Na^+K^+-ATPase, Abcam; 1:400 anti-MRP2, Abcam; 1:1000 anti-NS5A 9E10; 1:300 anti-CD81, Santa Cruz; 1:300 anti-SR-B1, Novus; 1:400 anti-EGFR, Santa Cruz; 1:400 anti-OCLN, Invitrogen; 1:100 anti-CLDN1, Santa Cruz) Following overnight incubation, the Matrigel was allowed to reform for 10 minutes at room temperature without shaking. Coverslips were washed 3 times, 20 minutes each, with wash buffer (0.1% BSA, 0.2% Triton x-100, and 0.005% Tween-20 in PBS). Alexa Fluor conjugated secondary antibody (488 or 594) was diluted 1:1000 in blocking solution and incubated with the Matrigel-embedded cells for 1 hour at room temperature, then rinsed 3 times with wash buffer (as above). CMFDA labeling (Invitrogen) occurred prior to fixation: CMFDA was incubated with the cells (1:1000) for 1 hour, then washed and incubated for an additional hour with

DMEM +10% FBS. Cells were then fixed and stained as above. For all samples, coverslips were mounted with ProLong Gold AntiFade with DAPI nuclear stain (Invitrogen) following the final rinse.

For immuno-staining of DiD-HCV particles, purified particles were added to poly-lysine treated coverslips and incubated at 37°C for 2 hours, then fixed in 3.6% paraformaldehyde for 30 minutes. Samples were washed with PBS, permeabilized in PBS with 0.2% Triton x-100 for 15 minutes, washed in PBS containing 0.1% Tween 20 (PBS/Tween), then blocked with 10% goat serum in PBS/Tween for 1 hour. Coverslips were incubated for 1 hour with primary antibody in blocking solution (1:100 anti-core, Virostat; 1:100 anti-E2 CBH5; 1:250 anti-Apo-E, Abcam). Following incubation with primary antibodies, samples were washed twice with PBS and incubated with fluorescently conjugated secondary antibodies at 1:1000 in blocking solution (488 or 350, AlexaFluor) for 1 hour. Coverslips were washed three times with PBS, then mounted with ProLong Gold AntiFade (Invitrogen).

Confocal Microscopy Analysis

Fixed cell imaging was performed on an Olympus DSU Spinning Disc Confocal with a 100X NA 1.45 oil-immersion objective. Using Slidebook imaging software, images were captured with a Hamamatsu back thinned EM-CCD camera set to an intensification of 255. Alexafluor 594 was visualized with the DsRed filter set; Alexafluor 488 was visualized with the EGFP filter set. Z-stacks of the organoids were acquired using slices taken every 0.3 µm. Following acquisition, images were processed with ImageJ (NIH). Z-stacks were normalized on Slidebook, then imported using BioFormats (LOCI). Images presented in the figures were duplicated out of the Z-stack, separated into individual channels, adjusted for contrast and smoothed, then reassembled.

Live Cell Imaging

Cells expressing CD81-GFP were mixed with Matrigel; 400 µL of the solution was seeded into a 48-well plate and maintained as described. After 7 days, organoids were extracted from Matrigel and resuspended in 1 mL imaging media containing DMEM-F12 without phenol red (Gibco) supplemented with 10% fetal bovine serum (FBS; Invitrogen), 0.1 mM nonessential amino acids (Gibco), 1% penicillin-streptomycin (Gibco), and 50 µM HEPES (Gibco). Organoids were then replated onto collagen-treated 35 mm imaging dishes with interlocking lids (Ibidi), 200 µL of the cell solution per plate. Imaging media was added to the dishes, and organoids were allowed to adhere for 6-8 hours. Just prior to imaging, DiD-labeled HCV was added to imaging dishes. Dishes were incubated on ice for 1 hour, then placed on an enclosed stage heated to 37°C on a Leica SP5 Tandem Scanner Spectral 2-Photon confocal microscope.

Cells were visualized using a 63x NA 1.4 oil-immersion objective. CD81-GFP was imaged with an Argon laser and a HyD detector set for the 495-535 nm wavelength range; DiD was imaged with a HeNe laser and a HyD detector using the 600-670 nm wavelength range. Videos were acquired through sequential exposures every 15-30 seconds up to 90 minutes post-temperatures shift. Images were processed using ImageJ.

HCV RNA quantitation

Following cell recovery, RNA was extracted using RNeasy 96 kit (Qiagen); samples were eluted with 150 µL water. Cellular and HCV RNAs were reverse-transcribed and PCR amplified using the SuperScript^{TM} III Platinum One-Step qRT-PCR System with Platinum Taq (Invitrogen) as previously described (Randall et al., 2007). HCV RNA was amplified using 300 nM forward

primer (5’ - CCG GGA GAG CCA TAG TGG TCT) and 300 nM reverse primer (5’ - CCA AAT CTC CAG GCA TTG AGC) and 200 nM probe (5’ - 6FAM-CAC CGG AAT TGC CAG GAC GAC CGG-MGBNFQ). Parallel reactions utilized 18S ribosomal RNA as an internal loading control, detected via rRNA TaqMan gene expression assay (Hs99999901_s1, Applied Biosystems). Reverse transcription-PCR (RT-PCR) amplification reaction parameters using an ABI 7300 system (Applied Biosystems) was as follows: 50°C for 30 min, 95 °C for 6 min, and then 50 cycles of <95 °C for 15 secs, 60 °C for 1 min>. HCV and 18S RNA copy numbers were determined via comparisons to concentration standards. Data was analyzed with SDS v1.4 software (Applied Biosystems). Absolute HCV RNA was normalized to the sample’s 18S RNA, then to the (normalized) 6-hour vehicle control for relative HCV RNA levels.

Results

DiD-HCV labeling and characterization

We previously published single particle tracking of HCV infection of 2D Huh-7.5 cells (Coller et al., 2009). In order to follow HCV in cells, we utilized a lipophilic dye, DiD, that binds to the virion’s highly lipidated envelope (see Figure 2 for schematic). HCV harvested from cells post-electroporation has a very poor specific infectivity (Figure 3A), meaning that the vast majority of particles are not infectious. In order to ensure we are following productive interactions, or those interactions leading to infection, we enrich for HCV with the lowest specific infectivity. DiD is first polyethylene glycol (PEG) concentrated, then labeled with the DiD dye. DiD-labeled HCV is then purified by density gradient ultracentrifugation on an iodixanol gradient, fractionated, and each fraction is assayed for specific infectivity. The fractions with the best specific infectivity

are concentrated by Amicon filter centrifugation. In the current study, the purified DiD-HCV stocks had a specific infectivity of 4.9 ± 4 (Figure 3).

In the previous work from our lab, DiD-labeled HCV was characterized to ensure the DiD puncta being tracked were viral particles. Levels of DiD co-localization with HCV core indicated specific labeling of virions. Successful immunodepletion of DiD-HCV with E2 antibodies demonstrated they were free virions. Entry and uncoating of DiD-HCV in Huh-7.5 cells required CD81 and endosomal acidification (Bartosch et al., 2003b; Blanchard et al., 2006; Coller et al., 2009; Koutsoudakis et al., 2006; Meertens et al., 2006), showing that these DiD-labeled particles had the same entry requirements as HCV.

In the current study, we co-labeled DiD-HCV with various components of the viral envelope to demonstrate specific labeling in our preps (Figure 4A). Particles showed almost complete colocalization of DiD with either HCV structural proteins Core and E2 or Core and Apolipoprotein E. In addition, to ensure these DiD-HCV samples were pure and not contained within exosomes, electron microscopy was performed (Figure 4B). Particles of the expected size and shape were observed, without the presence of exosomes. Immunogold E2 labeling confirmed these particles were marked by the envelope glycoprotein E2.

Hepatoma organoids display polarity similar to hepatocytes *in vivo*.

Polarized hepatocytes *in vivo* display a distinct morphology wherein the basolateral surface is exposed to extra-cellular virus traveling via the bloodstream, while the apical membrane, which forms the bile canaliculus, is flanked by tight junctions (Figure 1). Huh-7.5 hepatoma cells are poorly polarized when grown in standard two-dimensional (2D) cultures, as indicated by localization of the tight junction protein zona occludens-1 (ZO-1) throughout the plasma

membrane (Figure 6, top left). In contrast, Huh-7.5 cells grown in ECM form three-dimensional (3D) polarized cultures that resemble hepatocytes *in vivo* (Molina-Jimenez et al., 2012). The Matrigel-based ECM abuts the basolateral membrane; similarly, the sinusoidal face of hepatocytes is in contact with stellate cell-secreted ECM *in vivo*. To develop this Matrigel-based polarization system in our lab, we trypsinized Huh-7.5 cells and diluted them to a final concentration of $1x10^5$ cells/mL in 10% DMEM. Equal parts Matrigel and cell solution were mixed, then added to wells. Seeding at single-cell density allows for polarization as the cells grow in the extra-cellular matrix. After 6-8 days, sphere-like organoids of roughly 10-20 cells are apparent (Figure 5).

We tested the polarity of these cells by examining the localization of hallmark apical, basolateral, and tight junctional markers (Figure 6). In contrast to the unpolarized two-dimensional Huh-7.5 cells, Huh-7.5 organoids displayed a restricted ZO-1 sub-cellular localization at internal membrane interfaces that is consistent with tight junctions. The localization of MRP2, an apical protein that defines the bile canaliculus, was similarly restricted in Huh-7.5 organoids. Na^+K^+-ATPase, a basolateral marker, displayed an expected localization to lateral faces (between cells) as well as the external membranes.

To determine whether the hepatoma organoids display functional characteristics of polarization, we tested whether they retained the bile analog 5-chloromethylfluorescein di-acetate (CMFDA) at the apical membrane. CMFDA freely diffuses into cells, where it is converted to a cell-impermeant form after cleavage by esterases. Hepatoma organoids showed enrichment of CMFDA at the apical bile canaliculi, suggesting that the polarized cells are capable of export into the bile canalicular space. Thus, hepatoma organoids display the appropriate localization of cellular markers and functional characteristics of polarized hepatocytes.

Hepatoma organoids are susceptible to HCV infection.

We next tested whether Huh-7.5 organoids were susceptible to HCV infection. Cells were infected with HCV for 48 hours, then fixed and probed with an NS5A-specific antibody. NS5A expression was readily detected in all cells within the organoid (Figure 6, bottom right). Additionally, we compared kinetics of HCV replication and infectious virus production in 2D versus 3D Huh-7.5 cells. Viral RNA and supernatants were harvested at 24, 48, and 72 hours. Viral RNA copies (Figure 7A) and infectious virus titers (Figure 7B) increased over the time course of infection, indicating that the 3D cultures were productively infected with HCV. Comparison to the 2D cultures showed no significant difference in HCV replication or infectious virus production, validating the use of the 3D cultures to characterize HCV infection.

Localization of HCV entry factors in hepatoma organoids is consistent with their localization in hepatocytes.

HCV entry factor localization in Huh-7.5 organoids was then examined (Figure 8). EGFR primarily localized to the basolateral membrane, while SR-B1 and CD-81 localized to both basolateral and apical domains. CLDN1 and OCLN were restricted to the internal membrane interfaces, as would be expected for tight junctional proteins. To verify tight junctional localization of the HCV receptors, the Huh-7.5 organoids were immuno-probed for OCLN and ZO-1. OCLN and ZO-1 are fully colocalized, confirming that in this polarized system, the HCV tight junctional entry factors reside exclusively in and define the tight junction. As the localization of these entry factors resembles that of *in vivo* hepatocytes, this presents a more realistic system for investigating entry, which is based upon a series of associations with proteins in specific domains.

Live cell imaging of hepatoma organoids with DiD-HCV.

In order to trace the path of the virus in live cells, we utilized a Huh-7.5 CD81-GFP expressing cell line. Organoids expressing CD81-GFP allow for visualization of cellular architecture, with clear basolateral and apical domains. During the fixation process, most of the Matrigel is removed, allowing for clear visualization of the organoid on the coverslip. Imaging away from the coverslip, as would occur in Matrigel-embedded organoids, leads to a serious loss in resolution. Consequently, for live cell imaging, additional processing steps were taken. One day prior to imaging, organoids were extracted from Matrigel and replated onto collagen-treated imaging dishes. Overnight incubation (~8 hours) is sufficient for the organoids to adhere to the dishes without losing their polarization. The samples were then infected with DiD-HCV and incubated on ice for one hour to allow for binding, then imaged every 15-30 seconds to capture DiD-HCV localizations within the organoid (Figure 9). DiD-HCV particles displayed heterogeneous behavior. On the basal face, some particles remained static during imaging, while others exhibited somewhat random movement. Some particles, after attachment (Figure 9A) moved to the lateral face, progressing towards the tight junction (Figure 9B). In general, movement towards the tight junction was slow and non-processive. Due to the nature of 3D imaging and the extended period seemed to be required for tight junctional migration, we were unable to capture one particle moving from the basal surface to the tight junction. However, we did observe particles moving along the lateral face (Figure 9B) and lateral-to-tight junction transitions (Figure 9C). Additionally, over time, we saw accumulation of particles at the tight junction (Figure 9D). Given these observations, it is most likely the DiD-HCV particles bind at the basal membrane, then transit to the tight junction via the lateral face.

Discussion

One of the most essential components of studying HCV entry is specific visualization of the virus. Fluorescent DiD labeling results in less nonspecific, or background staining, as compared to antibodies directed against structural proteins. Unlike insertion of fluorescent proteins, which may affect interactions with host entry factors, lipophilic dyes bind easily to virions and do not affect infectivity. Additionally, dyes in the red/far red family, such as DiD, reduce background noise due to autofluorescence.

However, like many viruses, HCV has a very poor specific infectivity of roughly 2000 (Figure 3); to follow entry using such viral stock could result in extraneous associations that have no relevance to the entry process. Previous work with DiD, as in DENV, used fusion as a proxy for infectious viruses and only studied particles that progressed to this stage. Our lab, however, used multiple rounds of concentration and purification to obtain highly infectious virus (Coller et al., 2009). We also performed extensive characterization – triple staining of virions (of DiD, Core, and E2 or Core and ApoE) suggests specific labeling of viral particles (Figure 4A). Electron microscopy of purified stocks used for DiD imaging are pure, without extraneous particles or exosomes (Figure 4B). Furthermore, observed particles are within the size expected for virions and are immunogold labeled. We can therefore be fairly confident our labeled preps are specific for highly infectious HCV.

HCV entry is an unusually complex process, with many distinct host cofactors that either directly or indirectly modulate it. The differential subcellular localizations of these cofactors highlight the importance of cell polarity in studying HCV entry – as HCV requires two tight junction proteins, it is essential to study them in a relevant, polarized cell culture model. A Matrigel-based system of polarization is able to overcome the difficulties posed by alternative

polarization methods, such as bioreactors (Sainz et al., 2009) and HepG2 cell lines (Mee et al., 2008). Unlike cells generated by bioreactors, Matrigel-embedded cells display markers both markers of polarization and functional bile secretion (Figure 6). Additionally, they maintain similar kinetics and levels of virus production as in 2D unpolarized cells (Figure 7), making them feasible for study.

We find the hepatoma organoids to have many advantages over 2D Huh-7.5 cells in imaging HCV entry: (i) The entry cofactors have an appropriately restricted localization at their respective membrane compartments (Figure 8). HCV first encounters the ECM-associated basolateral membrane; virions *in vivo* most likely access hepatocytes' basolateral surfaces in the context of stellate cell-secreted ECM. (ii) The organoids establish *bona fide* tight junctions, as defined by the secretion and retention of bile analogs at the apical bile canaliculus (Figure 6). This restricts the virions' access to tight junctional entry cofactors CLDN1 and OCLN in the absence of virally induced signaling, replicating conditions *in vivo*. In the 2D system, our lab found entry away from areas of cell-cell contact, potentially due to the lack of spatially distinct domains (Coller et al., 2009). However, it remained a distinct possibility that such an entry pathway was due to a lack of polarization and did not represent a relevant route. Without accurate localization of these tight junction proteins, it is impossible to establish which, if any, model of entry holds true (Figure 1). Although the previous work in 2D did find colocalization with CLDN1, this could occur *in vivo* through relocalization to the tight junction or via disruption of tight junctional complexes, accessing tight junction proteins on the basolateral. Furthermore, either of these scenarios would require signaling in a polarized system. However, such a constraint may not be necessary in 2D, as CLDN1 and OCLN are readily available on the plasma membrane. (iii) The highly distinct localization patterns of the early basolateral receptors versus the tight junction entry factors enables

a simplified interpretation of virus-receptor colocalization, as compared to unpolarized cells, in which the receptors diffuse randomly and likely form inappropriate complexes. As mentioned before, a lack of polarization may obscure signaling events that have distinct spatial and temporal requirements. As the virus can associate with all entry factors at the membrane, there is potentially less need for diffusion across the plasma membrane. Additionally, without discrete steps – virion-based signaling leading to association with host factors and (re)localization to distinct domains – it is much more difficult to tease apart the contributions of individual entry factors. Thus, the spatially segregated cellular factors in the polarized system are not only essential but useful in determining the mechanism of HCV entry. (iv) Finally, we anticipate that properly polarized hepatoma cell models might reveal important differences at other stages of the viral life cycle. For instance, the Huh-7.5 organoids also have a polarized secretory pathway that likely impacts viral egress (data not shown).

Although we were unable to follow a single particle moving from the basolateral to the tight junction via live cell imaging of DiD-HCV, we did capture portions of this path: movement along the basal face, lateral face, and from the lateral face to the tight junction (Figure 9). Additionally, we saw accumulation of DiD-HCV particles at the tight junction over time (Figure 9D). This would suggest that DiD-HCV particles bind on the basal face, proceeding through the lateral face to the tight junction. This is the first study of HCV entry into fully polarized cells. The findings support the tight junctional migration model put forth by Evans et al., suggesting extrajunctional entry seen in two-dimensional cells was likely due to lack of polarization. This has the potential to change the model for HCV entry – if polarization can affect the path of the virus, then it may alter the cellular requirements as well. Kinetics, signaling, and potentially use of cellular factors might change as a result of the “new” requirements for HCV entry – as the

virus now seems to be forced to traffic to the tight junction. It remains to be seen whether HCV accesses CLDN1 and/or OCLN, and whether this association only occurs at the tight junction.

CHAPTER III

TRACING THE ROLE OF HOST FACTORS IN HCV ENTRY

Abstract

Hepatitis C virus (HCV) enters hepatocytes using a complex assortment of entry factors, including scavenger receptor BI (SR-B1), cluster of differentiation 81 (CD81), epidermal growth factor receptor (EGFR), claudin 1 (CLDN1) and occludin (OCLN). Given that CLDN1 and OCLN are not readily accessible to an infecting virion due to their tight junctional localization, HCV likely accesses them by either disrupting cellular polarity or migrating to the tight junction. In this study, we track HCV entry into a three-dimensional polarized hepatoma system that closely resembles the complex polarity of hepatocytes in vivo. We observe that HCV initially localizes with the early entry factors SR-B1, CD81, and EGFR at the basolateral membrane and then migrates to the tight junction in an actin-dependent manner. HCV associates with CLDN1 and then OCLN at the tight junction and is internalized by an active process that requires EGFR signaling. We also demonstrate CD81 and SRBI's role as early entry factors, as they are required for transit to the tight junction; OCLN, meanwhile, as a late entry factor, is required for internalization of the virus.

Introduction

HCV entry into hepatocytes is a highly intricate, multistep process involving numerous cellular factors. Initial attachment is proposed to occur via interactions of virion-associated ApoE with cell-associated glycosaminoglycans (Jiang et al., 2012), LDL receptor (Owen et al., 2009)

and syndecan1 (Shi et al., 2013). HCV E2 then interacts with two entry factors that are generally accepted to function as receptors: SR-B1 and the tetraspanin CD81; disrupting the interaction of E2 with SR-B1 or CD81 via siRNAs or blocking antibodies inhibits HCV entry (Bartosch et al., 2003b; Pileri et al., 1998; Scarselli et al., 2002; Zhang et al., 2004). SR-BI is thought to function both as an attachment factor (Maillard et al., 2006) and a receptor (Scarselli et al., 2002). Following nonspecific attachment of the virus to SR-BI, E2 is exposed and is then thought to directly associate with SR-BI in its capacity as a receptor (Catanese et al., 2010; Dao Thi et al., 2012; Scarselli et al., 2002; Zeisel et al., 2007). The E2-SR-BI interaction induces another conformational change, allowing E2 to bind CD81 (Bankwitz et al., 2010). Additionally, HCV entry into hepatocytes requires the tight junction proteins CLDN1 and OCLN (Evans et al., 2007; Liu et al., 2009; Ploss et al., 2009; Zheng et al., 2007). CD81 may mediate the HCV receptor complex interaction with CLDN1 (Davis et al., 2012; Harris et al., 2008; Krieger et al., 2010), which seems to be critical for successful entry (Harris et al., 2010; Krieger et al., 2010).

Beyond the core set of entry factors, EGFR is the most fully validated potential entry factor to date. EGFR expression, but more specifically its activation, are required for HCV entry (Lupberger et al., 2011). EGFR has been demonstrated to interact with CD81 (Diao et al., 2012; Zona et al., 2013). Furthermore, binding of HCV to CD81 or antibody-mediated crosslinking of CD81 can activate EGFR (Diao et al., 2012). A follow-up study also found that EGFR-mediated downstream signaling via the MAPK pathway played a role in HCV entry (Zona et al., 2013). Based on work in unpolarized cells in the absence of infection, several EGFR inhibitors limited CD81 lateral diffusion and CD81-CLDN1 interaction (Zona et al., 2013). Zona et al. consequently hypothesized that EGFR signaling may be required for HCV migration to and interaction with the tight junction.

Although many receptors have been identified and some their interactions have been mapped, their role in entry remains unclear. Furthermore, HCV virions and envelope proteins have not been shown to interact directly with CLDN1 or OCLN, suggesting that the entry factors either play an indirect role in HCV entry, or alternatively, that conformational changes in the envelope proteins, likely resulting from initial receptor engagement, are required for HCV binding to CLDN1 and OCLN. In support of the latter interpretation, antibodies directed to extra-cellular domains of CLDN1 and OCLN block HCV entry (Evans et al., 2007; Fofana et al., 2013; Sourisseau et al., 2013). If, as these studies suggest, HCV associates with CLDN1 and OCLN, the virion cannot readily access these required host factors from the bloodstream. One model proposes that HCV migrates to the tight junction following engagement of the early receptors SR-BI and CD81 (Evans et al., 2007). Another alternative involves HCV association with extrajunctional forms of CLDN1 and OCLN, potentially due to disruption of tight junction barrier function (Harris et al., 2008; Mee et al., 2009). However, the models remain largely untested due to a lack of relevant cell culture systems.

Our lab's previous work investigated HCV entry, using DiD-HCV particles in unpolarized cells (Coller et al., 2009). They found DiD-labeled HCV colocalized with host entry factors CD81 and CLDN1; DiD-HCV was also found to interact with components of clathrin-mediated endocytosis, the actin cytoskeleton, ubiquitylated receptor sorting, and endosomal acidification pathways. Although particles did colocalize with the tight junction protein CLDN1, they were found to enter away from areas of cell-cell contact. Another study in partially polarized HepG2 cells also seemed to support this second model of HCV entry. They found polarization interfered with rates of HCV infection; disrupting cell polarity (and therefore causing CLDN1 to localize away from the cell-cell junctions) increased infection (Mee et al., 2009). While these results might

suggest HCV does not utilize the tight junction for entry, such a conclusion cannot be drawn in cells lacking discrete tight junctional domains.

In this study, we used single particle tracking of DiD-labeled HCV particles to follow HCV entry in Matrigel-polarized Huh-7.5 organoids. We find that DiD-HCV particles colocalize with early entry factors CD81, SR-B1, and EGFR at the basolateral membrane and that over time, these fluorescent HCV particles accumulate at the tight junction, localizing with CLDN1 and OCLN in an actin-dependent manner. We also investigated the temporal requirements for each of these factors. CD81 and SR-B1, hypothesized early factors, are required for relocalization to the tight junction; the late factor OCLN is required for internalization. EGFR signaling was not required for DID-HCV accumulation at the tight junction, as has been previously suggested, but was instead essential for particle internalization at the tight junction.

Materials and Methods

Cell culture

To induce polarization, Huh-7.5 cells were embedded in Matrigel (Growth Factor Reduced, Phenol Red-free; BD Biosciences). Matrigel was first thawed on ice. Huh-7.5 cells were then trypsinized and diluted in DMEM + 10% FBS to a final concentration of 1 x10^5 cells/mL. Equal volumes of Matrigel and diluted cells were mixed and seeded into plates. The Matrigel solution was allowed to polymerize for 30 minutes at 37°C before adding DMEM + 10% FBS to cover. Cells were cultured for 6-8 days, changing media every other day.

Huh-7.5 cells CRISPR'D for entry factors (Huh-7.5_CD81'CR, Huh-7.5_SRBI'CR, Huh-7.5_OCLN'CR, Huh-7.5_CLDN'CR) were a generous gift from Matthew Evans (Icahn School of Medicine, Mount Sinai).

Pseudoparticle Transduction

A construct containing shEGFR, pLKO.1-puro shEGFR, was obtained from Sigma (SCHLDN MISSION shRNA DNA clone Oligo TRCN0000010329). pBABE-EGFR (Addgene plasmid # 11011) was a gift from Matthew Meyerson (Greulich et al., 2005).

pLPCX-SR-BI was digested with HindIII and ClaI. pLPCX-SR-BI was used as a template for two separate, overlapping PCR reactions: 1) HindIII forward primer (5'- CTC CGC GGC CCC AAG CTT ATG) and mutation reverse primer; (2) mutation forward primer and SalI reverse primer (5'- TAA AAT CTT TTA TTT TAT CGA TCT ACA GTT TTG CTT CCT GCA GC). Primers to create the mutations on the SR-BI background are as follows: K469R reverse (5' – TAC TAC TAC TCC AAA ATA AAT AGC ATC TCT CTT G), K469R Forward (5' – CAA ATC CGG AGC CAA GAG AGA TGC TAT TTA TTT TGG AG),
Y471F reverse (5' – CCA AAA TAA AAA GCA TTT CTC TTG GCT CCG GAT), Y471F Forward (5' – GGA GCC AAG AGA AAT GCT RTT TAT TTT GGA GTA GTA GT), Y490F reverse (5' – GGG ATT CAG AAA AGG CCT GAA TGG CCT C), Y490F Forward (5' – TTC AGG CCT TTT CTG AAT CCC TGA TGA CAT). Amplified fragments were inserted into the pLPCX vector via the In-Fusion cloning kit. Wild type and mutant SR-BI constructs were then amplified with pLVX overhangs, forward primer (5'-GGA TCT ATT TCC GGT GAA TTC ATG GGC TGC TCC GCC AAA G) and reverse primer (5'- ATC CGC GGC CGC TCT AGA

CTA CAG TTT TGC TTC CTG CAG CAC AG), then amplified fragments were inserted into the digested pLVX vector with the In-Fusion cloning kit.

To produce retroviral stocks, ~70% confluent p100 plates of 293T cells were transfected with 8 µg MMLV gag-pol, 4 µg vesicular stomatitis virus glycoprotein G, and 12 µg construct. Plasmids were transfected using Lipofectamine 2000 (Life Technologies), as per manufacturer's guidelines. Supernatants were harvested 48 hours post-transfection, filtered through a 0.22 µM filter, then used to transduce cells. Huh-7.5 cells were incubated with pseudoparticles and 8 µg/mL polybrene for 5 hours. Cells transduced with shEGFR were puromycin selected, then expanded from single cell clones. For the complemented cell line, shEGFR stable cells were transduced with EGFR pseudoparticles and polybrene, then selected with puromycin. Cells were probed for EGFR expression via Western Blot to check for successful complementation. For live cell imaging, cells were transduced with CD81-GFP lentivirus (Coller et al., 2009).

Highly infectious virus preparation

Stocks of HCV genotype 2a RNA (infectious clone pJFHxJ6-CNS2C3) were generated as previously described (Berger et al., 2009; Coller et al., 2009; Coller et al., 2012; Mateu et al., 2008). Briefly, viral supernatants were collected for up to 5 passages after electroporation, then filtered through a 0.22 micron nitrocellulose filter and stored at 4°C protected from light. Viral titer was determined via limiting dilution and subsequent immunohistochemical staining with a monoclonal NS5A antibody (9E10, generous gift of Charles Rice, Rockefeller University) as described (Randall et al., 2006).

Viral stocks were concentrated via PEG (polyethylene glycol 8000; Fisher) precipitation (Blight et al., 2002; Coller et al., 2009). Viral supernatant was mixed with PEG (final concentration

8%) and incubated overnight at 4°C. Following centrifugation (20 minutes, 8000xg), pellet was resuspended in 15 mLs of the original supernatant; resuspended sample was spun down again (15 minutes, 8000xg) and pellet was resuspended in supernatant for a final concentration of 1/100 of the starting volume. 5 µL of DiD (Invitrogen), was added to 1 mL concentrated virus and incubated for 90 minutes with shaking, protected from light. Labeled virus was layered onto a 10–60% weight/volume iodixanol gradient (OptiPrep, Sigma) in sterile water and centrifuged for 16.5 hours (34,000 RPMs at 4°C). The gradient was separated into 1 mL fractions; each fraction was subsequently analyzed for HCV RNA levels (following Trizol-LS extraction; Invitrogen) and infectious viral titer (Randall et al., 2006). Fractions with the best specific infectivity were added to Amicon Ultra 100k filters (Millipore) and spun for 20 minutes at 14000xg. Filters were then inverted in a new tube and spun for 2 minutes at 2000xg. The resulting supernatants were pooled for use in imaging studies.

Cell Recovery from Matrigel

Matrigel-polarized cells were harvested with Matrigel cell recovery media (BD Biosciences). Briefly, cells were shaken for 1 hour with 500 µL cell recovery media, then centrifuged at 300g for 5 minutes. Supernatant was removed, and the pellet was washed twice in PBS.

HCV RNA quantitation

Following cell recovery, RNA was extracted using RNeasy 96 kit (Qiagen); samples were eluted with 150 µL water. Cellular and HCV RNAs were reverse-transcribed and PCR amplified using the SuperScript^{TM} III Platinum One-Step qRT-PCR System with Platinum Taq (Invitrogen)

as previously described (Randall et al., 2007). HCV RNA was amplified using 300 nM forward primer (5' - CCG GGA GAG CCA TAG TGG TCT) and 300 nM reverse primer (5' - CCA AAT CTC CAG GCA TTG AGC) and 200 nM probe (5' - 6FAM-CAC CGG AAT TGC CAG GAC GAC CGG-MGBNFQ). Parallel reactions utilized 18S ribosomal RNA as an internal loading control, detected via rRNA TaqMan gene expression assay (Hs99999901_s1, Applied Biosystems). Reverse transcription-PCR (RT-PCR) amplification reaction parameters using an ABI 7300 system (Applied Biosystems) was as follows: 50°C for 30 min, 95 °C for 6 min, and then 50 cycles of <95 °C for 15 sec, 60 °C for 1 min>. HCV and 18S RNA copy numbers were determined via comparisons to concentration standards. Data was analyzed with SDS v1.4 software (Applied Biosystems). Absolute HCV RNA was normalized to the sample's 18S RNA, then to the (normalized) 6-hour vehicle control for relative HCV RNA levels.

Inhibitors

CD-81 blocking antibody (JS-81, BD Pharmingen) and its mouse IgG1 isotype control (Novus Biologicals) were used at 10 µg/mL. Inhibitor concentrations were as follows: 10 µM Cytochalasin D (Sigma) and 15 µM Erlotinib (Santa Cruz). Chemical inhibitors used in HCV replication analysis were incubated with Matrigel-embedded cells 5 days post-plating for two hours prior to addition of HCVcc (MOI=3).

Infectious time course and fixed cell immunofluorescence microscopy

Unpolarized cells (wild type Huh-7.5, Huh 7.5_shEGFR, and Huh-7.5_shEGFR+pEGFR) were seeded onto coverslips in 24-well plates. One day after seeding, cells were washed twice in PBS, then fixed for 20 minutes with 3.6% paraformaldehyde. Samples were washed three times in

PBS, incubated with blocking solution (20% goat serum, .05% saponin in PBS) for 1 hour, then incubated with anti-EGFR (1:400, Santa Cruz) in blocking solution for 1 hour. Coverslips were washed twice in PBS, then incubated with Alexa Fluor conjugated secondary antibody (488), diluted 1:1000 in blocking solution, for 1 hour. Samples were washed twice in PBS and mounted with ProLong Gold AntiFade with DAPI nuclear stain (Invitrogen).

Matrigel-cell mixtures were prepared as described above, and 75 µL of the solution was placed onto coverslips in 24-well plates. Matrigel-embedded samples were preincubated on ice for 20 minutes. If infected, DiD-labeled HCV, mixed 1:1 with supplemented DMEM + 10% FBS, was added to cells and incubated, covered, on ice for an additional hour. Cells were then transferred to 37°C (time of temperature shift: t=0) and fixed at various points after the shift in 3.6% paraformaldehyde (PFA) for 20 minutes at room temperature. Cells were permeabilized with room temperature 0.5% Triton x-100 in PBS for 10 minutes, and then rinsed with 0.1 M Glycine in PBS 3 times for 10 minutes each. Cells were incubated for 2 hours in blocking solution (0.1% BSA, 0.2% Triton x-100, 0.005% Tween-20, and 20% goat serum in PBS). Coverslips were incubated overnight at 4°C with primary antibodies diluted in blocking solution. (1:500 anti-ZO-1, Invitrogen; 1:300 anti-CD81, Santa Cruz; 1:300 anti-SR-B1, Novus; 1:400 anti-EGFR, Santa Cruz; 1:400 anti-OCLN, Invitrogen; 1:100 anti-CLDN1, Santa Cruz; 1:350 anti-Core, Virostat) Following overnight incubation, the Matrigel was allowed to reform for 10 minutes at room temperature without shaking. Coverslips were washed 3 times, 20 minutes each, with wash buffer (0.1% BSA, 0.2% Triton x-100, and 0.005% Tween-20 in PBS). Alexa Fluor conjugated secondary antibody (488 or 594) was diluted 1:1000 in blocking solution and incubated with the Matrigel-embedded cells for 1 hour at room temperature, then rinsed 3 times with wash buffer (as above). Actin staining utilized the same protocol (PFA fixation, permeabilization, glycine wash, and

block), followed by incubation for 1 hour at room temperature with Alexa Fluor 488 Phalloidin (1:40, Invitrogen), then washed 3 times in wash buffer. CMFDA labeling (Invitrogen) occurred prior to fixation: CMFDA was incubated with the cells (1:1000) for 1 hour, then washed and incubated for an additional hour with DMEM +10% FBS. Cells were then fixed and stained as above. For all samples, coverslips were mounted with ProLong Gold AntiFade with DAPI nuclear stain (Invitrogen) following the final rinse.

Confocal Microscopy Analysis

Fixed cell imaging was performed on an Olympus DSU Spinning Disc Confocal with a 100X NA 1.45 oil-immersion objective. Using Slidebook imaging software, images were captured with a Hamamatsu back thinned EM-CCD camera set to an intensification of 255. DiD-labeled HCV and Alexafluor 594 were visualized with the DsRed filter set; Alexafluor 488 was visualized with the EGFP filter set. Z-stacks of the organoids were acquired using slices taken every 0.3 µm. Following acquisition, images were processed with ImageJ (NIH). Z-stacks were normalized on Slidebook, then imported using BioFormats (LOCI). DiD puncta were assayed for their localization within the organoid and/or colocalization with selected antibodies; ‘n’ values reflect the total number of DiD puncta quantified per treatment. Images were quantified for colocalization using RGB profiler (Christophe Laummonerie) and colocalization highlighter. Images presented in the figures were duplicated out of the Z-stack, separated into individual channels, adjusted for contrast and smoothed, then reassembled.

Cell Viability Assay

Cell viability was determined using CellTiter-Glo Luminescent Cell Viability Assay (Promega). Results were normalized to vehicle control in chemical inhibitor studies.

Western Blot Analysis

Unpolarized cells were serum starved for 4 hours, then treated (if indicated) with 200 nM EGF (Life Technologies) for 30 minutes before lysis. Cells were lysed in 100 µL 5% NP40 buffer (150 mM NaCl, 20 mM Tris-HCL [pH 7.5], 10% glycerol, 2 mM EDTA) supplemented with 1 mM protease inhibitors (cOmplete Mini, Roche) and 1 mM sodium orthovanadate (Fisher). Proteins were separated on a 4 to 20% SDS-PAGE gel (BioRad) and transferred to PVDF. Membrane was incubated in blocking solution (10% BSA and 0.1% Tween-20 in 1xPBS), followed by overnight incubation at 4°C with primary antibodies (1:1000 anti-actin, Sigma; 1:500 anti-EGFR, Cell Signaling; 1:800 anti-phospho-EGFR 1045, Cell Signaling) diluted in 5% BSA (0.1%Tween-20, 1xPBS). Blots were then incubated for 1 hour with horseradish peroxidase-conjugated secondary antibodies (goat anti-rabbit and rabbit anti-mouse, Thermo Scientific), followed by detection using SuperSignal West Femto Maximum Sensitivity substrate (Thermo Scientific) and exposure to film.

Statistical Analysis

Data shown as mean ± standard deviation. Statistical significance was determined using two-tailed Student's *t* test.

Results

Single particle tracking of HCV entry into polarized hepatoma organoid cultures

To determine whether HCV migrates to the tight junction in polarized cell systems, we visualized DiD-HCV co-localization with ZO-1 over a time course of infection. Huh-7.5 organoids were incubated with DiD-HCV at 4ºC for one hour. This allowed for partial depolymerization of the ECM gel, aiding movement of DiD-HCV through the ECM substrate while preventing any HCV fusion events. Cells were then transferred to 37ºC, fixed at various time points, and immuno-probed for ZO-1 (Figure 10A). At the temperature shift (t=0), DiD-HCV localized to the external (basolateral) membrane, tight junction, and at intermediate points between. As the time course of infection progressed, DiD-HCV showed increasing accumulation at the tight junction, with ~93% tight junctional localization at 90 minutes post temperature shift (Figure 10B). This suggests that DiD-HCV traffics to the tight junction in hepatoma organoids.

HCV infection can be inhibited through blocking antibodies to CD81 with earlier kinetics than with blocking antibodies specific to CLDN1 or OCLN, indicating that HCV-CD81 interaction occurs prior to a requirement for CLDN1 or OCLN (Evans et al., 2007; Sourisseau et al., 2013). If HCV-CD81 engagement were required for migration of HCV to the tight junction, then CD81 blocking antibodies should prevent the tight junctional accumulation of DiD-HCV. We tested this prediction by incubating the hepatoma organoids with the CD81 blocking antibody prior to infection with DID-HCV in a parallel entry time course. The CD81 blocking antibody prevented accumulation of DiD-HCV at the tight junction, with most particles localized basolaterally (Figure 10A, bottom panel). At all time points, there was a significant decrease in DiD-HCV/ZO-1 co-localization (Figure 10B), indicating that association of HCV with CD81 is critical for tight

junctional migration of HCV. In addition, RT-PCR analysis of HCV RNA levels in cells incubated with CD-81 blocking antibody showed a significant decrease in HCV RNA levels as compared to cells incubated with control IgG (Figure 10C). Altogether, the results demonstrate that, unlike previous work in unpolarized systems, DiD-HCV relocalizes to the tight junction in polarized hepatoma organoids. The tight junctional trafficking of DiD-HCV and subsequent infection is dependent on the HCV-CD81 interaction.

Localization of DiD-HCV with its entry factors

We next determined the membrane localization of DiD-HCV with its entry factors. We hypothesized that early entry factors, such as CD81 and SR-B1, should initially colocalize with HCV at the basolateral membrane, as it is the first (and only) accessible cellular surface to extra-cellular virus. Additionally, CD81 should maintain DiD-HCV co-localization throughout the entry process, as we previously observed CD81 co-trafficking and internalization with DiD-HCV in 2D Huh-7.5 cells (Coller et al., 2009). We repeated the DiD-HCV time course of infection, probing with indicated entry factor antibodies. Samples were then visualized via confocal microscopy and quantified for DiD-HCV-entry factor colocalization at the different domains (‘basolateral’ for exterior colocalization and ‘internal’ for association at the inner domain of the organoid, likely to be tight junctional). We observed high colocalization of DiD-HCV with CD81, SR-B1, and EGFR at both the external basolateral membrane and interior domains in the vicinity of tight junctions. (Figure 11A). Quantitation of co-localization indicated that 73-98% of DiD-HCV was localized with the individual entry factors at the basolateral and internal membranes (Figure 11C). This suggests an HCV-receptor complex containing SR-B1, CD81 and EGFR forms at the basolateral membrane and then migrates to the tight junction.

We previously observed co-localization of DiD-HCV with CLDN1 outside of intra-cellular membranes in 2D Huh-7.5 cells (Coller et al., 2009), raising the possibility that either HCV-CLDN1 interactions occur outside of the tight junction; or alternatively, that the 2D Huh-7.5 cells were not forming tight junctions (as we observed in Figure 6). In probing the co-localization of DiD-HCV with CLDN1 and OCLN during infection of the hepatoma organoids, we did not detect any co-localization of DiD-HCV with CLDN1 or OCLN at the basolateral membrane (Figure 11C). However, we observed extensive co-localization of DiD-HCV with CLDN1 and OCLN in the internal, tight junction membrane (Figure 12B and 12C). Co-staining of DiD-HCV with CMFDA during the entry time course showed that CMFDA was retained at the bile canaliculus during HCV infection, indicating that tight junctional integrity is maintained during HCV infection (Figure 12). These data demonstrate that the HCV association with CLDN1 and OCLN is restricted to the tight junction of polarized hepatocytes. It also suggests that CLDN1 and OCLN are indeed part of the receptor complex promoting HCV internalization.

DiD-HCV accumulation at the tight junction is dependent on actin.

We previously defined a series of roles for actin in HCV entry into 2D Huh-7.5 cells (Coller et al., 2009). DiD-HCV traveled from filopodial projections to the plasma membrane via retrograde actin flow, followed by actin nucleation and virion internalization in association with actin stress fibers. However, most DiD-HCV particles at the plasma membrane of 2D Huh-7.5 only colocalized transiently with actin and displayed primarily random movements that are characteristic of diffusion. This suggested that events driving active lateral movement of HCV at the plasma membrane failed to occur in unpolarized Huh-7.5 cells. In order to investigate the role of actin in polarized cell entry, we repeated the time course of HCV infection in hepatoma

organoids and stained for F-actin. DiD-HCV localized with actin basolaterally, often in association with actin-rich clusters (Figure 13A, left panel, indicated by arrow). DiD-HCV also colocalized with actin filaments parallel to the basolateral membrane, which likely represent virions in transit to the tight junction (Figure 13A, B). DiD-HCV displayed full colocalization with actin at the tight junction, a site of actin enrichment. We observed no global reorganization of the actin cytoskeleton during infection.

To determine whether actin was required for DiD-HCV movement in hepatoma organoids, we pretreated cells with 10μM cytochalasin D (CytoD), an inhibitor of actin polymerization, or DMSO control. After incubation on ice, cells were fixed at 90 minutes after the temperature shift and stained for F-actin (Figure 14A). Quantification of DiD-HCV localization showed that 88% of particles in DMSO treated cells accumulated at the internal membranes, consistent with tight junction localization. In CytoD treated cells, there was a significant reduction of internally localized DiD-HCV (36% of total), with the majority of DiD-HCV remaining at the basolateral membrane (Figure 14B). The results indicate that DiD-HCV localizes extensively with actin at all membranes and that the trafficking of DiD-HCV to the tight junction requires an intact actin cytoskeleton.

Requirements for individual entry factors in the HCV entry process

As we have established the kinetics of colocalization with the various entry factors, we next explored at which stage these factors are required for entry. We obtained cells knocked out for the various entry factors via CRISPR. These cells were seeded into Matrigel, infected with DiD-HCV over a time course of infection, then assayed for tight junctional relocalization and internalization via the ZO-1 colocalization assay.

DiD-HCV infected Huh-7.5_CD81'CR organoids (wild type cells lacking CD81) show a significant defect in tight junction localization at 90 mps (Figure 15), which is consistent with its proposed role as an early entry factor. Huh-7.5_SRBI'CR cells also display a defect in tight junction localization at 90 mps, although it is not as severe as with CD81'CR cells (Figure 16).

Unlike CD81, SRBI has an extended cytoplasmic domain with multiple residues responsible for signaling and recruiting adaptors (Rhainds and Brissette, 2004); phosphorylation or ubiquitination of these residues could be critical for HCV entry. To determine which, if any, residues are required for HCV entry, we mutated a panel of C-terminal SRBI residues. These mutants were then used to complement the Huh-7.5_SRBI'CR cell line. Analysis of HCV infection via RT-PCR shows a defect in RNA levels in the SRBI'CR cells that is restored by complementation with wild type SRBI (Figure 17). However, two tyrosine residues, 471 and 490, show decreased RNA levels, suggesting they may play a role in entry.

Finally, we tested the requirement of one of the tight junction proteins, OCLN, in the DID-HCV infectious time course assay. Colocalization analysis showed comparable levels of DiD-HCV at the tight junction as in wild type organoids at both 0 and 90 mps (Figure 18). However, OCLN'CR organoids maintain significantly higher colocalization of ZO-1 at 360 mps, indicating an internalization defect in cells lacking OCLN.

EGFR signaling is required for DiD-HCV internalization but not migration to the tight junction.

Although EGFR signaling is required for HCV entry, its role is less defined. In unpolarized 2D Huh-7.5 cells, it was proposed to be required either for membrane diffusion of CD81 and subsequent CLDN1 association (Zona et al., 2013) or alternatively, for HCV internalization (Diao

et al., 2012). We confirmed that the EGFR inhibitor erlotinib, used in the Lupberger et al. paper, also inhibited HCV replication in hepatoma organoids. Cells were seeded into Matrigel, infected for 36 hours, then assayed for RNA replication and cell viability. Erlotinib treatment impaired RNA replication (Figure 19A) without impacting cell viability (Figure 19B).

We first examined the requirement of EGFR signaling for DiD-HCV accumulation at the tight junction in association with CLDN. We performed an extended time course of HCV infection in the presence of erlotinib or DMSO control. In DMSO-treated cells, DiD-HCV co-localization with CLDN1 peaked 90 minutes after temperature shift, then decreased at 360 minutes, likely due to internalization and uncoating of DiD-HCV (Figure 20 A, B). Erlotinib-treated cells showed similar DiD-HCV colocalization with CLDN1 at 90 minutes post shift, indicating that EGFR signaling is not required for DiD-HCV trafficking to the tight junction and association with CLDN1 in hepatoma organoids. However, we did observe an obvious difference at 360 minutes post shift: DID-HCV remained co-localized with CLDN1 in the presence of erlotinib (Figure 20 A, B). This indicates that erlotinib inhibits the internalization and uncoating of DiD-HCV and that DID-HCV remains associated with CLDN1 at the tight junction.

We further tested this possibility by analyzing the effects of erlotinib in our previously published DiD-HCV uncoating assay (Coller et al., 2009). Intact virions are visualized as a co-localization of DiD with core, while DiD in the absence of core signifies an uncoated particle, in which the lipophilic dye has intercalated the endosomal membrane where fusion has occurred. We examined the effects of erlotinib on HCV uncoating over a time course of infection. At early time points (0 and 90 minutes post temperature shift), virtually all DiD-HCV co-localized with core, indicating that they are intact virions (Figure 21A, B). At 360 minutes post shift, only 16% of DiD-HCV and core co-localized in DMSO treated cells, indicating the majority of DiD-HCV had

undergone uncoating. In contrast, we observed high levels of DiD-HCV and core co-localization in erlotinib-treated cells throughout the time course, indicating virions did not uncoat. Thus, EGFR signaling is required for DiD-HCV internalization at the tight junction.

To validate a role for EGFR in HCV internalization, we created a Huh-7.5 cell line expressing EGFR shRNA (shEGFR) and a cell line that was virally transduced to complement this defect via an shRNA-resistant EGFR (shRNA +pEGFR). Both cell lines were validated for EGFR expression and signaling via Western Blot and immunofluorescence (Figure 22). The shEGFR cell line was defective in HCV entry, in that HCV RNA and infectious virus production was decreased following HCV infection; however, when entry was bypassed via electroporation of HCV RNA, infectious virus production was unaffected. The restoration of EGFR expression via shRNA resistant EGFR rescued the entry defect (Figure 23). We next infected Huh-7.5, shEGFR, or shEGFR+pEGFR organoids with DiD-HCV and analyzed the colocalization of DiD-HCV with the tight junction marker ZO-1 over a time course of infection. Similar to erlotinib treatment of Huh-7.5 cells, we observed that DiD localized to the tight junction of shEGFR cells but failed to internalize (Figure 24). However, such an internalization defect was restored in the complemented cell line.

Discussion

Single particle tracking of HCV infection of the polarized hepatoma organoids presented the first opportunity to directly test models of HCV entry (Figure 1). Evans et al. identified CLDN1 as a late HCV entry factor and proposed that HCV may migrate to the tight junction following interactions with SR-B1 and CD81 (Evans et al., 2007). This model is conceptually similar to the entry pathway of Coxsackie virus B3 (Coyne and Bergelson, 2006). Alternatively, HCV could

disrupt the tight junction to gain access to CLDN1 or OCLN. Other viruses are known to disrupt tight junctions, including another member of the Flaviviridae, West Nile virus (Medigeshi et al., 2009; Xu et al., 2012). Since a physical interaction of HCV virions or structural proteins with CLDN1 and OCLN has not been demonstrated, it was also possible that HCV has an indirect requirement for CLDN1 and OCLN in HCV entry. We find that indeed, HCV virions traffic to the tight junction in a manner that requires a CD81 interaction (Figure 10). There is no gross perturbation of tight junctional integrity, as visualized by CMFDA retention (Figure 12). Initially, HCV colocalizes with its early receptors SR-B1 and CD81; we have also observed early, basolateral colocalization with EGFR as well (Figure 11). Although physical interactions between CD81 and EGFR have been reported (Zona et al., 2013), this is the first demonstration that EGFR is also localized with the HCV-receptor complex. Given the sensitivity limits of conventional fluorescent microscopy, it is likely the receptor multimers are likely present, either due to multiple virion-receptor contacts or as part of a "tetraspanin web" directed by CD81. This HCV-receptor complex (CD81, SRBI and EGFR) is detected at the basolateral membrane and at internal localizations consistent with the tight junction, indicating lateral movement of HCV-receptors to the tight junction (Figure 11).

Our previous single particle tracking studies of DiD-HCV movements at the plasma membrane of 2D unpolarized Huh-7.5 cells found that the majority of the virions randomly diffuse at the plasma membrane, indicating the absence of signaling processes to direct virion migration (Coller et al., 2009). In the polarized organoids, virions actively travel ~25 μm in the organoids from the basolateral membrane to the tight junction in association with actin, indicating an active signaling process to drive HCV-receptor lateral migration. Indeed, we found that DiD-HCV particles colocalize with actin (Figure 13) and require its polymerization for relocalization to the

tight junction (Figure 14). However, which entry factor/signaling process drives this movement to the tight junction is still unknown. The distance required to get to the tight junction and the lack of processivity seen in live cell imaging (Figure 9) may help to explain why relocalization to the tight junction is such a slow process, especially compared to 2D entry.

One of the major advantages of the 3D polarized system is the spatial separation of signaling events. Entry in 2D cells did not require much if any plasma membrane diffusion; entry factors were not segregated into domains. Matrigel-polarized cells, however, have two clear sets of signaling events: those required to get to the tight junction and those required to internalize at the tight junction. Not only does this disentangle the role of individual entry factors (early vs late), the spatial separation provides a clear readout of factors or signaling required for each stage. As seen with the CD81 blocking antibodies (Figure 10), defects can be readily assayed with DiD-HCV imaging in the Matrigel-polarized cells. Lack of tight junctional (co)localization is an indicator of factors required for movement to the tight junction; particles stuck at the tight junction is indicative of an internalization defect.

Using this idea, we explored the roles of the various entry factors. As with the CD81 blocking antibody, knockdown of CD81 resulted in a significant drop of DiD-HCV particles at the tight junction (Figure 16). This is not surprising, as it is thought to be an early entry factor as well as the central mediator of viral-host interactions. Huh-7.5 cells CRISPR'D for SRBI also showed a large decrease in tight junction-localized DiD-HCV particles, although not as severe as with CD81 (Figure 16). Recent evidence suggests SRBI may be less of a receptor and more of an attachment factor, playing a redundant role in concert with LDLR. However, as EGFR signaling is not responsible for tight junctional relocalization (Figure 20) and CD81 lacks a cytoplasmic domain, we explored SRBI signaling for a potential role in traffic to the tight junction. Mutagenesis

of its cytoplasmic residues revealed two tyrosines that show defects in RNA levels when complemented onto an SRBI'CR background (Figure 17). Potentially, activation of SRBI by HCV could lead to phosphorylation of such residues, binding of c-Cbl (a known interactor) and ubiquitination. In uninfected cells, activation of c-Cbl can lead to plasma membrane movement of the SRBI complex (Rhainds and Brissette, 2004). Among residues tested, however, other expected adaptors were not found to affect HCV RNA levels. PDZK1, an SRBI adaptor, can bind to the actin skeleton and was an ideal mediator of actin-based relocalization to the tight junction. Other groups have suggested it plays a role in HCV entry. However, we found mutating the residue that binds PDZK1 had no effect on HCV RNA levels (data not shown). As this study was done in 2D cells, it remains a formal possibility that 3D polarized cells might indeed show a defect. Finally, we found that cells lacking OCLN show an internalization defect (Figure 18). This further confirms the hypothesis that tight junction proteins (or at least OCLN) are only required at the tight junction. Preliminary evidence suggests cells lacking CLDN1 are also deficient in internalization (data not shown). The question remains why the virus needs two tight junctional proteins, as they do not play redundant roles (evidenced by the CRISPR data). One may be involved in recruiting the complex while the other provides a scaffold for recruitment of the endocytic machinery. Another option we are currently exploring is these proteins' role in activating EGFR.

Surprisingly, given prior reports, EGFR signalizing was not required for tight junction accumulation of DiD-HCV or CLDN1 colocalization. The treatment of Huh-7.5 organoids with erlotinib or knockdown of EGFR did not prevent HCV colocalization with the tight junction, although it did inhibit HCV entry (Figure 20, 24). This is in contrast to studies performed in unpolarized 2D Huh-7.5 cells that found erlotinib inhibited CD81-CLDN1 interactions, as assayed via fluorescent resonance energy transfer (FRET) (Zona et al., 2013). It is difficult to interpret

FRET experiments in unpolarized cells using over-expressed receptor-fluorescent protein fusions however, since the receptors were not properly localized nor were they studied in the context of HCV infection. It remains possible, although perhaps unlikely, that polarization may make an EGFR-dependent signaling pathway redundant for HCV-receptor migration to the tight junction and localization with CLDN1.

As mentioned, this was the first analysis of HCV entry in fully polarized cells, allowing us to (further) test the various models of HCV entry. It revealed a different entry pathway than seen in two-dimensional cells – HCV traffics to the tight junction. Additionally, our work was able to distinguish between the membrane relocalization and internalization of the particle, allowing us to pull apart the relative contributions of each of the host factors to the entry process. With this system, EGFR is found to mediate internalization, not migration to the tight junction as previously proposed. We hope these findings reinforce the importance of a polarized cell culture system when studying events that rely on proper protein localization. Furthermore, identification of EGFR as an internalization factor provides new insight into endocytosis of the virus, a poorly understood and less studied aspect of the entry process.

Based on our data, we propose a revised model for HCV entry into polarized hepatocytes (Figure 25). HCV first associates with hepatocytes via interactions of the virion-associated ApoE with attachment factors, including LDLR, heparan sulfate, and Syndecan-1 (Barth et al., 2003; Jiang et al., 2012; Owen et al., 2009). Once the virion is associated with its attachment factors, HCV E2 binds SR-BI, then CD81 (Pileri et al., 1998; Scarselli et al., 2002); the HCV-receptor complex also associates with EGFR at the basolateral membrane, likely via the CD81-EGFR interaction. This complex then migrates to the tight junction in an actin-dependent, but EGFR-independent fashion. Once at the tight junction, HCV encounters the late receptor CLDN1. The

interaction of CD81 and CLDN1 localizes the HCV-receptor complex in proximity to OCLN, which is likely associated with internalization in concert with EGFR signaling. We speculate that HCV interaction with its early receptors produces a conformation that enables a direct E2-OCLN interaction. Alternatively, HCV may not need to directly interact with EGFR or CLDN1, since CD81 is capable of binding them in the absence of HCV infection (Diao et al., 2012). At least one important question remains in regard to this model: which signaling pathways, if not EGFR, stimulate HCV-receptor migration to the tight junction?

CHAPTER IV

HCV UTILIZES EGFR SIGNALING TO INTERNALIZE VIA CLATHRIN-MEDIATED ENDOCYTOSIS

Abstract

Studying HCV entry in the morphologically relevant three-dimensional polarized hepatoma cells has revealed multiple differences with unpolarized entry. Most significantly, EGFR and its associated signaling seem to be responsible for internalization of the virus. In order to explore the molecular determinants of HCV internalization in these organoids, we utilized both biochemical and immunofluorescence approaches in which we tracked fluorescently labeled HCV with various cellular components. We find that the virus internalizes via clathrin-mediated endocytosis, traffics through early endosomes, and uncoats in a manner which requires endosomal acidification. Spatiotemporal analysis of EGFR demonstrated activated EGFR associated with HCV at the tight junction at times associated with clathrin recruitment and internalization. Mutagenesis of EGFR residues potentially involved in signaling or adaptor binding revealed a pair of tyrosines required for HCV infection. EGFR expression and signaling were required for recruitment of clathrin and components of the clathrin endocytic machinery (growth factor receptor-bound protein (Grb)2 and Casitas B-lineage lymphoma (c-Cbl) to the DiD particle. Altogether, this suggests EGFR plays a role in HCV internalization via clathrin-mediated endocytosis. EGFR activation may lead to association with key proteins involved in this endocytic process via residues on its cytoplasmic tail, resulting in internalization of the HCV-receptor complex.

Introduction

Several hypotheses have been put forward regarding HCV entry. However, to this date, entry has only been studied in poorly polarized systems. As the virus infects the highly polarized hepatocytes of the liver and requires proteins with specific localizations, entry of the virus must be examined in cell culture systems with the proper makeup. Earlier studies described in this thesis used a three-dimensional polarized organoid system to trace the initial steps in HCV entry. We found initial attachment occurred on the basolateral face, much like in polarized hepatocytes. Fluorescently (DiD)-labeled HCV was used to trace associations with known entry factors. As previously hypothesized, DiD-HCV colocalized with the "early" entry factors SR-BI and CD81 as well as EGFR. The virus then migrated to the tight junction in association with these three entry factors; once at the tight junction, DiD-HCV colocalized with the "late" factors CLDN1 and OCLN as well. These results support the tight junctional relocalization model of HCV, which had been previously untested due to lack of relevant systems.

EGFR is a transmembrane glycoprotein and a member of the erbB receptor tyrosine kinase family. Activation via EGF (epidermal growth factor) or EGF-like ligands leads to its autophosphorylation and initiations of downstream signaling cascades (Herbst, 2004). These signaling cascades are critical to the cell, often involving migration, differentiation, proliferation, and survival. Due to its key role in these processes, it is often upregulated in cancer. After its discovery as a required entry factor following a kinase screen (Lupberger et al., 2011), Zona et al. proposed downstream signaling was important for CD81 lateral diffusion and CD81-CLDN1 interaction, thus hypothesizing EGFR was required for migration to the tight junction (Zona et al., 2013). However, our work demonstrated EGFR did not affect relocalization to the tight junction; instead, EGFR signaling seems to be required for internalization of the viral particle.

While we have found internalization to occur at the tight junction, it is unclear as to the roles each of the tight junction proteins plays. CLDN1 is known to associate with CD81 (Davis et al., 2012; Harris et al., 2008; Krieger et al., 2010); this interaction may help localize the HCV-entry factor complex to the tight junction where it can access OCLN. However, it is unknown if and how these tight junction proteins facilitate internalization. Our work with CRISPR knockout lines suggests that HCV internalization in organoids lacking OCLN expression is blocked at the tight junction.

Furthermore, not much is known about the internalization process of the virus. In unpolarized cells, HCV internalizes via clathrin-mediated endocytosis (Blanchard et al., 2006; Codran et al., 2006; Coller et al., 2009; Meertens et al., 2006); our lab also showed CD81 internalizes with the viral particles (Coller et al., 2009). After internalization, HCV is thought to traffic in early endosomes (Coller et al., 2012; Meertens et al., 2006), then fuses in a pH-dependent manner (Blanchard et al., 2006; Haid et al., 2009; Hsu et al., 2003; Kobayashi et al., 2006; Koutsoudakis et al., 2006; Lavillette et al., 2006; Meertens et al., 2006; Tscherne et al., 2006).

In the current study, we traced the internalization pathway of HCV into polarized organoids. We find that, as in unpolarized cells, the viral particle internalizes via clathrin-coated vesicles into early endosomes and fuses in acidified endosomes. Activation of EGFR seems to be temporally associated with tight junctional localization and internalization of the virus. This is confirmed via immunofluorescence – DiD-HCV particles consistently colocalize with total EGFR at the basolateral and tight junction; this association is also fairly steady throughout the entry process. Colocalization with the activated (phosphorylated) form of EGFR, however, is restricted to the tight junction; the kinetics are also in line with tight junctional accumulation and internalization. Mutational analysis suggests two residues play a role in the entry process; these

residues are associated with the MAPK pathway and may serve as adaptor binding sites. Additional studies of adaptor association via immunofluorescence shows DiD-HCV colocalizes with components of the clathrin endocytic machinery (clathrin, Grb2, c-Cbl), but such association requires EGFR activation. This data leads to a model wherein HCV-receptor complex localization to the tight junction (perhaps mediated by CD81-CLDN) activates EGFR. Phosphorylation of key residues on its cytoplasmic tail lead to the binding of adaptors, subsequent recruitment of clathrin, and endocytosis of the virion.

Materials and Methods

Cell culture

Huh-7.5 cells (Blight et al., 2002) were maintained in Dulbecco's modified high glucose media (DMEM; Gibco) supplemented with 10% fetal bovine serum (FBS; Invitrogen), 0.1 mM nonessential amino acids (Gibco), and 1% penicillin-streptomycin (Gibco). Cells were grown at 37°C with 5% CO_2. To induce polarization, Huh-7.5 cells were embedded in Matrigel (Growth Factor Reduced, Phenol Red-free; BD Biosciences). Matrigel was first thawed on ice. Huh-7.5 cells were then trypsinized and diluted in DMEM + 10% FBS to a final concentration of 1 $x10^5$ cells/mL. Equal volumes of Matrigel and diluted cells were mixed and seeded into plates. The Matrigel solution was allowed to polymerize for 30 minutes at 37°C before adding DMEM + 10% FBS to cover. Cells were cultured for 6-8 days, changing media every other day.

Pseudoparticle Transduction

pBABE-EGFR was digested with BglII and SalI. pBABE-EGFR was used as a template for two separate, overlapping PCR reactions: 1) BglII forward primer (5'-

AATCCCTGCCAGCGAGATCTC) and mutation reverse primer; (2) mutation forward primer and SalI reverse primer (5'- ACACATTCCACAGGGTCGACC). Primers to create the mutations on the EGFR background are as follows: Y1045F reverse (5'- TCT GAG CTG AAT CGC TGC AAG AAG), Y1045F forward (5'- CAG CGA TTC AGC TCA GAC CCC AC), Y1068F reverse (5'- CTG GTT TAT GAA TTC AGG CAC TGG GAG), Y1068F forward (5'- TGC CTG AAT TCA TAA ACC AGT CCG TTC), Y1086F reverse (5'- ATT GTG AAA GAC AGG ATT CTG CAC AGA GC), Y1086F forward (5'- TCC TGT CTT TCA CAA TCA GCC TCT GAA C), Y1148F reverse (5'- TCC TGC TGG AAG TCA GGG TTG TCC), Y1148F forward (5'- CCC TGA CTT CCA GCA GGA CTT CTT TC), Y1173F reverse (5'- CCC TTA GGA ATT CTG CAT TTT CAG CTG TG), Y1173F forward (5'- GCA GAA TTC CTA AGG GTC GCG C). The two amplified segments were inserted into the digested pBABE vector via the In-Fusion Cloning kit. Double and triple mutants were constructed using the same procedure. Briefly, Y1086F mutant primers were used on the Y1068F mutant construct; Y1173F mutant primers were used on the Y1148F mutant construct. Once double mutants were obtained, these were amplified using the Y1045F mutant primers to create triple mutants of each double mutant. For insertion into pLVX, the vector was digested with EcoRI and XbaI. Wild type and mutant EGFR constructs were amplified with pLVX overhangs, forward primer (5'- GGA TCT ATT TCC GGT GAA TTC ATG CGA CCC TCC GGG ACG G) and reverse primer (5'- ATC CGC GGC CGC TCT AGA TCA TGC TCC AAT AAA TTC ACT GCT TTG TGG C), then amplified fragments were inserted into the digested pLVX vector with the In-Fusion cloning kit.

To produce retroviral stocks, ~70% confluent p100 plates of 293T cells were transfected with 8 µg MMLV gag-pol, 4 µg vesicular stomatitis virus glycoprotein G, and 12 µg construct. Plasmids were transfected using Lipofectamine 2000 (Life Technologies), as per manufacturer's

guidelines. Supernatants were harvested 48 hours post-transfection, filtered through a 0.22 μM filter, then used to transduce cells. Huh-7.5 cells were incubated with pseudoparticles and 8 μg/mL polybrene for 5 hours. For the complemented cell line, shEGFR stable cells were transduced with EGFR pseudoparticles and polybrene, then selected with puromycin. Cells were probed for EGFR expression via Western Blot to check for successful complementation.

Highly infectious virus preparation

Stocks of HCV genotype 2a RNA (infectious clone pJFHxJ6-CNS2C3) were generated as previously described (Berger et al., 2009; Coller et al., 2009; Coller et al., 2012; Mateu et al., 2008). Briefly, viral supernatants were collected for up to 5 passages after electroporation, then filtered through a 0.22 micron nitrocellulose filter and stored at 4°C protected from light. Viral titer was determined via limiting dilution and subsequent immunohistochemical staining with a monoclonal NS5A antibody (9E10, generous gift of Charles Rice, Rockefeller University) as described (Randall et al., 2006).

Viral stocks were concentrated via PEG (polyethylene glycol 8000; Fisher) precipitation (Blight et al., 2002; Coller et al., 2009). Viral supernatant was mixed with PEG (final concentration 8%) and incubated overnight at 4°C. Following centrifugation (20 minutes, 8000xg), pellet was resuspended in 15 mLs of the original supernatant; resuspended sample was spun down again (15 minutes, 8000xg) and pellet was resuspended in supernatant for a final concentration of 1/100 of the starting volume. 5 μL of DiD (Invitrogen), was added to 1 mL concentrated virus and incubated for 90 minutes with shaking, protected from light. Labeled virus was layered onto a 10–60% weight/volume iodixanol gradient (OptiPrep, Sigma) in sterile water and centrifuged for 16.5 hours (34,000 RPMs at 4°C). The gradient was separated into 1 mL fractions; each fraction was

subsequently analyzed for HCV RNA levels (following Trizol-LS extraction; Invitrogen) and infectious viral titer (Randall et al., 2006). Fractions with the best specific infectivity were added to Amicon Ultra 100k filters (Millipore) and spun for 20 minutes at 14000xg. Filters were then inverted in a new tube and spun for 2 minutes at 2000xg. The resulting supernatants were pooled for use in imaging studies.

Cell Recovery from Matrigel

Matrigel-polarized cells were harvested with Matrigel cell recovery media (BD Biosciences). Briefly, cells were shaken for 1 hour with 500 µL cell recovery media, then centrifuged at 300g for 5 minutes. Supernatant was removed, and the pellet was washed twice in PBS.

HCV RNA quantitation

Following cell recovery, RNA was extracted using RNeasy 96 kit (Qiagen); samples were eluted with 150 µL water. Cellular and HCV RNAs were reverse-transcribed and PCR amplified using the SuperScript^{TM} III Platinum One-Step qRT-PCR System with Platinum Taq (Invitrogen) as previously described (Randall et al., 2007). HCV RNA was amplified using 300 nM forward primer (5' - CCG GGA GAG CCA TAG TGG TCT) and 300 nM reverse primer (5' - CCA AAT CTC CAG GCA TTG AGC) and 200 nM probe (5' - 6FAM-CAC CGG AAT TGC CAG GAC GAC CGG-MGBNFQ). Parallel reactions utilized 18S ribosomal RNA as an internal loading control, detected via rRNA TaqMan gene expression assay (Hs99999901_s1, Applied Biosystems). Reverse transcription-PCR (RT-PCR) amplification reaction parameters using an ABI 7300 system (Applied Biosystems) was as follows: 50°C for 30 min, 95 °C for 6 min, and

then 50 cycles of <95 °C for 15 secs, 60 °C for 1 min>. HCV and 18S RNA copy numbers were determined via comparisons to concentration standards. Data was analyzed with SDS v1.4 software (Applied Biosystems). Absolute HCV RNA was normalized to the sample's 18S RNA, then to the (normalized) 6-hour vehicle control for relative HCV RNA levels.

Inhibitors

Inhibitor concentrations were as follows: 15 μM Erlotinib (Santa Cruz) and 20 μM Ammonium Chloride (Fisher). Chemical inhibitors used in HCV replication analysis were incubated with Matrigel-embedded cells 5 days post-plating for two hours prior to addition of HCVcc (MOI=3).

Infectious time course and fixed cell immunofluorescence microscopy

Matrigel-cell mixtures were prepared as described above, and 75 μL of the solution was placed onto coverslips in 24-well plates. Matrigel-embedded samples were preincubated on ice for 20 minutes. If infected, DiD-labeled HCV, mixed 1:1 with supplemented DMEM + 10% FBS, was added to cells and incubated, covered, on ice for an additional hour. Cells were then transferred to 37°C (time of temperature shift: t=0) and fixed at various points after the shift in 3.6% paraformaldehyde (PFA) for 20 minutes at room temperature. Cells were permeabilized with room temperature 0.5% Triton x-100 in PBS for 10 minutes, and then rinsed with 0.1 M Glycine in PBS 3 times for 10 minutes each. Cells were incubated for 2 hours in blocking solution (0.1% BSA, 0.2% Triton x-100, 0.005% Tween-20, and 20% goat serum in PBS). Coverslips were incubated overnight at 4°C with primary antibodies diluted in blocking solution. (1:500 anti-ZO-1, Invitrogen; 1:100 anti-CLDN1, Santa Cruz; 1:350 anti-Core, Virostat; 1:200 anti-Clathrin LC,

Santa Cruz; 1:900 anti-Rab5a, Abcam; 1:600 anti-EEA1, Abcam; 1:75 anti-phospho-EGFR 1045, Cell Signaling; 1:175 anti-Grb2, Santa Cruz; 1:300 anti c-Cbl, Santa Cruz) Following overnight incubation, the Matrigel was allowed to reform for 10 minutes at room temperature without shaking. Coverslips were washed 3 times, 20 minutes each, with wash buffer (0.1% BSA, 0.2% Triton x-100, and 0.005% Tween-20 in PBS). Alexa Fluor conjugated secondary antibody (488 or 594) was diluted 1:1000 in blocking solution and incubated with the Matrigel-embedded cells for 1 hour at room temperature, then rinsed 3 times with wash buffer (as above). Cells were then fixed and stained as above. For all samples, coverslips were mounted with ProLong Gold AntiFade with DAPI nuclear stain (Invitrogen) following the final rinse.

For immuno-staining of DiD-HCV particles, purified particles were added to poly-lysine treated coverslips and incubated at 37°C for 2 hours, then fixed in 3.6% paraformaldehyde for 30 minutes. Samples were washed with PBS, permeabilized in PBS with 0.2% Triton x-100 for 15 minutes, washed in PBS containing 0.1% Tween 20 (PBS/Tween), then blocked with 10% goat serum in PBS/Tween for 1 hour. Coverslips were incubated for 1 hour with primary antibody in blocking solution (1:100 anti-core, Virostat; 1:100 anti-E2 CBH5; 1:250 anti-Apo-E, Abcam). Following incubation with primary antibodies, samples were washed twice with PBS and incubated with fluorescently conjugated secondary antibodies at 1:1000 in blocking solution (488 or 350, AlexaFluor) for 1 hour. Coverslips were washed three times with PBS, then mounted with ProLong Gold AntiFade (Invitrogen).

Confocal Microscopy Analysis

Fixed cell imaging was performed on an Olympus DSU Spinning Disc Confocal with a 100X NA 1.45 oil-immersion objective. Using Slidebook imaging software, images were captured

with a Hamamatsu back thinned EM-CCD camera set to an intensification of 255. DiD-labeled HCV and Alexafluor 594 were visualized with the DsRed filter set; Alexafluor 488 was visualized with the EGFP filter set. Z-stacks of the organoids were acquired using slices taken every 0.3 μm. Following acquisition, images were processed with ImageJ (NIH). Z-stacks were normalized on Slidebook, then imported using BioFormats (LOCI). DiD puncta were assayed for their localization within the organoid and/or colocalization with selected antibodies; 'n' values reflect the total number of DiD puncta quantified per treatment. Images were quantified for colocalization using RGB profiler (Christophe Laummonerie) and colocalization highlighter. Images presented in the figures were duplicated out of the Z-stack, separated into individual channels, adjusted for contrast and smoothed, then reassembled.

Cell Viability Assay

Cell viability was determined using CellTiter-Glo Luminescent Cell Viability Assay (Promega). Results were normalized to vehicle control in chemical inhibitor studies.

Western Blot Analysis

Unpolarized cells were serum starved for 4 hours, then treated (if indicated) with 200 nM EGF (Life Technologies) for 30 minutes before lysis. For immunoblot analysis in polarized cells, Huh-7.5 cells were seeded into Matrigel (500 μL/well) and cultured for 8 days as described above. Cells were serum starved 8 hours prior to experiment. Cells were infected with PEG-concentrated HCV, then incubated on ice for one hours before transferring to 37°C incubator. One hour prior to lysis, cells were extracted from Matrigel (as described above). Following the last wash, supernatant was removed, and the pellet was lysed

All cells were lysed in 100 µL 5% NP40 buffer (150 mM NaCl, 20 mM Tris-HCL [pH 7.5], 10% glycerol, 2 mM EDTA) supplemented with 1 mM protease inhibitors (cOmplete Mini, Roche) and 1 mM sodium orthovanadate (Fisher). Proteins were separated on a 4 to 20% SDS-PAGE gel (BioRad) and transferred to PVDF. Membrane was incubated in blocking solution (10% BSA and 0.1% Tween-20 in 1xPBS), followed by overnight incubation at 4°C with primary antibodies (1:1000 anti-actin, Sigma; 1:500 anti-EGFR, Cell Signaling; 1:800 anti-phospho-EGFR 1045, Cell Signaling; 1:1000 anti-phospho-EGFR 1148, Cell Signaling; anti-1:1000 phospho-EGFR 1173, Cell Signaling) diluted in 5% BSA (0.1%Tween-20, 1xPBS). Blots were then incubated for 1 hour with horseradish peroxidase-conjugated secondary antibodies (goat anti-rabbit and rabbit anti-mouse, Thermo Scientific), followed by detection using SuperSignal West Femto Maximum Sensitivity substrate (Thermo Scientific) and exposure to film.

Statistical Analysis

Data shown as mean ± standard deviation. Statistical significance was determined using two-tailed Student's *t* test.

Results

Dissecting the HCV internalization pathway in 3D organoids

DiD-HCV enters 2D Huh-7.5 cell via clathrin-mediated endocytosis to early endosomes (Coller et al., 2009); however, it remained a formal possibility that polarization might alter this process. Huh-7.5 organoids were infected with DiD-HCV particles over a time course and probed for clathrin light chain (LC), a component of clathrin triskelions. At the temperature shift (t=0),

some DiD-HCV-clathrin-LC colocalization was evident (Figure 26A), mostly occurring basolaterally. At 90 minutes post shift, when most DiD-HCV particles are localized to the tight junction, clathrin light chain association with DID-HCV particles increased, suggesting the initiation of clathrin-mediated endocytosis. Colocalization of DiD-HCV and clathrin-LC decreased at 360 minutes, a time at which most DiD-HCV particles have uncoated (Figure 26B).

To determine whether DiD-HCV internalizes to early endosomes, we infected the Huh-7.5 organoids with DiD-HCV over a time course as before. To further confirm that EGFR signaling is required for internalization (and thus colocalization with early endosomes), cells were incubated with either DMSO or erlotinib and probed for Rab5a colocalization. We observed minimal colocalization of DiD-HCV and Rab5a at t=0, which is expected since infection at 4ºC prevents particle internalization. Rab5a-DiD-HCV co-localization peaked at 150 minutes and then decreased, likely as a result of uncoating (Figure 27 A,B), thus confirming traffic of DiD-HCV particles in early endosomes. Erlotinib prevented DiD-HCV/Rab5a colocalization at all time points, indicating that EGFR signaling is required for internalization of DiD-HCV into early endosomes.

During internalization, the HCV envelope is thought to fuse with the early endosome in a pH-dependent manner. Ammonium chloride (NH_4Cl), which inhibits endosomal acidification, has been shown to block HCV entry (Tscherne et al., 2006) and prevents DiD-HCV uncoating (Coller et al., 2009). To investigate whether HCV uncoating requires endosomal acidification in polarized cells, we repeated the DiD-HCV uncoating assay in the presence and absence of NH_4Cl. In the absence of NH_4Cl, DiD-HCV colocalized with core at 0 and 90 minutes, then displayed decreased colocalization at 360 minutes, indicating most particles have uncoated (Figure 28 A,B). However, in NH_4Cl treated cells, DiD remained colocalized with core throughout the time course, indicating

that uncoating of DiD-HCV requires endosomal acidification (Figure 28 A, B). We then validated that NH_4Cl inhibits HCV replication in hepatoma organoids without impacting cell viability (Figure 28 C, D). Thus, HCV uncoating and replication in polarized 3D Huh-7.5 cells requires endosomal acidification.

Activation of EGFR cytoplasmic residues occurs at the tight junction and is required for HCV infection.

As EGFR signaling is required for HCV internalization, we investigated whether activated, phosphorylated EGFR is associated with DiD-HCV. After extended serum starvation, organoids were infected with DiD-HCV over a time course, fixed and probed for either EGFR or phospho-EGFR (at amino acid 1045). DiD-HCV colocalized with EGFR throughout the time course, while it preferentially colocalized with phospho-EGFR at later time points of infection (90 and 120 minutes) (Figure 29A, C). While DiD-HCV colocalized with EGFR at both the external basolateral and internal membrane domains, phospho-EGFR colocalization with DiD-HCV particles was generally restricted to internal membrane domains near the tight junction (Figure 29D, E). Activated EGFR became enriched over time, forming cups underneath DiD-HCV particles (Figure 29B). Internalized particles can also be seen to localize within phospho-EGFR containing vesicles (Figure 29A). We then validated the EGFR phosphorylation kinetics by immunoblot. EGFR phosphorylation peaks at 90-150 minutes after infection (Figure 29 F), with multiple residues displaying activation. Thus, although DiD-HCV colocalizes with EGFR at the basolateral membrane, EGFR is selectively activated following HCV-receptor accumulation at the tight junction. The kinetics of EGFR phosphorylation mirror the kinetics of HCV internalization.

As several EGFR cytoplasmic residues probed via Western Blot showed activation following HCV infection, we performed mutagenesis to determine which residues are required for HCV infection. We chose residues consistent with the previously identified MAPK signaling pathway (Lupberger et al., 2011; Zona et al., 2013) as well as those that have been implicated in recruiting adaptors important for internalization. As many of these pathways could utilize several residues, we initially tested double and triple mutants. Using these constructs, we complemented the hairpin EGFR knockdown with wild type and mutant EGFR via lentiviral transduction and assayed RNA levels via RT-PCR. The hairpin knockdown showed a significant decrease in RNA levels which was rescued by the wild type EGFR construct (Figure 30A). Residue 1045, implicated in binding c-Cbl, showed no defect in RNA levels. Additionally, while the 1068/1086 double mutant (as well as the triple mutant with residue 1045) showed no defect, the 1148/1173 residue set demonstrated RNA replication levels similar to the hairpin knockdown. To determine whether one or both of the residues was required, the single mutants were also tested. Both 1148 and 1173 showed defects in RNA replication, with the double mutant displaying a more severe defect than the single mutants alone (Figure 30B).

Activated EGFR is associated with and required for internalization of the viral particle via clathrin-mediated endocytosis.

We next investigated the function of EGFR in HCV internalization. EGFR utilizes clathrin-mediated endocytosis during its internalization (McMahon and Boucrot, 2011); we therefore asked whether EGFR signaling is required for recruitment of clathrin to DiD-HCV puncta. We performed a time course of infection in the presence of erlotinib or DMSO, then probed for clathrin LC. DiD-HCV had increased colocalization with clathrin LC, which was abrogated by erlotinib treatment

(Figure 31 A, B). Similarly, shEGFR cells were defective in clathrin LC colocalization with DiD-HCV as compared to the parental Huh-7.5 cells. (Figure 31 C, D) This suggests that EGFR signaling is required for the recruitment and assembly of clathrin components during HCV clathrin-mediated endocytosis.

As EGFR signaling affects colocalization of DiD-HCV with clathrin, we examined whether it is also required for association with other components of the clathrin endocytic machinery. We seeded Huh-7.5 cells into Matrigel and pretreated with erlotinib, as before. A time course of infection was performed, fixing cells infected with DiD-HCV at 120 minutes. The two proteins studied, Grb2 and c-Cbl, are both involved in clathrin-mediated endocytosis. Both showed colocalization with DiD-HCV in the DMSO control, indicating their role in the endocytic process (Figure 32). However, inhibition of EGFR abrogated such colocalization, suggesting EGFR activation is required for such downstream colocalization events.

Discussion

Our previous work in polarized organoids demonstrated the important of using cell culture systems that closely mimic the *in vivo* architecture of the highly polarized hepatocyte. Unlike what was observed with unpolarized cell culture systems, in polarized cells, the HCV-receptor complex, including EGFR, relocalized to the tight junction. Studies from other labs using unpolarized cells suggested EGFR signaling mediated CD81-based migration to the tight junction (Zona et al., 2013). However, in our polarized system, trafficking to the tight junction was unaffected; EGFR expression and signaling were instead required for internalization of the viral particle. Based on these findings, we investigated the HCV internalization process as well as how EGFR may be required.

Following DiD-HCV in organoids, we found the virus internalized via clathrin mediated endocytosis (Figure 26) then localized to early endosomes (Figure 27). The particles then underwent fusion in a pH-dependent fashion; blocking acidification prevented uncoating and resulted in a defect in HCV RNA replication (Figure 28). This aspect of HCV entry mirrors what is seen in unpolarized cells.

EGFR signaling was initially implicated in mediating CD81 lateral diffusion and resulting CD81-CDLN1 interactions (Zona et al., 2013). In this study, EGFR is not phosphorylated with either the kinetics or localization to influence HCV-receptor migration to the tight junction (Figure 29). While DiD-HCV colocalizes with total EGFR at the basolateral membrane, there is very little colocalization with the activated form of EGFR; colocalization with pEGFR instead occurs at the tight junction. This is seen in temporal comparisons of colocalization – association with total EGFR remains fairly consistent while pEGFR colocalization increases over time, peaking at points where DiD-HCV is at the tight junction or internalized. This is also mirrored by the biochemical data; the kinetics of HCV-induced activation of the various EGFR residues is consistent with the virion's localization to the tight junction or internalization.

With our previous work, it is clear that EGFR signaling is required for HCV virion internalization and uncoating. Given that CLDN1 and OCLN have constitutive endocytosis, it was possible that HCV may not need to trigger endocytosis once establishing an interaction with them. However, DiD-HCV remained localized at the tight junction with CLDN1 for ≥6 hours in the presence of erlotinib. This suggests that HCV/SR-B1/CD81 bring EGFR to the tight junction to stimulate HCV-receptor internalization at the tight junction.

EGFR is an attractive target for pathogen entry and known to be used by other viruses to induce internalization. Larger viruses such as vaccinia and respiratory syncytial virus utilize

EGFR-based macropinocytosis for entry (Krzyzaniak et al., 2013; Mercer et al., 2010a); influenza A virus uses an as-yet unidentified mechanism for EGFR-based internalization (Eierhoff et al., 2010). Interestingly, the chlamydial invasin Pmp21 is also endocytosed via EGFR in vesicles containing activated EGFR (Molleken et al., 2013). These pathogens all coopt EGFR to induce their own internalization. When activated in uninfected cells, the protein dimerizes, which stimulates its tyrosine kinase activity. Autophosphorylation of its cytoplasmic domain often leads to downstream signaling; adaptors and downstream signaling molecules can associate with EGFR through its phosphorylated tyrosine residues. Based on the ligand binding and concentration, EGFR will undergo endocytosis. Although there is still some debate, it is thought that high levels of activation lead to macropinocytosis while lower levels induce clathrin mediated endocytosis. Once EGFR is activated, the binding of Grb2 and c-Cbl have been found to be sufficient to induce endocytosis via clathrin (Madshus and Stang, 2009). Residues 1068 and 1086 are binding sites for Grb-2, which can induce ERK1/2 signaling, often through Ras or Raf. Grb2-recruited c-Cbl can then bind EGFR via residue 1045.

As with HCV, the chlamydial invasion Pmp21 activates the MAPK/ERK cascade; this activation also seems to be induced by EGFR (Molleken et al., 2013). Internalization requires EGFR residues 1068/1086 as well as 1045. *C. pneumoniae* was also found to colocalize with Grb2 and c-Cbl during infection, suggesting that they play a role in endocytosis.

In order to explore the genetic requirements for EGFR-mediated internalization, we mutated these residues as well as 1148 and 1173, as they are also implicated in the MAPK cascade important in HCV entry (Zona et al., 2013). Although 1045, 1068, and 1086 were not required for HCV infection, mutations in either 1148 or 1173 decreased RNA replication (Figure 30). In addition, DiD-HCV colocalization analysis suggested EGFR and its associated signaling was

required for colocalization with clathrin (Figure 31). Taken together, this suggests EGFR activation and subsequent adaptor recruitment via residues 1148 and 1173 may contribute to HCV internalization. In support of this, DiD-HCV was found to colocalize with Grb2 and c-Cbl; this association was abrogated when EGFR activation was blocked (Figure 32).

The parallels between Pmp21 and HCV are notable, suggesting that these two pathogens may utilize similar mechanisms for stimulating endocytosis. Although HCV does not use the "classical" Grb2 residue, studies have demonstrated binding of Grb2 to 1173 (Batzer et al., 1994), suggesting HCV may use an alternate binding site to associate with this protein. We have not fully fleshed out the components of the clathrin machinery required, nor which proteins bind to the required EGFR residues. However, we hypothesize an EGFR-mediated model for HCV internalization (Figure 33):

Following migration across the basolateral face, the HCV-receptor complex links up to the tight junction via CD81-CLDN1 associations. These interactions may allow for binding to OCLN. Once at the tight junction, EGFR is activated. This may be due to associations with one of the tight junction proteins or to EGFR clustering (known to induce EGFR activation). Activation of EGFR leads to phosphorylation of its cytoplasmic residues; binding of these phospho-tyrosine by clathrin adaptors leads to recruitment of the clathrin endocytic machinery and subsequent internalization in clathrin-coated vesicles. The largest question remaining is the source of EGFR activation. Furthermore, if EGFR can be activated in the absence of the tight junction proteins, what function do they serve?

CHAPTER V

CONCLUSION

Interactions of a virus with its potential host cell are critical for initiating entry and subsequent productive infection. To do this, HCV makes use of their own structural proteins as well as host factors embedded in the host membrane that envelops the virion. These viral components associate with host cell factors in order to initiate viral attachment, internalization, endosomal trafficking, and genome release.

The HCV virion is a unique structure, termed a lipoviroparticle due to its associations with lipoproteins. Such properties are due to its maturation and secretion, which is linked to the VLDL biosynthesis pathway (Chang et al., 2007; Gastaminza et al., 2008; Gastaminza et al., 2006; Huang et al., 2007); lower density viral fractions (that contain more LDL/VLDL) display increased HCV infectivity (Hijikata et al., 1993; Lindenbach et al., 2006). These lipoproteins play an essential role in entry, allowing for initial attachment of the virus to its host cell. Although a HCV virion contains many apolipoproteins, only ApoE is known be required for its infectivity (Gastaminza et al., 2008; Huang et al., 2007; Jiang and Luo, 2009; Maillard et al., 2006; Merz et al., 2011; Owen et al., 2009), as it is demonstrated to serve as the binding partner for initial host attachment factors (Andre et al., 2002; Dao Thi et al., 2012; Hishiki et al., 2010; Jiang et al., 2012; Maillard et al., 2006; Owen et al., 2009).

As HCV is a blood borne pathogen, it enters the liver via the bloodstream, first encountering hepatocytes via sinusoid capillaries. Before it reaches the hepatocytes, it passes through the Space of Disse, an area rich in ECM proteins (Perrault and Pecheur, 2009). ApoE can

interact with components of the ECM, especially heparan sulfate. At the hepatocyte itself, initial low-affinity contacts with the host cell's basolateral face involve Syndecan-1, LDLR, and SR-BI (Albecka et al., 2012; Catanese et al., 2010; Dao Thi et al., 2012; Koutsoudakis et al., 2006; Maillard et al., 2006; Shi et al., 2013). It is then thought that SR-BI can modulate the HCV E2 glycoprotein conformation, allowing the virus to bind CD81 (Bankwitz et al., 2010). The virus then is thought to interact with two tight junction proteins, CDLN1 and OCLN (Evans et al., 2007; Ploss et al., 2009), then internalize via clathrin-mediated endocytosis (Blanchard et al., 2006; Codran et al., 2006; Coller et al., 2009; Meertens et al., 2006) and uncoat in acidified endosomal compartments (Blanchard et al., 2006; Haid et al., 2009; Hsu et al., 2003; Kobayashi et al., 2006; Koutsoudakis et al., 2006; Lavillette et al., 2006; Meertens et al., 2006; Tscherne et al., 2006).

Although the cellular requirements of HCV have been defined, there has been some debate as to how these components are utilized during HCV entry. As mentioned, the virus first comes into contact with hepatocytes at its basolateral face and has ready access to the early-acting receptors CD81 and SR-BI. Localization of the late receptors CLDN1 and OCLN is potentially problematic however. These two tight junction proteins are inaccessible to the virus at the basolateral face. Accordingly, various models in the field center around how the virus resolves this.

One theory suggested CLDN and OCLN, while required, only serve in a signaling capacity; the virus does not need to come into contact with them. However, recent studies have suggested the virus may interact directly with these two proteins. HCV E1 develops a compensatory mutation when passaged in cells with CLDN6 but not CLDN1 (Hopcraft and Evans, 2015). OCLN-directed antibodies block HCV in an isolate-specific fashion, again suggesting direct interaction

(Sourisseau et al., 2013). Furthermore, humanized forms of OCLN are required for an infectable mouse model (Dorner et al., 2011).

Additional theories focus on where the virus accesses these proteins. Evans et al. proposed a model wherein the virus transits to the tight junction to access the two proteins. An alternative model suggests disruption of tight junction integrity, resulting in mislocalization of CLDN1 and OCLN to the basolateral face where the virus could interact with them. There is some evidence to support this second hypothesis. Partially polarized HepG2 cells are characterized by a high proportion of CLDN1 localized to junctional regions. Disrupting polarity allows CLDN1 to escape these junctional domains and was found to boost HCV infection (Mee et al., 2009). This might suggest that extrajunctional CLDN1 (and OCLN) are conducive to HCV infection and that HCV might also disrupt tight junction polarity for increased access to these proteins. In our lab's earlier work with HCV entry, they used DiD-labeled virus to follow interactions with host components. Live cell imaging of DiD-HCV in conjunction with CD81-GFP demonstrated virion internalization away from areas of cell-cell contact (Coller et al., 2009), again suggesting HCV does not require these junctional regions for entry.

However, current cell culture systems, both Huh-7.5 and HepG2 cells, are unpolarized. This is in contrast, as mentioned, to the highly polarized nature of hepatocytes *in vivo*. Studies in unpolarized cells not only lose the complexity of interactions in the hepatocyte, they are biased towards nonjunctional entry. Without the domain restrictions of a polarized cell, HCV may not need to relocalize. However, although HCV can enter extrajunctionally given the opportunity, one cannot infer this is the relevant entry pathway. Furthermore, as proteins do not have precise localizations in these cell culture systems, with proteins present all across the plasma membrane, spatiotemporal requirements of signaling may be lost. We argue HCV entry studies should be done

in more morphologically relevant cell culture systems, not only to avoid artifacts of poor cell polarization, but to understand the nuances of HCV entry.

To this end, we utilized a Matrigel-based polarization system of Huh-7.5 hepatoma cells (Molina-Jimenez et al., 2012). Seeded at single-cell density into ECM-rich gel, the cells polarize as they grow, forming spheres, or organoids. These organoids exhibit markers of polarity and some of the capabilities of hepatocytes, with functional bile secretion into the interior (apical) space. The architecture of the organoids also mimics what the virus would encounter *in vivo* – HCV in the liver passes through an ECM-rich milieu before reaching the basolateral face of the hepatocyte, much like the virus would encounter Matrigel-based ECM before encountering the basolateral face of the organoid. Most importantly for our study, HCV entry factors now correctly localize in these polarized cells; CLDN1 and OCLN are restricted to the inner tight junctional region, completely colocalize with the tight junction marker ZO-1, and are inaccessible to the incoming virion without virally-induced signaling (either disruption or relocalization). In order to clearly visualize interactions with the virus, we optimized live and fixed cell imaging. In addition, we further characterized populations of highly infectious DiD-labeled HCV for use in imaging assays. Purified DiD-HCV specifically labeled virus and was free from any extraneous cellular components that might interfere with HCV entry analysis, such as exosomes.

Studying the entry process in these polarized organoids vastly changed how the virus behaved during entry. Binding at the basolateral face, the virus associated with SR-BI, CD81 and EGFR. It maintained these associations with host factors as it trafficked to the tight junction, where it also associated with CLDN1 and OCLN. Following tight junction localization, the virus internalized via clathrin-mediated endocytosis into early endosomes; the virus fused in acidified endosomal compartments. Unlike in the unpolarized two-dimensional system, HCV traffics to the

tight junction; we found no association of DID-HCV with CLDN1 or OCLN outside of the tight junction. Along with evidence that tight junction integrity is not grossly perturbed during HCV entry, this suggests to us that HCV must traffic to the tight junction in order to associate with its two tight junction entry factors. This is the first validation of a model in a relevant cell culture system and again underscores the necessity of studying entry in a system that adequately represents the native environment.

Additionally, we found that actin played an essential role in trafficking to the tight junction. In unpolarized cells, there is very little diffusion across the plasma membrane; diffusion was mostly random and did not require actin (Coller et al., 2009). However, due to the large-scale relocalization that now takes place, virions require active transport to drive its movement ~25 μm to the tight junction. This is also the first study that demonstrated colocalization with EGFR, which was found to associate with the particle early, at the basolateral, and maintain association throughout the migration to the tight junction.

With the observation that HCV utilizes the tight junctional relocalization model, it becomes much easier to tease apart the various stages of HCV entry. Using immunofluorescence, we can assay for defects in DiD-HCV localization upon perturbation of the system. One can imagine factors involved in binding will show decreased basolateral colocalization at early time points, factors involved tight junctional relocalization will display accumulation of particles at the basolateral rather than tight junction, internalization factors will accumulate at the tight junction, and factors involved in trafficking/fusion will be trapped in a pre-fusion state.

We used this assay to determine the stages at which the different entry factors participate. SR-BI, CD81, and OCLN were CRISPR'D while we used a hairpin knockdown for EGFR. SR-B1 and CD81, consistent with their role as early factors, showed defects in tight junction

relocalization; cells lacking OCLN led to particle accumulation at the tight junction, indicating its role in internalization. EGFR, although it had been hypothesized to play a role in trafficking to the tight junction (Lupberger et al., 2011; Zona et al., 2013), is instead required for internalization.

Given our unexpected finding, we further explored the role of EGFR in internalization. Biochemical and colocalization data suggest that EGFR is activated at the tight junction prior to internalization. Mutagenesis of potential residues involved in adaptor binding or signaling identified two tyrosine residues on EGFR's cytoplasmic tail that are required for HCV infection; tyrosine 1173 may function as an alternate adaptor for Grb2. Further tracing the role of EGFR in endocytosis, we found colocalization of DiD-HCV with components of the clathrin endocytic machinery. This association, however, was dependent on EGFR activation. Our study is the first to propose a potential mechanism for HCV endocytosis. Additionally, as mentioned, our study has clarified previous work looking at the role of EGFR signaling in HCV entry.

Moving forward, we would initially like to utilize the CRISPR system to determine the requirements for individual receptors. Preliminary evidence suggests CLDN1 knockout also results in an internalization defect. We would next like to study the individual knockouts to clarify the temporal pattern of the interactions with the virus during HCV entry – is SR-BI indeed required for CD81 association? Which of the early entry factors are required for association with EGFR? Is CLDN1 required for OCLN interaction? Complementation of these CRISPR'D cell lines with mutants of entry factors could also aid in understanding of these patterns. For example, the residues involved in CLDN1-CD81 and CLDN1-E1 associations are known; how do viral localization and interaction patterns change when a CLDN1 knockout cell line is complemented back with residues mutated for CD81 or E1 association?

Mutagenesis of the residues potentially involved in signaling and adaptor binding could also shed light on additional host factors required for entry. One of the largest remaining questions is how the virus relocates to the tight junction. Although we have identified one cytoskeletal component, how this actin-based relocalization is initiated is still unknown. CD81 does not contain a cytoplasmic tail and is consequently not a target for such mutagenesis. SR-BI, however, contains a large C-terminal tail with multiple residues available for phosphorylation or ubiquitination. Our initial data suggests mutation of two tyrosine residues leads to a decline in RNA replication. However, it still remains to be determined how these residues participate in HCV entry. Using our ZO-1 localization study, it will be possible to determine if these mutants have defects in relocalization to the tight junction. Furthermore, it would be useful to investigate whether PKA is involved in activation of SR-BI. PKA has been demonstrated to lead to relocalization of SR-BI via transcytosis (Burgos et al., 2004). Although PKA has also been implicated in CD81-CLDN1 association (Farquhar et al., 2012), tight junction migration acts upstream of this; PKA inhibitors and mutagenesis may aid in elucidation of its role and possible interaction with SR-BI. Additionally, c-Cbl is a known interactor of SR-BI and induces migration of SR-BI. Immunofluorescence and biochemical analysis (looking at the ubiquitination of SR-BI during infection) can help elucidate whether the c-Cbl interaction is relevant for HCV entry. While double labeling of c-Cbl and SR-BI in cells has so far been problematic, triple staining with DiD-HCV may provide an initial clue as to whether c-Cbl is involved in the early stages of entry. Mutagenesis of c-Cbl and resulting ZO-1 colocalization studies may also be useful. Finally, we have not investigated whether the lipid transfer function of SR-BI plays a role in polarized entry. However, preliminary work suggests addition of HDL, in some cases, leads to an accumulation of SR-BI at

the tight junction. If this is the case, SR-BI may be involved in migration to the tight junction in a manner linked to lipid transfer.

Our initial studies of EGFR suggest its activation is necessary for internalization. As mentioned, we have established EGFR activation-dependent association of clathrin components with DiD particles as well as identified residues on the cytoplasmic tail necessary for viral internalization. However, it remains to be seen whether these residues directly bind clathrin adaptors or induce ERK/MAPK signaling that is required for internalization. To test the second option, drug inhibitors and mutagenesis could be combined with DiD-HCV localization studies to identify which stage of HCV entry requires these downstream kinases. They may participate in initial internalization; alternatively, the downstream signaling could be used to drive endocytic trafficking of the virus. In this scenario, particles would internalize but may display altered trafficking and/or fusion. Studying HCV entry in the context of the mutant residues will also provide clues as to their role in entry. Using the ZO-1 localization assay will determine whether these mutant EGFR residues cause an internalization defect; colocalization of Grb2 and c-Cbl with DiD-HCV in mutant cell lines can help shed light on their role in recruitment of these adaptors. C-Cbl has already been shown to be required for HCV entry in 2D; knockdown and mutagenesis of Grb2 would establish its role in entry as well. Furthermore, colocalization studies (in combination with mutagenesis) will also determine whether other components of the clathrin machinery (e.g. epsin, Eps15, SOS) are required for viral internalization.

A significant question remains – how is EGFR activated? EGFR seems to be activated when HCV particles have reached the tight junction. While EGFR activation is only required for internalization and not migration to the tight junction, it remains formally possible that EGFR is instead activated at the basolateral but in quantities too small to be detected. As EGFR activation

is enriched over time, this hypothesis could be tested by blocking actin-based relocalization to the tight junction. Particles would then be trapped at the basolateral face; incubation over time would allow for an observable increase in phosphorylation. If HCV is indeed activated at the tight junction, one of the tight junction proteins may participate in its activation. The CRISPR cell lines can be utilized to assay for EGFR activation through immunofluorescence (colocalization) and pEGFR protein levels (via western blot) in the absence of either CLDN1 or OCLN. If, in fact, one of these proteins is responsible, is this their sole function in the entry process? If exogenous stimulation of EGFR can overcome the absence of that tight junction protein (observed via successful internalization/uncoating of the particle), it may function solely to activate EGFR. *In silico* analysis of CLDN1, OCLN, and the glycoproteins could also reveal an EGF-like domain, or a domain that can activate EGFR.

CD81 has been shown to internalize with the viral particle (Coller et al., 2009). Our work suggests EGFR is also internalized, as pEGFR coated vesicles can sometimes be seen to colocalize with DiD-HCV. However, it is unclear whether other members of the HCV-receptor complex internalize as well. Colocalization studies post-internalization would clarify this step in the pathway. But a larger question is whether internalization of these components is necessary or just a consequence of their localization in the entry complex.

Analyzing the components of the entry complex at each stage would help elucidate the kinetics of entry factor usage, the composition of the entry complex at each stage (especially adaptor proteins), as well as shed light on how these proteins form a complex. However, biochemical isolation of these complexes is difficult, and the variable rates of entry across the population of HCV particles creates a very noisy sample. Drugs, blocking antibodies, or protein knockouts would allow for study of a homogeneous population of entry complexes blocked at a

particular stage. For example, inhibiting actin polymerization enriches for pre-migration complexes. Dynamin-induced blockage of internalization would capture the complex pre-endocytosis. This biochemical approach is also ideal for an in-depth look at the change in composition of an entry complex in a receptor knockout cell line; receptor knockout cell lines also provide an inherent block in HCV entry. (As a side note, these findings can be confirmed using drug treatments, etc. and probing for association of the virus with various proteins via immunofluorescence.) In order to better isolate these HCV-entry factor complexes, we could make use of the lipoprotein content of the virion. ApoE is only used for attachment, so fluorescent labeling of such a protein (as opposed to labeling one of the envelope glycoproteins) is less likely to interfere with the entry process. Initial work has demonstrated Huh-7.5 cells stably expressing ApoE-mCherry produce ApoE-mCherry labeled viral particles; such particles do not show a significant drop in infectivity. It remains to be seen whether these particles undergo the same entry process as unlabeled particles. However, this provides an opportunity for more specific capture of entry complexes. APEX (Ascorbate peroxidase) allows for enzyme-based proximity labeling; the enzyme generates biotin-phenoxyl radicals that bind to nearby proteins (Rees et al., 2015). Attaching APEX to a protein on the host cell surface would result in nonspecific labeling; however, substituting APEX into the ApoE construct would provide an APEX-tagged virus that could be used to label host components in close proximity, i.e. the host entry complex and associated adaptors. Immunoprecipitation of biotinylated proteins would provide an unprecedented view into the entry process. Furthermore, it might help elucidate downstream events such as endocytic trafficking and uncoating, of which little is known.

APPENDIX

FIGURES

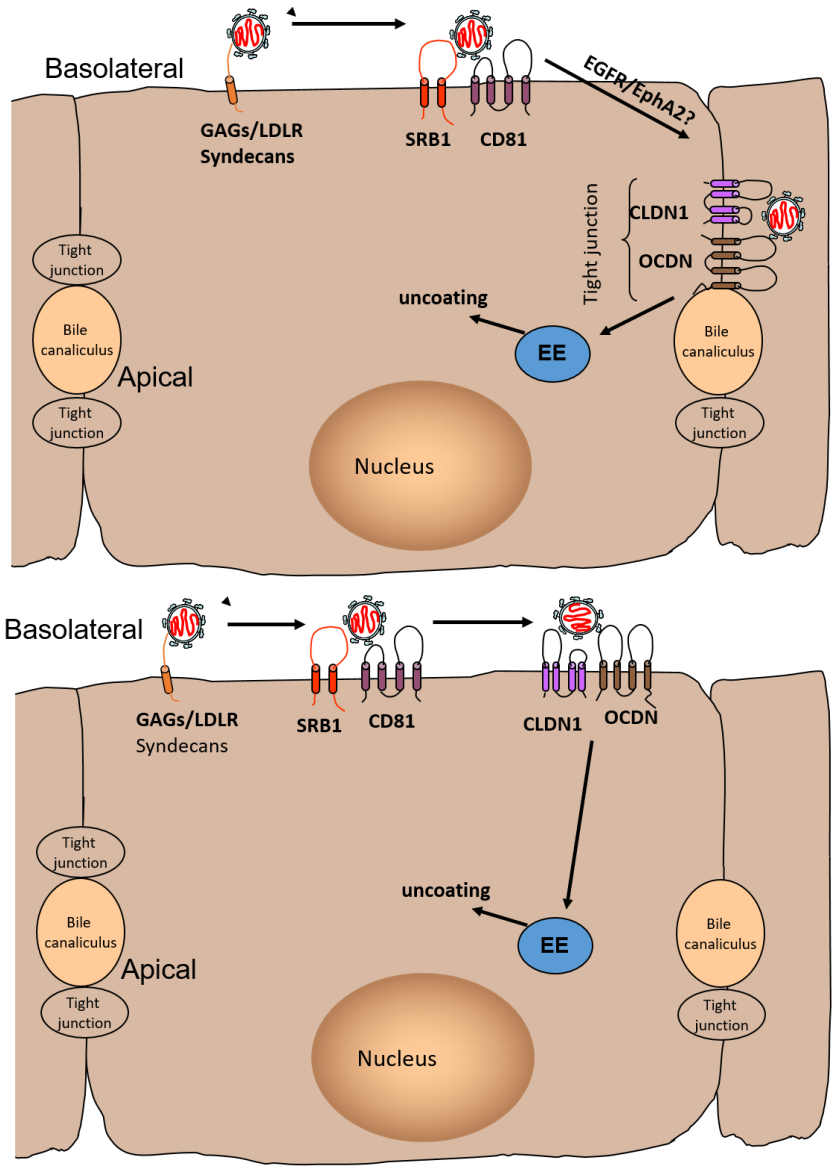

Figure 1. Potential models for HCV entry. As HCV entry requires the tight junction proteins CLDN1 and OCLN, there have been several hypothesized models for the virion's pathway into the cell. These tight junction proteins may play an indirect role in HCV entry, and thus would not require direct interaction (visual not shown). Alternatively, they may be involved in the entry factor/receptor complex that directly interacts with the virus. If this is the case, virions cannot access these two proteins from the bloodstream. One model (top) hypothesizes that the virion, after interacting with early receptors CD81 and SR-BI, relocalizes to the tight junction in order to interact with these two proteins. An alternative hypothesis involves extrajunctional association of HCV with CLDN1 and OCLN, potentially through disruption of barrier function.

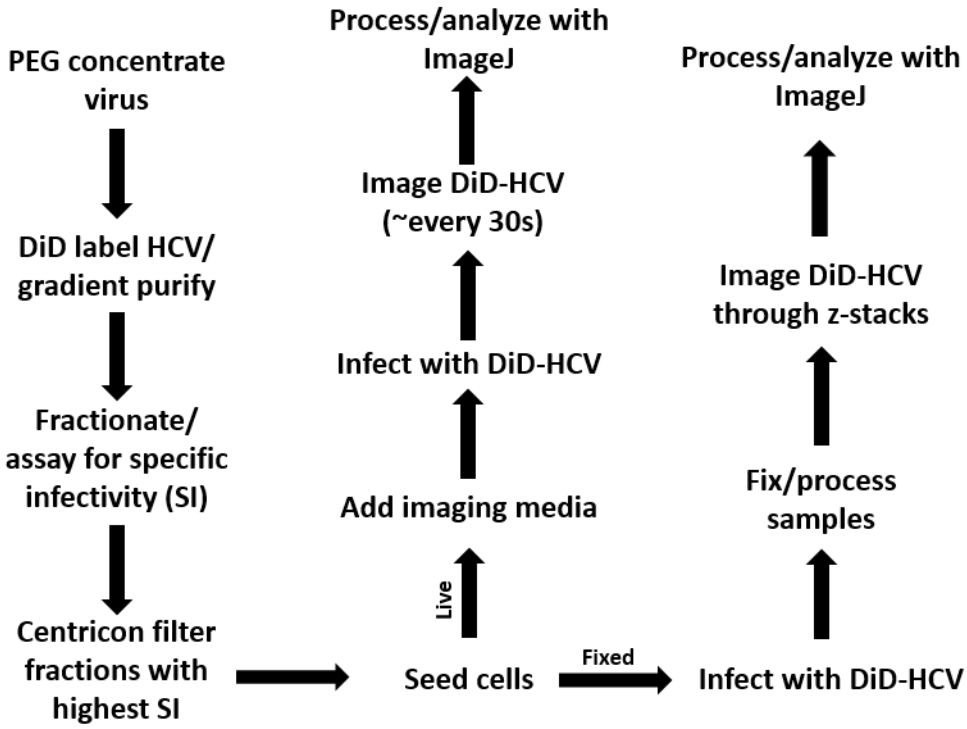

Figure 2. Workflow for DiD labeling of HCV. HCV is first PEG-concentrated, then labeled with the lipophilic dye DiD. Following iodixanol gradient ultracentrifugation and fractionation, each fraction is assayed for specific infectivity. The fraction with the best (lowest) specific infectivity is then concentrated/purified via Centricon filtration. Cells are seeded into Matrigel one week prior to imaging. If performing live cell, cells are (re)seeded into imaging dishes a day prior to imaging. Cells are incubated with DiD-HCV on ice. During live cell, a series of images are then acquired every 30 seconds. Fixed cells are also infected, incubated on ice for one hour, then fixed and processed for immunofluorescence. Resulting images are then processed and analyzed with ImageJ.

Virus	Specific Infectivity (SI)
HCV	2194 (±697)
Concentrated HCV	869 (±468)
DiD-HCV	728 (±915)
Purified DiD-HCV	4.9 (±4.1)

Figure 3. Concentration and gradient purification improves specific infectivity of HCV. Comparison of specific infectivity (SI) between HCVcc supernatant, polyethylene glycol (PEG)-concentrated viral supernatant, DiD-HCV, and selected fractions from gradient purified DiD-HCV

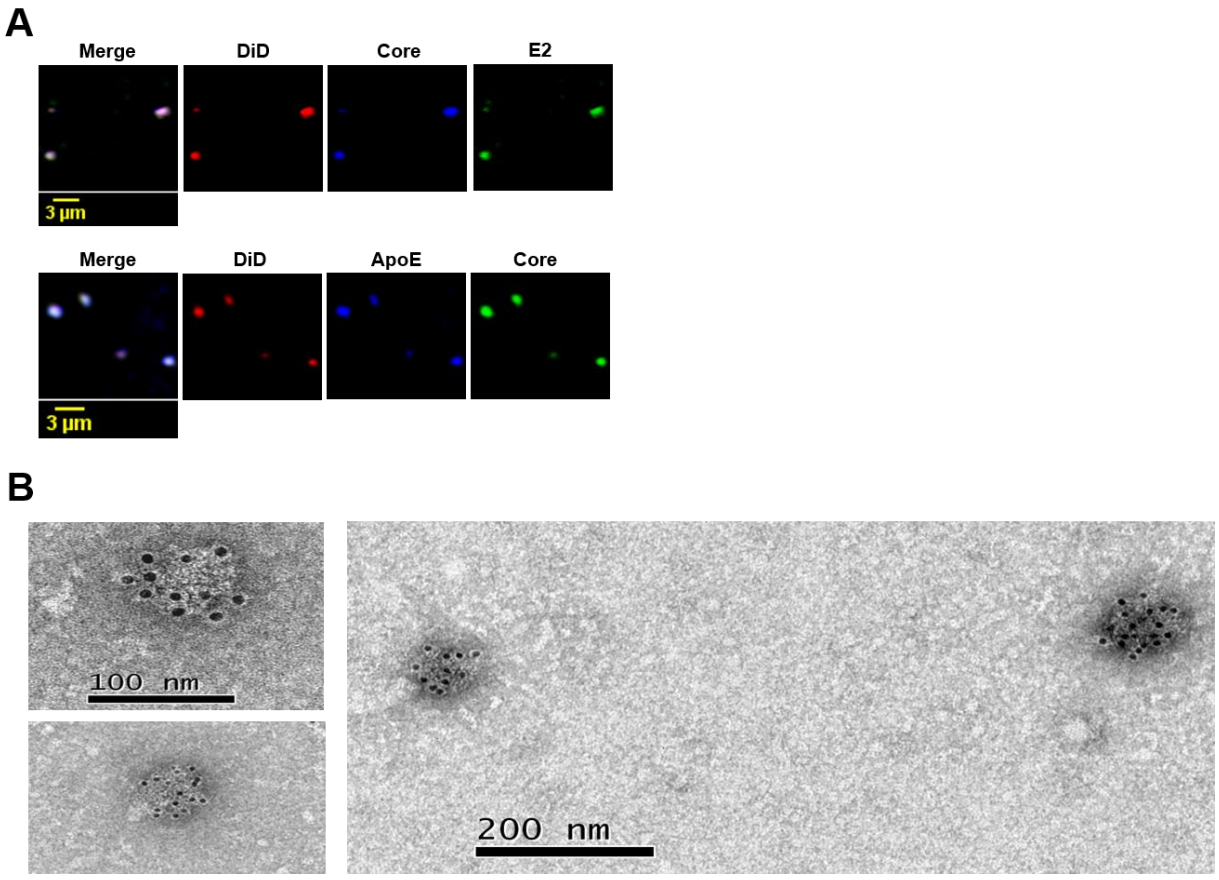

Figure 4. DiD labeling is specific for HCV particles. (A) Purified DiD-HCV (red) was spotted onto poly-L-lysine treated coverslips, fixed, and probed with indicated antibodies. (B) Purified DiD-HCV particles were fixed and processed for electron microscopy using an anti-HCV E2 antibody and 10 nm colloidal gold IgG.

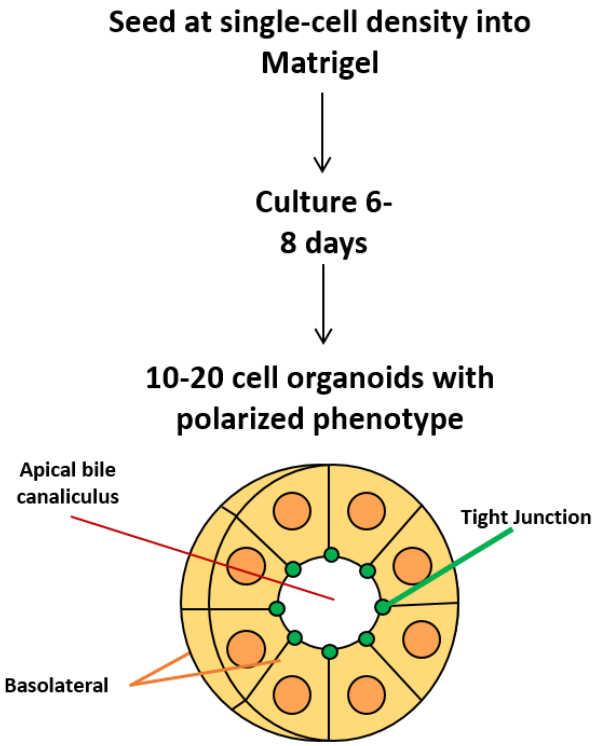

Figure 5. Schematic for polarizing cells. In order to induce polarization, cells were trypsinized and diluted in 10% DMEM to a concentration of 1 x10^5 cells/mL. Equal parts diluted cell solution and Matrigel were mixed, then seeded onto plates. The Matrigel was allowed to polymerize for 30 minutes at 37°C before adding 10% DMEM. Cells were grown for 6-8 days, changing the media every other day. At this time, had formed polarized "organoids" that greatly resemble the architecture of a hepatocyte in vivo (bottom diagrammatic). Organoids are composed of an exterior/lateral basolateral domain as well as an interior apical region, delimited by tight junctions.

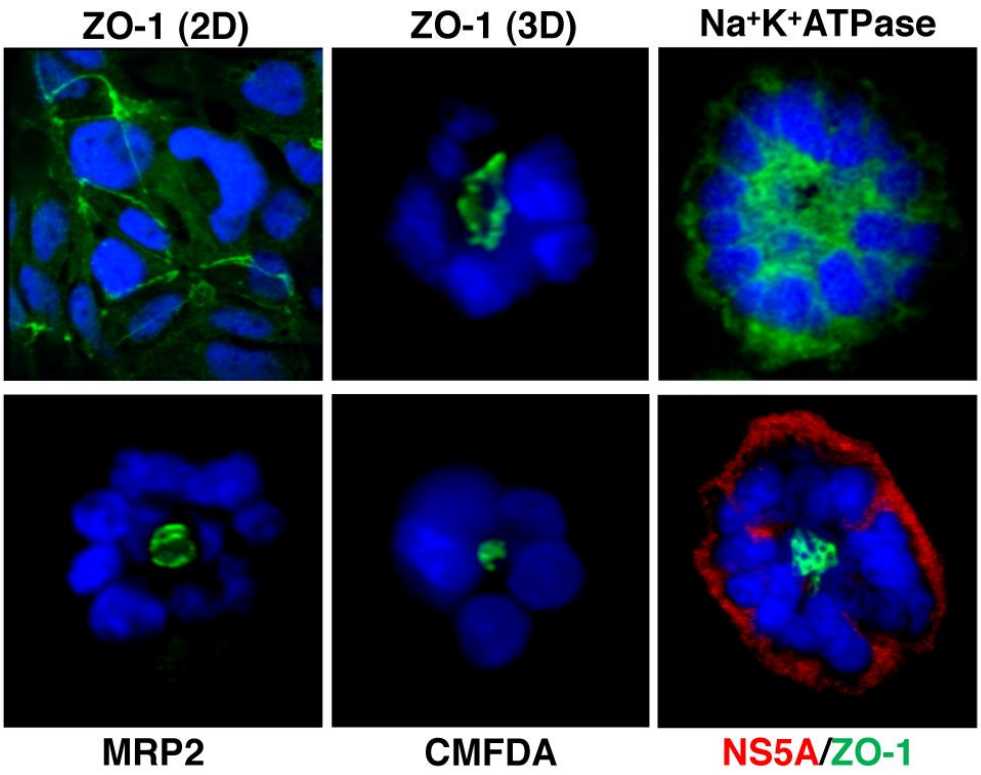

Figure 6. ECM-embedded Huh-7.5 cells display hallmarks of polarization and are susceptible to infection. (top left) Huh-7.5 cells were grown under 2D conditions, then fixed and stained for ZO-1. Nuclei are stained with DAPI (blue). (remaining panels) Trypsinized Huh-7.5 cells, diluted to $1x10^5$ cells/mL, were mixed 1:1 with thawed Matrigel solution, allowed to polymerize, and incubated for 7 days to form organoids. Cells were then fixed and probed with indicated antibodies. (bottom right) Huh-7.5 organoids were infected with HCVcc, then fixed at 48 hours post infection (hpi) and probed for ZO-1 (green) and NS5A (red).

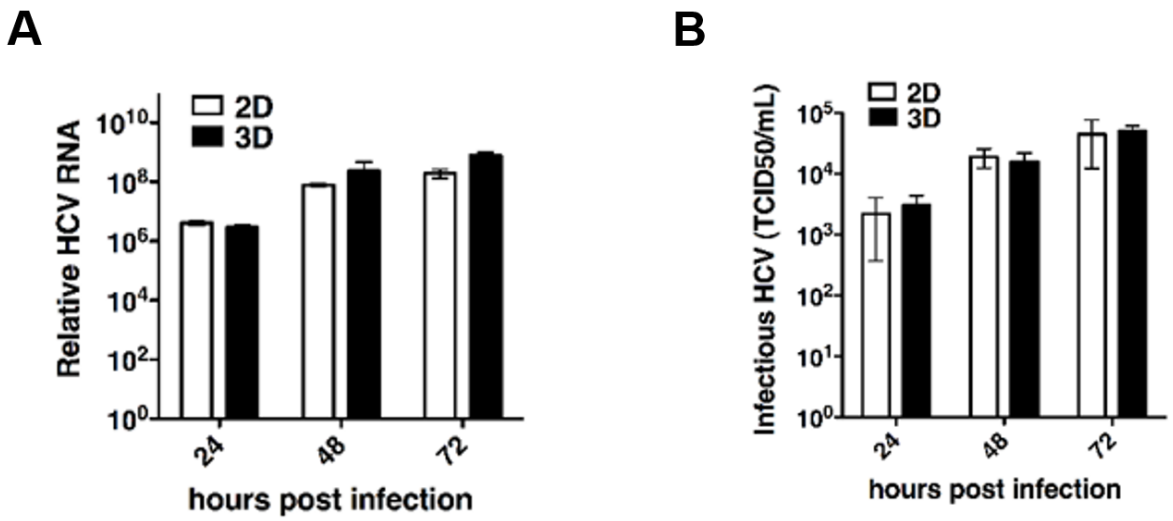

Figure 7. ECM-embedded Huh-7.5 cells are susceptible to HCV infection. (A) HCV replication and (B) virus production were quantified in 2D or 3D Huh-7.5 cells at the indicated times. To ensure that the ECM itself was not altering the kinetics of HCV infection, an ECM overlay was added to the 2D cultures just prior to infection. After an 8-hour incubation with HCV, the media was changed and ECM was removed in the 2D samples to prevent any partial polarization; means ± SD.

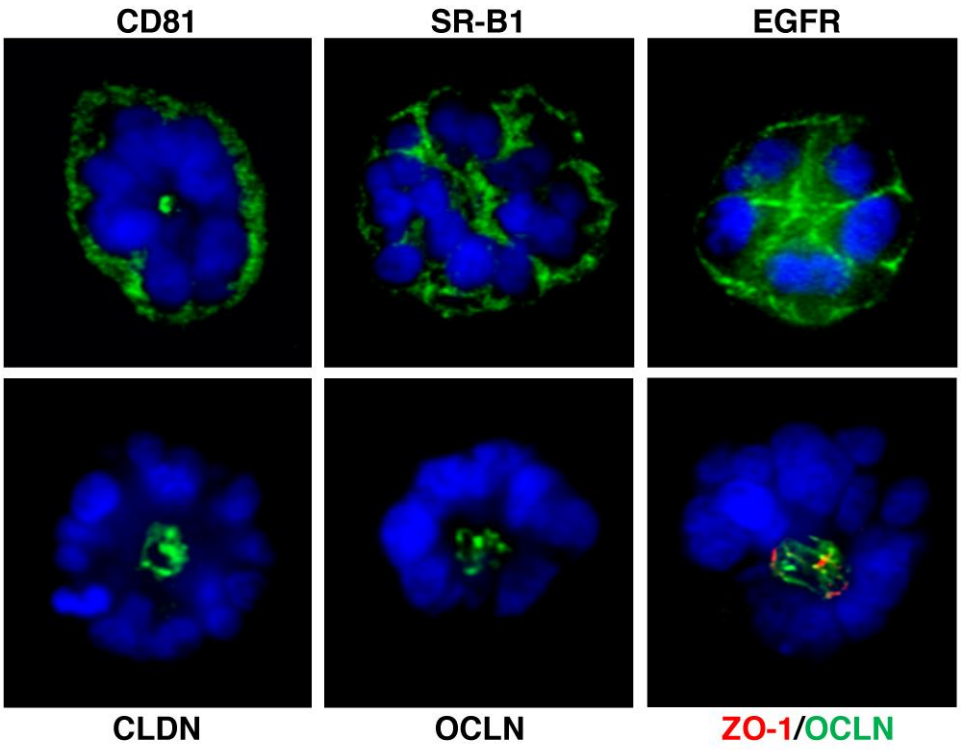

Figure 8. HCV entry factor localization in polarized Huh-7.5 organoids. Huh-7.5 organoids were fixed and probed with antibodies specific to the indicated HCV entry factors (green) or ZO-1 tight junctional protein (red). Nuclei are stained with DAPI (blue).

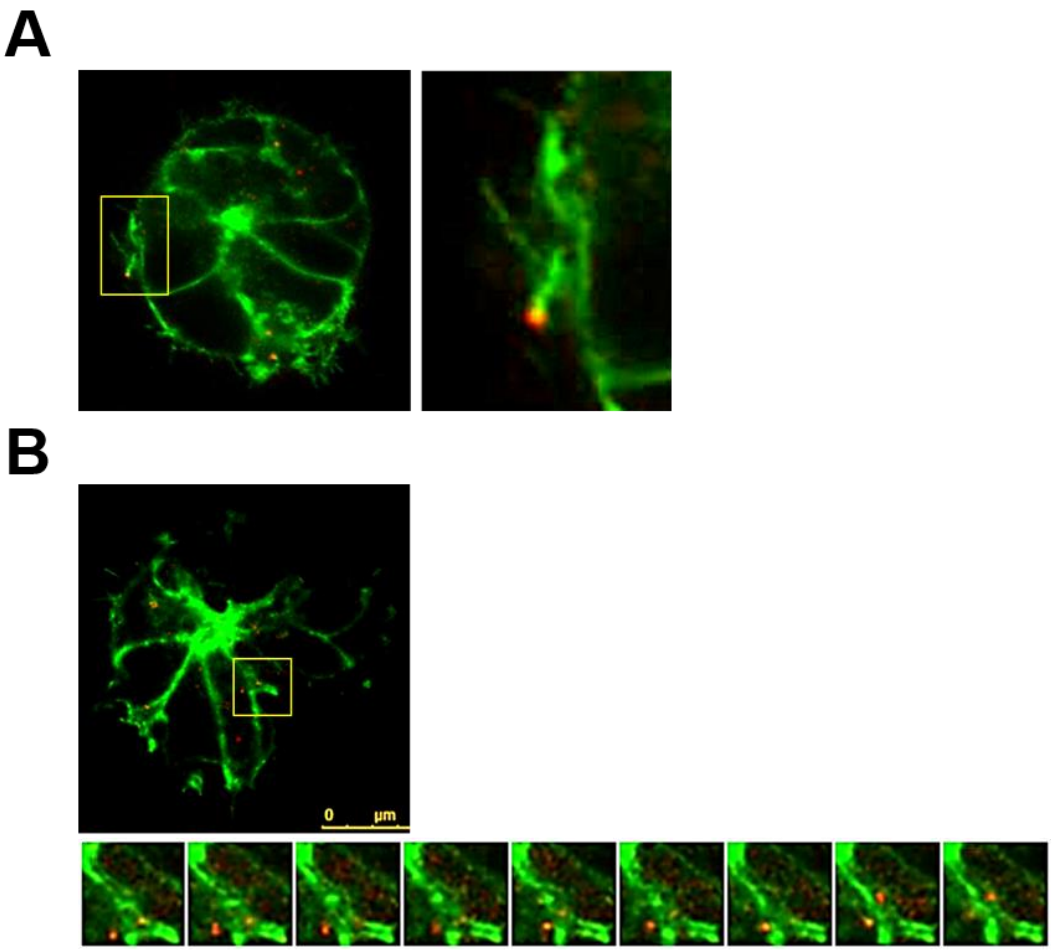

Figure 9. Live Cell Imaging of DiD-HCV Entry into Polarized Organoids. Huh-7.5 cells stably expressing CD81-GFP were seeded into Matrigel and cultured for 6 days. Organoids were then extracted from Matrigel, replated onto imaging dishes, and allowed to adhere. Cells were then infected with DiD-HCV, incubated on ice for 1 hour, then imaged every 15-30 seconds. Images show representative kymographs from live cell imaging CD81-GFP (green) and DiD-HCV (red). (A) Particle localized to filopodia. (B) Kymograph showing movement particles along lateral face. Yellow box denotes location of kymograph.

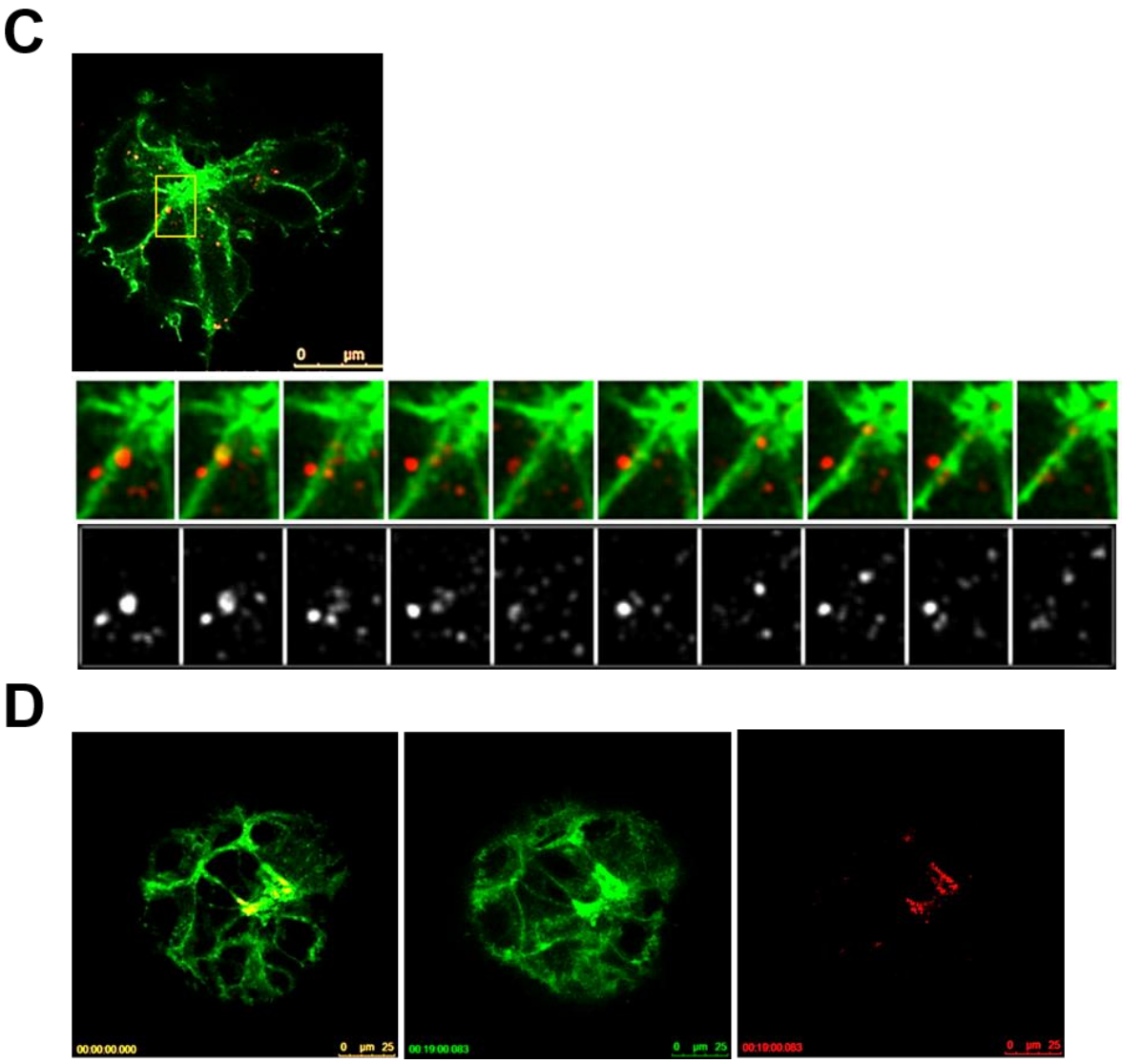

Figure 9 (continued). Live Cell Imaging of DiD-HCV Entry into Polarized Organoids. (C) Movement of DiD particles from lateral face to the tight junction. Yellow box denotes location of kymograph. Top kymograph: merge of CD81-GFP and DiD-HCV. Bottom kymograph: DiD-HCV particles only. (D) Particles accumulated at the tight junction. Right: Merged image of CD81-GFP and DiD.

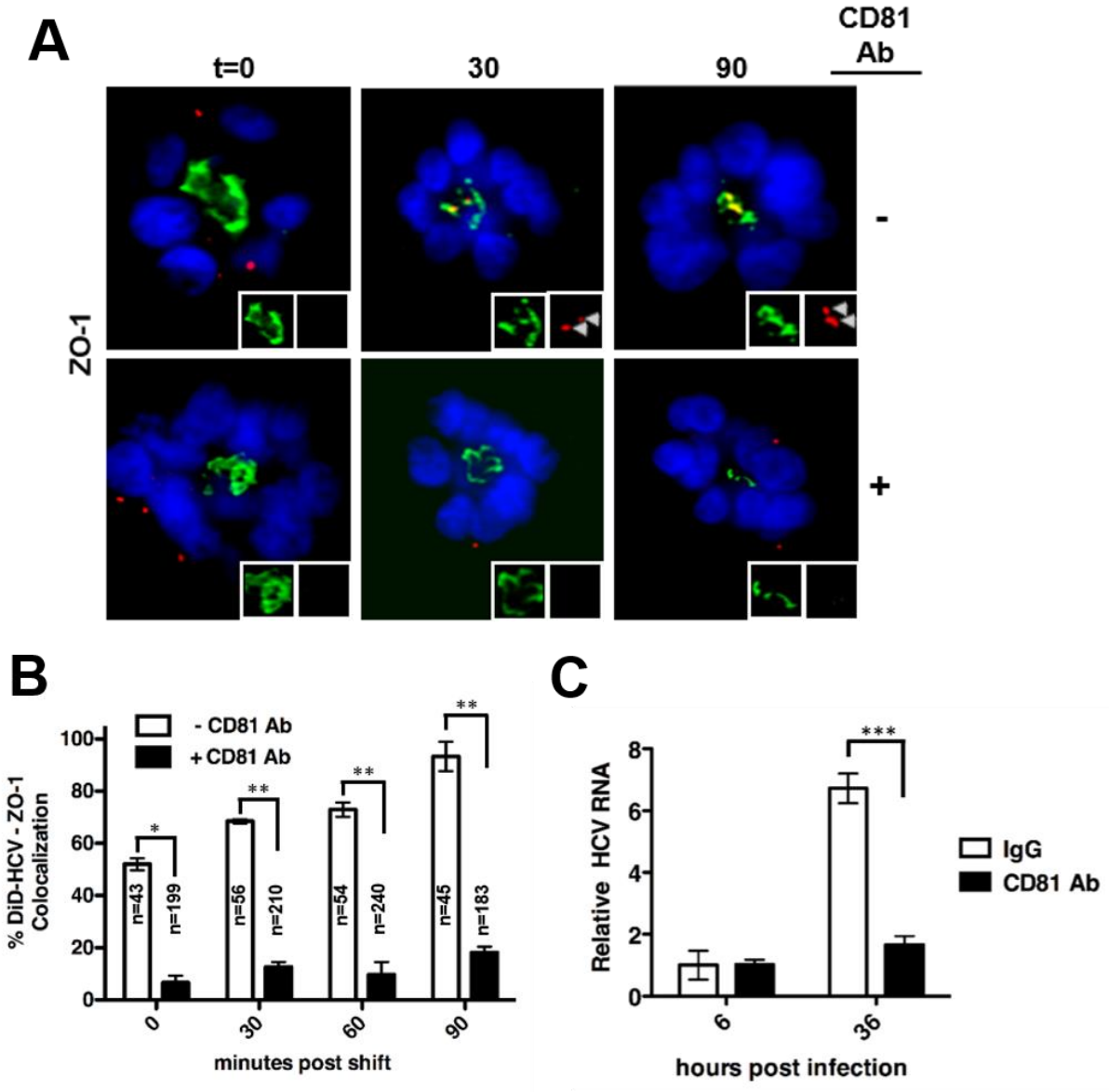

Figure 10. DiD-HCV accumulates at the tight junction during infection of Huh-7.5 organoids. (A) Huh-7.5 organoids were pretreated with or without 10 µg/mL CD81 blocking antibody JS-81 for 1 hour, infected with DiD-HCV for 1 hour at 4°C, shifted to 37°C (t=0) for the indicated amount of time (in minutes), fixed, and probed for ZO-1 (green). Nuclei are stained with DAPI (blue). Insets display the tight junctional region: ZO-1 (left) and DiD-HCV (right). (B) Quantitation of (A). n=total DiD puncta imaged at each time point, error bars=SD. (C) Huh-7.5 organoids were preincubated for 2 hours with 10 µg/mL JS-81 blocking antibody or control IgG. Cells were infected with HCVcc for 6 hours, washed twice, and replaced with fresh media. RNA was isolated at 6 and 36 hours and quantified via RT-PCR, normalized first to their respective cellular RNA levels, then to control IgG at 6 hpi. Experiments were performed in triplicate; error bars=SD. *p<0.05. **p<0.01. ***p<0.001.

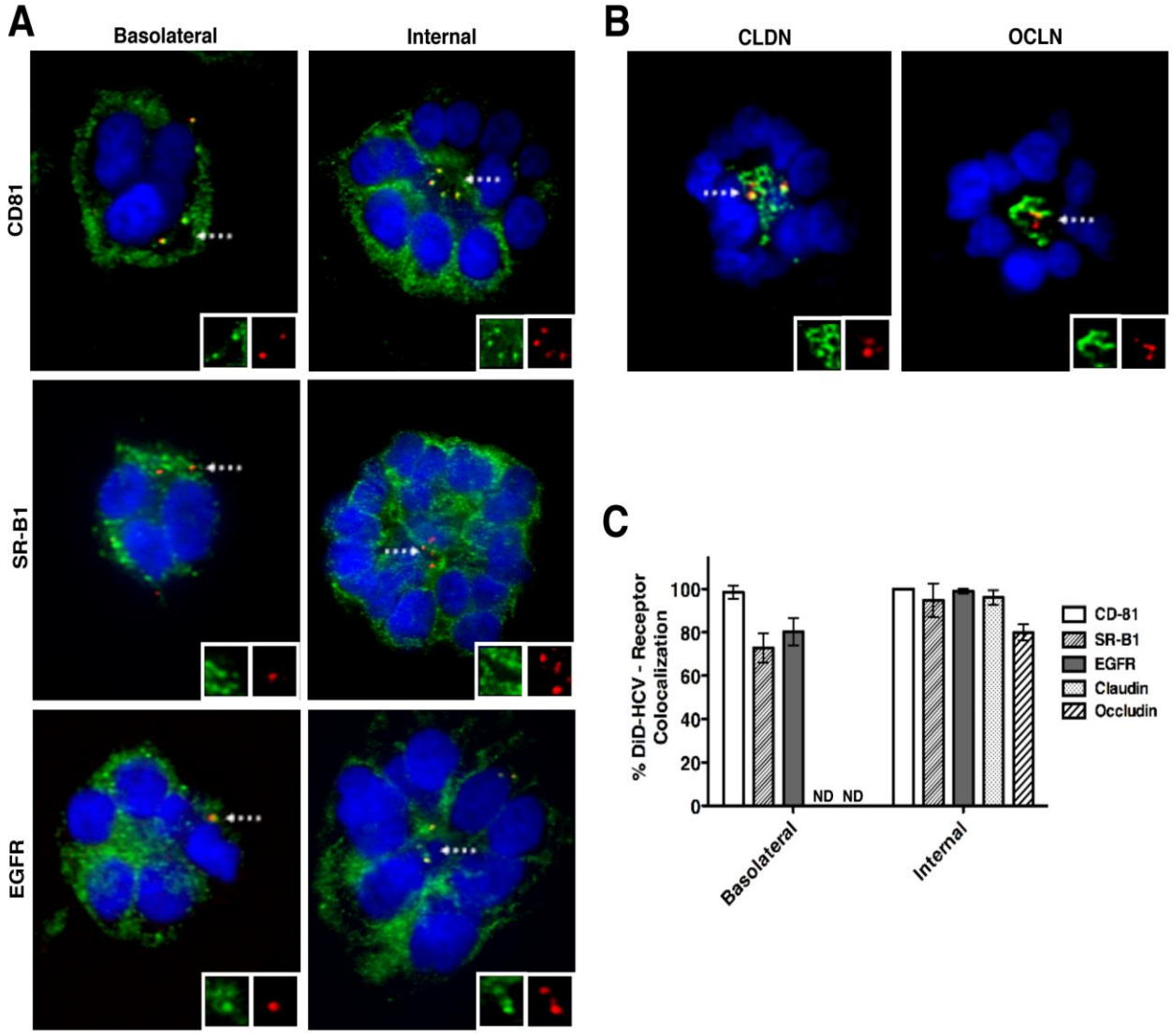

Figure 11. Co-localization of DiD-HCV with entry factors. Huh-7.5 organoids were infected with DiD-HCV for 1 hour at 4ºC, shifted to 37ºC for 0 to 90 minutes, then fixed, and probed for (A) CD-81, SR-B1, EGFR, (B) CLDN1, or OCLN. Nuclei were stained with DAPI (blue). Arrows indicate the portion of the image enlarged in insets. Left: HCV entry factor (green), right: DiD-HCV (red). In images shown, all DiD particles colocalize with selected entry factor with the exception of OCLN, in which 3 of 4 particles colocalize. (C) Percent DiD-HCV colocalization with each entry factor at the basolateral or internal/tight junctional portion of the cluster, as determined by Z-stack analysis. n-values (total DiD signal) range from 81 to 276 for each sample; error bars=SD, ND=not detected.

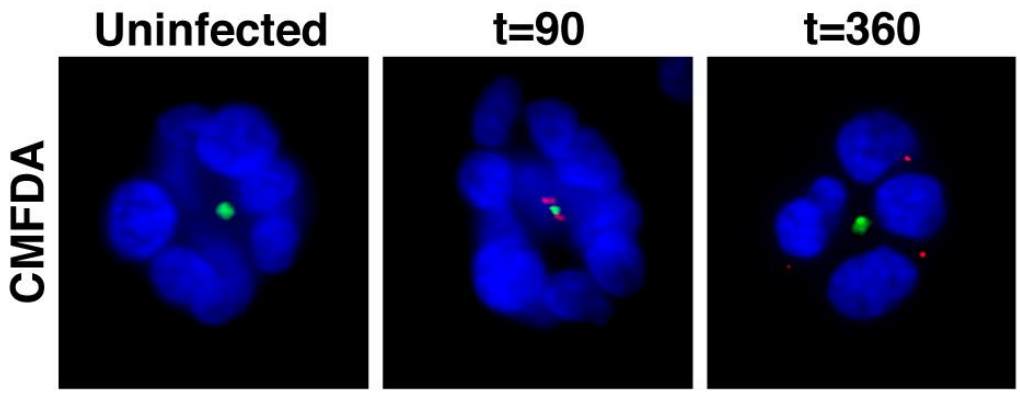

Figure 12. DiD-HCV entry into Huh-7.5 organoids does not alter bile canaliculi function. Huh-7.5 organoids were incubated with or without DiD-HCV for 1 hour on ice, then shifted to 37^{o}C for the specified time. Uninfected cells were fixed at 360 minutes post shift. Two hours prior to fixation, CMFDA (green) was added to the media, incubated for 1 hour, then washed with DMEM + 10% FBS and incubated for an additional hour. Nuclei were stained with DAPI (blue).

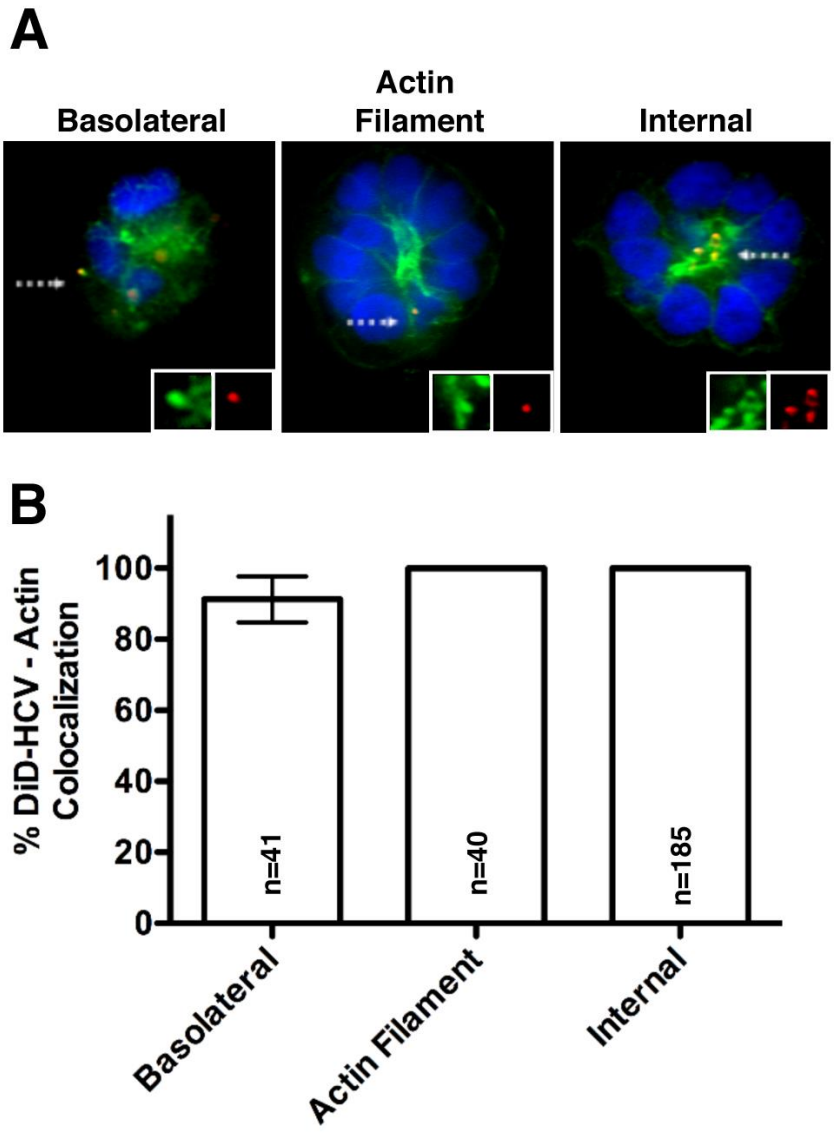

Figure 13. DiD-HCV traffics in association with actin. Huh-7.5 organoids were infected with DiD-HCV for 1 hour at 4ºC, shifted to 37ºC for 0 to 90 minutes, fixed, and probed with Phalloidin. Nuclei were stained with DAPI (blue). (A) Representative images of actin colocalization with DiD-HCV localized to basolateral (left), actin filament (middle), and internal (right) portions of the cluster; insets displaying actin colocalization labeled with dashed arrows. Left: actin (green), right: DiD-HCV (red). (B) Percentage of DiD-HCV particles colocalized with Phalloidin-labeled actin at each domain. n=total DiD signal; mean +/- SD. ***p<0.001.

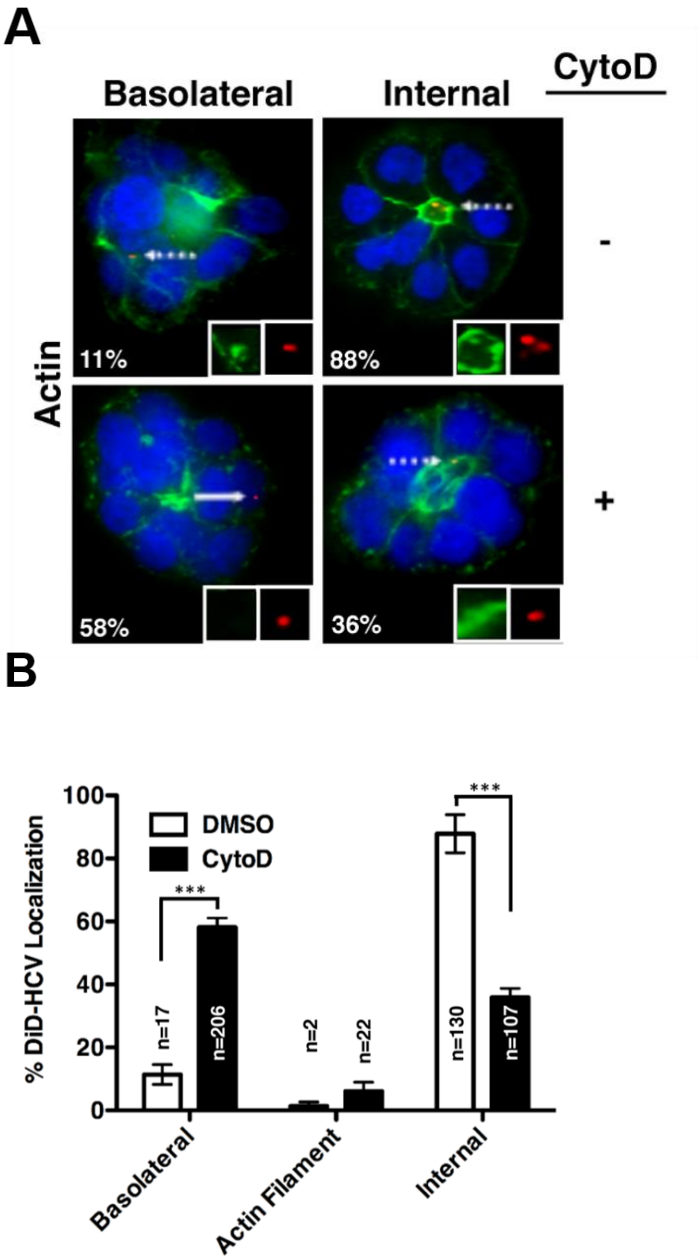

Figure 14. DiD-HCV requires actin for tight junction relocalization. Huh-7.5 organoids were incubated with either 10 uM cytochalasin D or DMSO control for 1 hour. Cells were infected with DiD-HCV for 1 hour on ice, shifted to 37^{o}C for 90 minutes, then fixed and stained with Phalloidin. Nuclei were stained with DAPI (blue). (A) Representative images of DiD localization with and without cytochalasin D treatment. Arrows mark portion of area enlarged in insets, dashed arrow indicates colocalization. Left: actin (green), right: DiD-HCV (red). Percent localization to each membrane (basolateral or internal) is indicated in each panel. (B) DiD-HCV particles were then quantified for their localization within the cluster. n=total DiD signal; mean +/- SD. ***p<0.001.

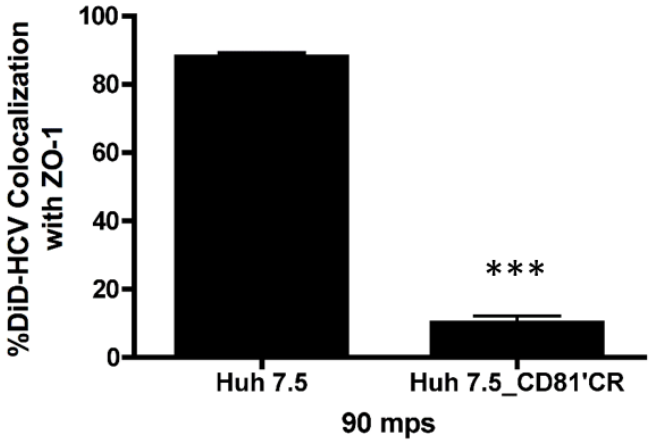

Figure 15. DiD-HCV requires CD81 for relocalization to the tight junction. Huh-7.5 wild type and CD81-CR organoids were infected with DiD-HCV for 1 hour at 4ºC, shifted to 37ºC for 90 minutes, fixed, and probed with ZO-1. Graph shows percentage of DiD-HCV particles colocalized with ZO-1. n=total DiD signal; mean +/- SD. ***p<0.001.

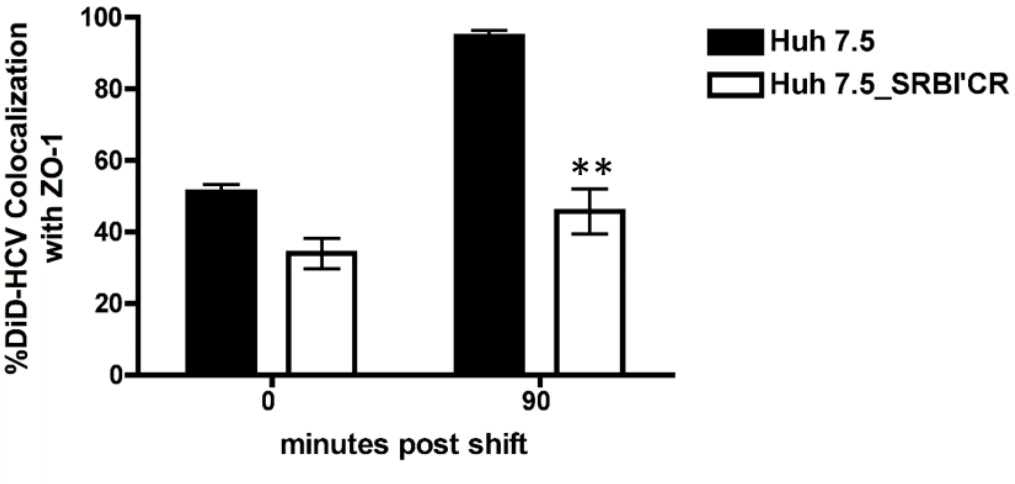

Figure 16. Cells lacking SR-BI show a defect in localization to the tight junction. Huh-7.5 wild type and SR-BI-CR organoids were infected with DiD-HCV for 1 hour at 4^{o}C, shifted to 37^{o}C for 0 and 90 minutes, fixed, and probed with ZO-1. Graph shows percentage of DiD-HCV particles colocalized with ZO-1. n=total DiD signal; mean +/- SD. **p<0.01.

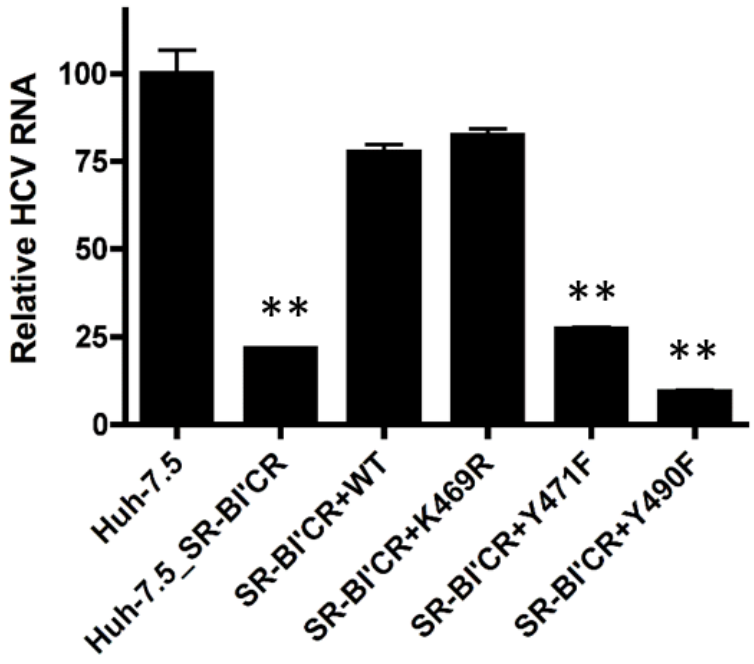

Figure 17. SR-BI Tyrosine residues are required for HCV Entry. Wild type, SR-BI'CR, or complemented cells were seeded onto 96 well plates, infected with HCVcc for 48 hours then analyzed for relative HCV RNA levels. error bars=SD. **p<0.01.

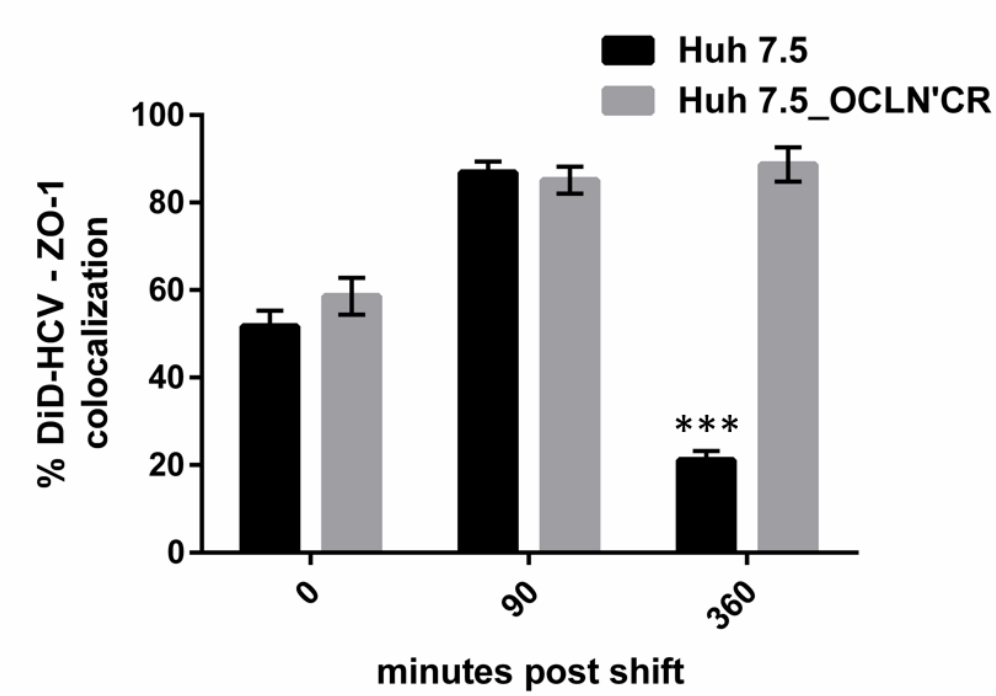

Figure 18. DiD-HCV does not internalize in cells lacking OCLN. Huh-7.5 wild type and OCLN-CR organoids were infected with DiD-HCV for 1 hour at 4ºC, shifted to 37ºC for 0, 90, and 360 minutes, fixed, and probed with ZO-1. Graph shows percentage of DiD-HCV particles colocalized with ZO-1. n=total DiD signal; mean +/- SD. ***p<0.001.

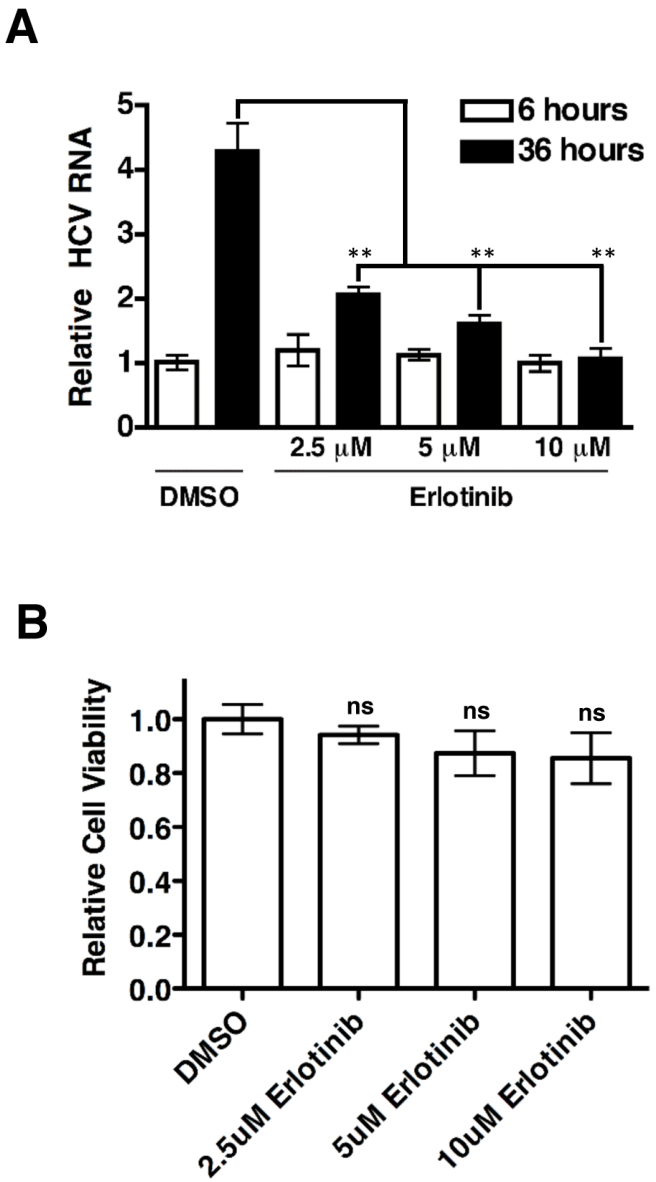

Figure 19. HCV requires EGFR activation for infection. (A, B) Huh-7.5 organoids were incubated with the indicated concentrations of Erlotinib for 2 hours, infected with HCVcc for 6 hours; cells were recovered using Matrigel cell recovery media at 6 and 36 hours and quantified for (A) Relative HCV RNA levels or (B) Cell viability. **p<0.01

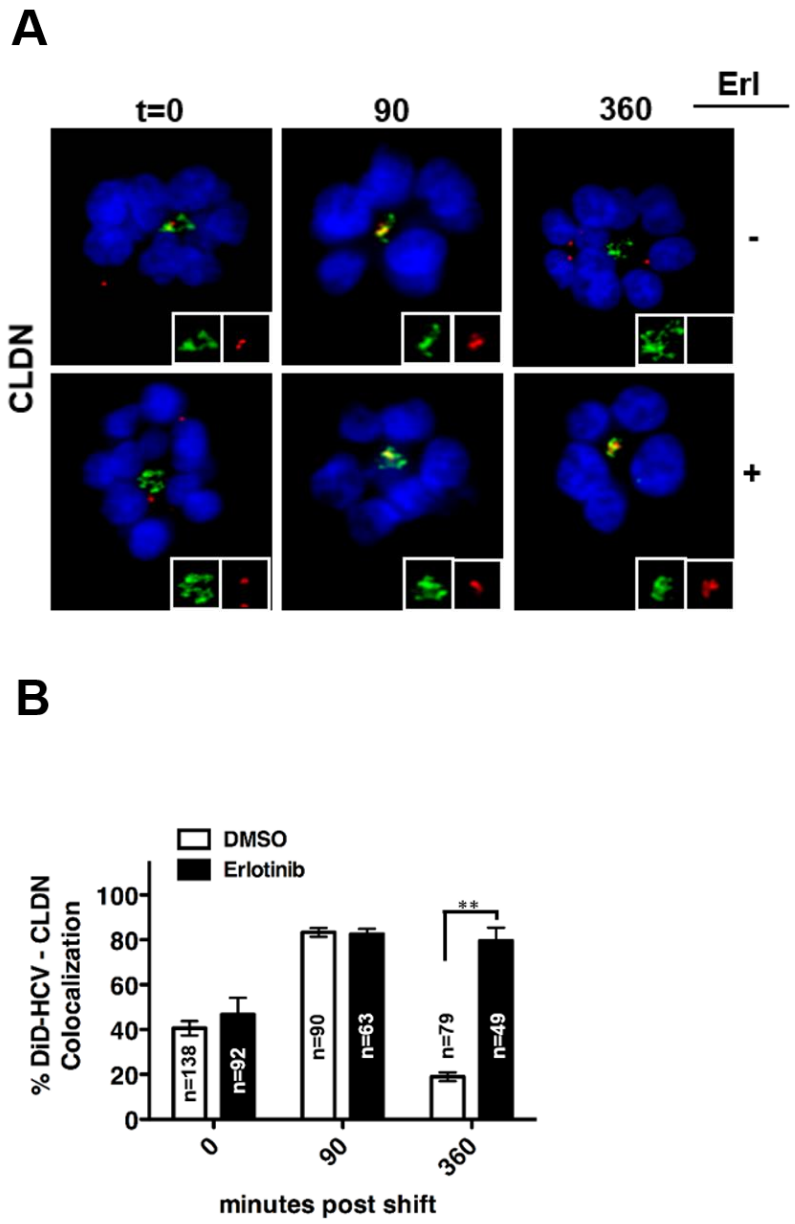

Figure 20. Inhibition of EGFR signaling with erlotinib prevents internalization but not tight junctional localization of DiD-HCV. Huh-7.5 organoids were incubated with 15 uM Erlotinib (Erl) or DMSO for 1 hour, infected with DiD-HCV for 1 hour at 4ºC, shifted to 37ºC for the indicated times, fixed, and probed for Claudin-1. (A) Tight junction region is shown in the inset. Left: Claudin (green), Right: DiD-HCV (red). (B) Quantitation of (A). n=total DiD signal, mean +/- SD. **p<0.01.

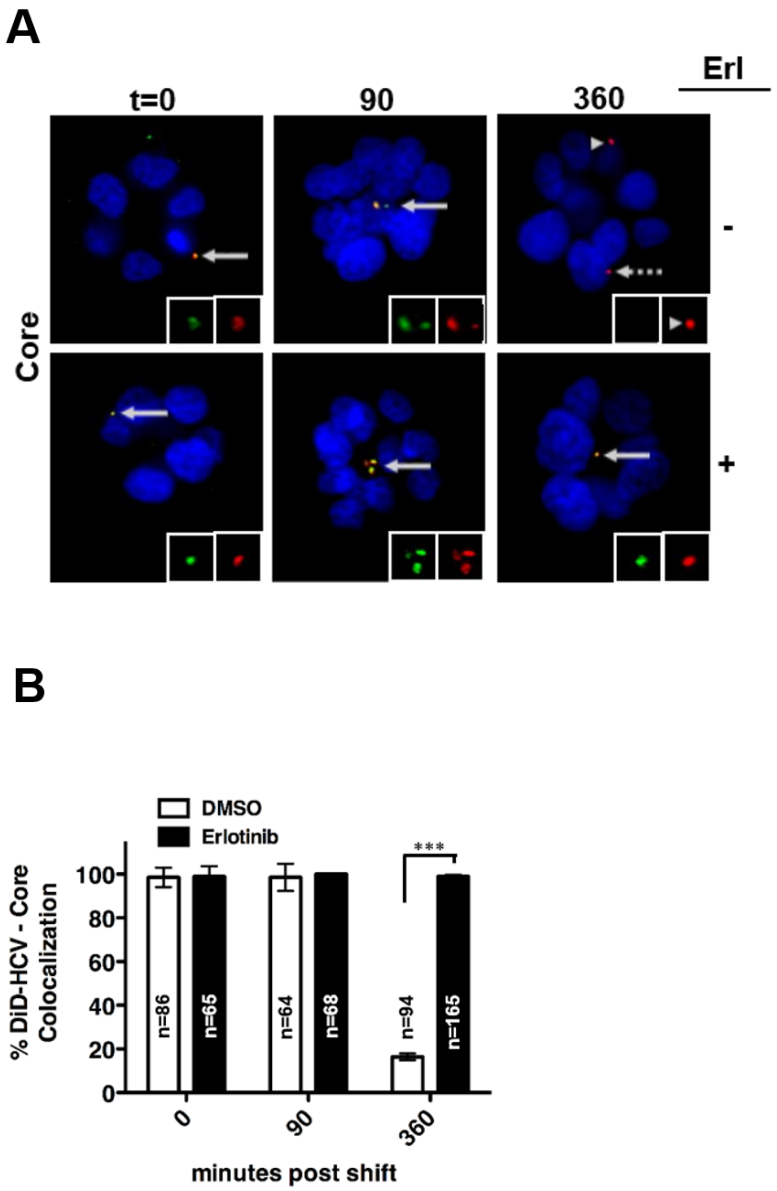

Figure 21. Inhibition of EGFR signaling with erlotinib blocks uncoating. Huh-7.5 organoids were incubated with 15 uM Erlotinib (Erl) or DMSO for 1 hour, infected with DiD-HCV for 1 hour at 4ºC, shifted to 37ºC for the indicated times, fixed, and probed for Core (A) Arrows indicate DiD-HCV particles enlarged in insets, dashed arrows and arrowhead represent colocalization with Core. Left: Core (green), Right: DiD-HCV (red). Lack of DiD-HCV colocalization with Core antibody, seen in DMSO treated cluster at 360 minutes post shift, indicates an uncoating event. (B) Quantitation of (A). n=total DiD signal, mean +/- SD. ***p<0.001

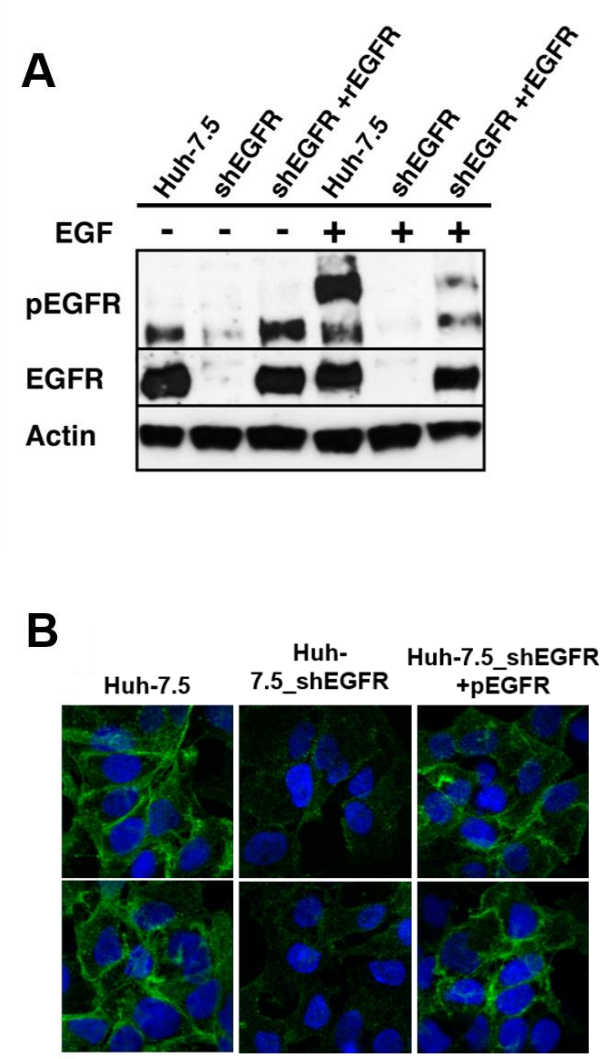

Figure 22. Complementation restores EGFR expression and signaling in Huh-7.5_shEGFR cells. (A) Huh-7.5, shEGFR, and shEGFR+pEGFR cells were seeded into 6 well plates, serum starved, treated +/- EGF, lysed, and analyzed by immunoblot with indicated antibodies. (B) Huh-7.5, shEGFR, and shEGFR+pEGFR cells were seeded onto coverslips in 24-well plates, fixed, and stained for EGFR expression.

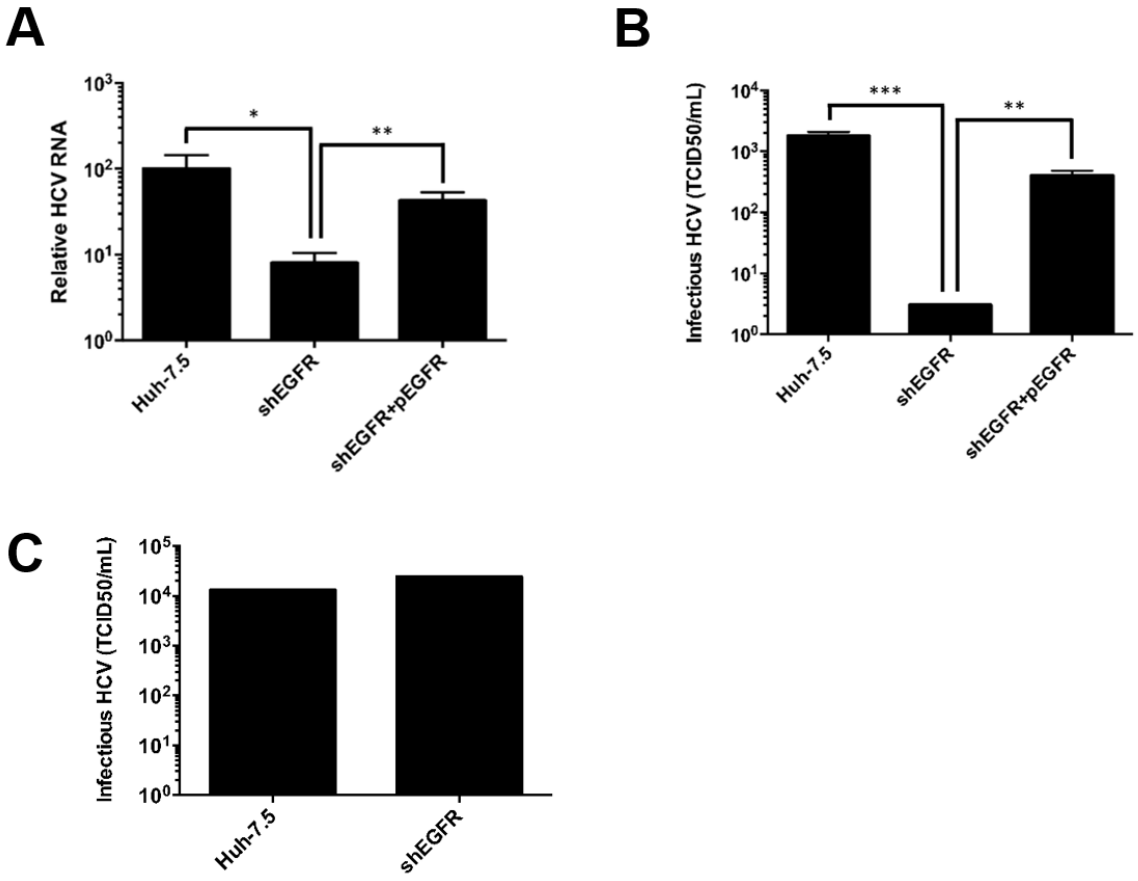

Figure 23. EGFR complementation restores HCV infection. Huh-7.5, shEGFR, and shEGFR+pEGFR cells were infected with HCVcc for 24 hours and analyzed for (A) relative HCV RNA levels or (B) infectious virus production. mean +/- SD. *$p<0.05$. (C) Huh-7.5 or Huh-7.5_shEGFR were electroporated with HCV RNA, maintained 48 hours, and infectious extra-cellular HCV was quantified **$p<0.01$. ***$p<0.001$

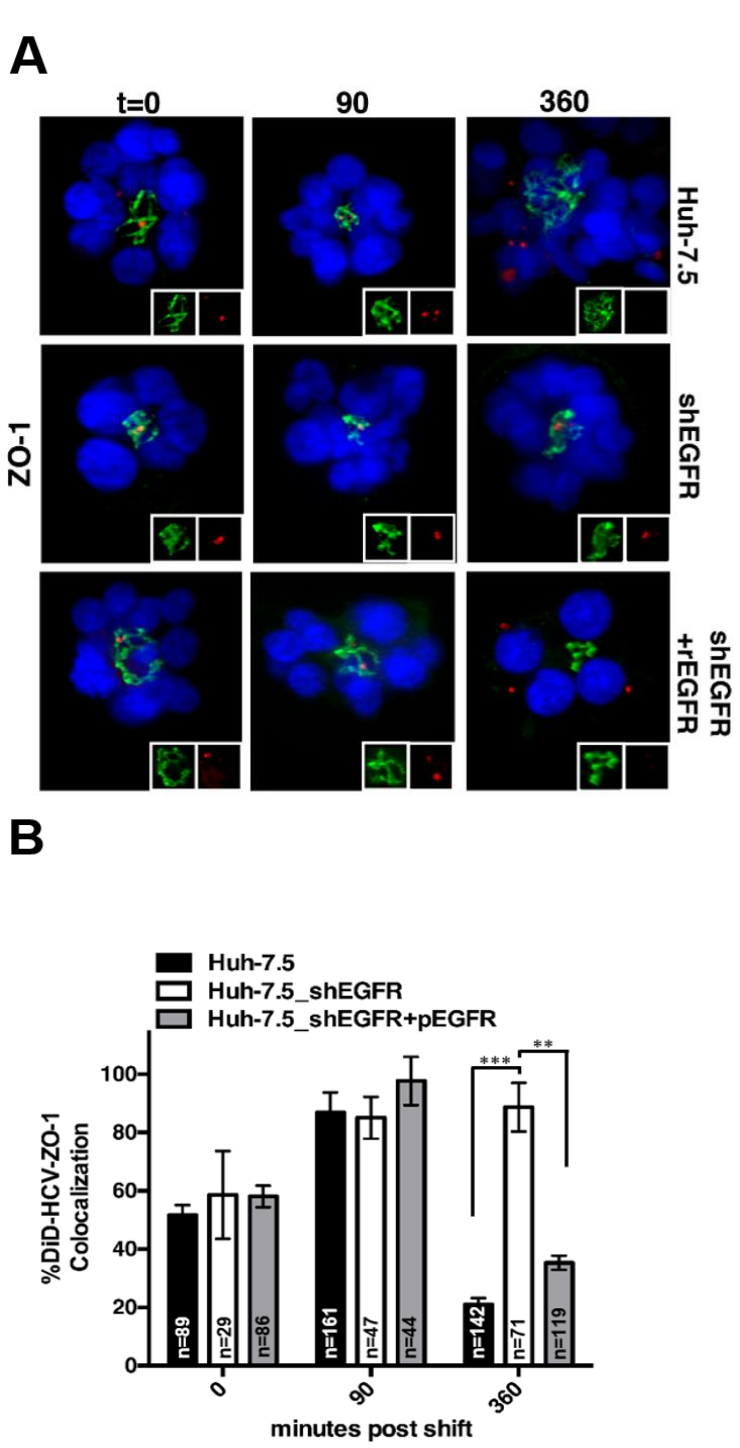

Figure 24. Knockdown of EGFR prevents internalization but not tight junctional localization of DiD-HCV. Matrigel was seeded with either wild type Huh-7.5, shEGFR, or shEGFR+pEGFR cells. Huh-7.5 organoids were infected with DiD-HCV for 1 hour at 4ºC, shifted to 37ºC for the indicated times, fixed, and probed for ZO-1. (A) Tight junction region is shown in the inset. Left: ZO-1 (green), Right: DiD-HCV (red). (B) Quantitation of (A). n=total DiD signal, mean +/- SD. **p<0.01. ***p<0.001

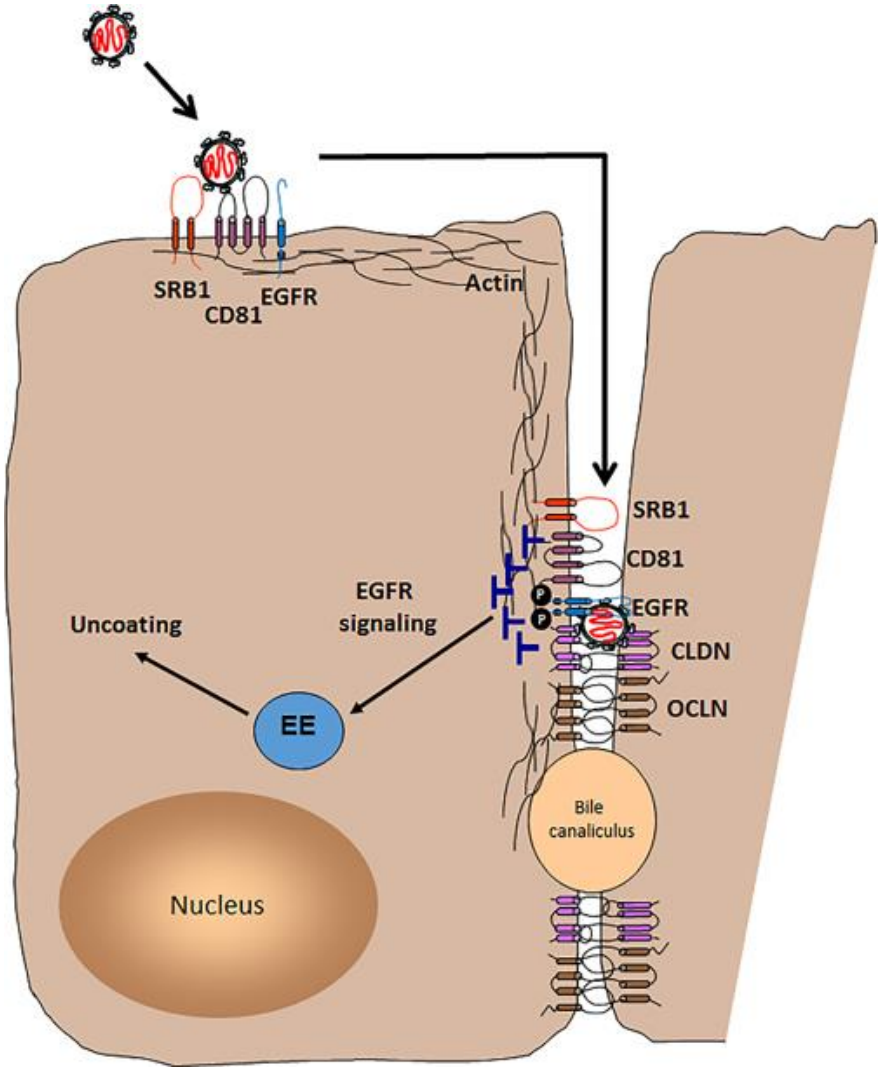

Figure 25. Proposed model of HCV entry into polarized hepatocytes. HCV most likely first associates with hepatocytes via low-affinity interactions of the virion-associated ApoE with various attachment factors (such as LDLR, heparan sulfate, and Syndecan-1). Following attachment, HCV E2 binds SR-BI and CD81. The HCV-receptor complex also associates with EGFR at the basolateral membrane, potentially mediated by CD81. This complex then migrates to the tight junction, requiring actin but not EGFR signaling. At the tight junction, the virus can now associate with CLDN1 and OCLN, promoting internalization of the virus.

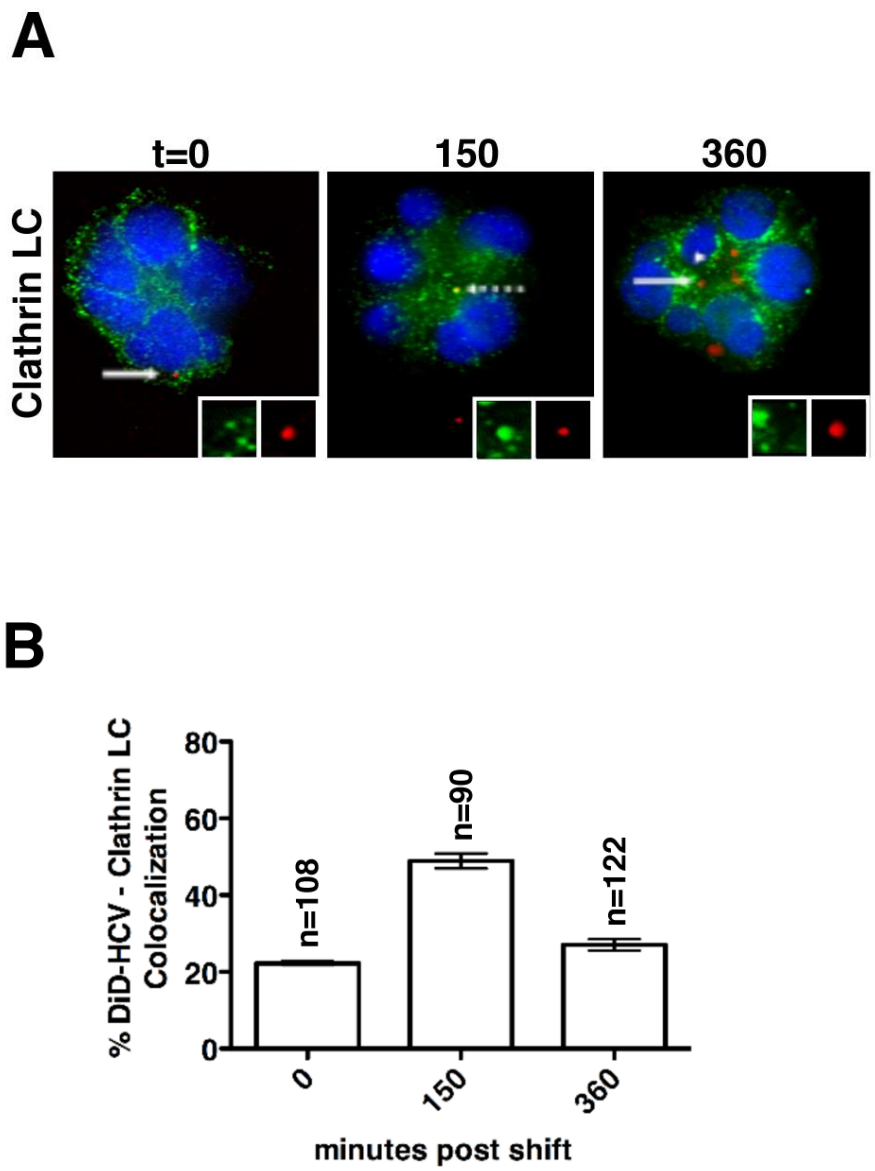

Figure 26. DiD-HCV is internalized via clathrin mediated endocytosis. Huh-7.5 organoids were infected with DiD-HCV for 1 hour 4^{o}C, shifted to 37^{o}C for the indicated times, fixed, and probed for Clathrin LC. Arrow indicates area enlarged in inset. Dashed arrows and arrowhead mark DiD particles colocalized with Clathrin LC. (B) Quantification of (A). n=total DiD signal, mean +/- SD.

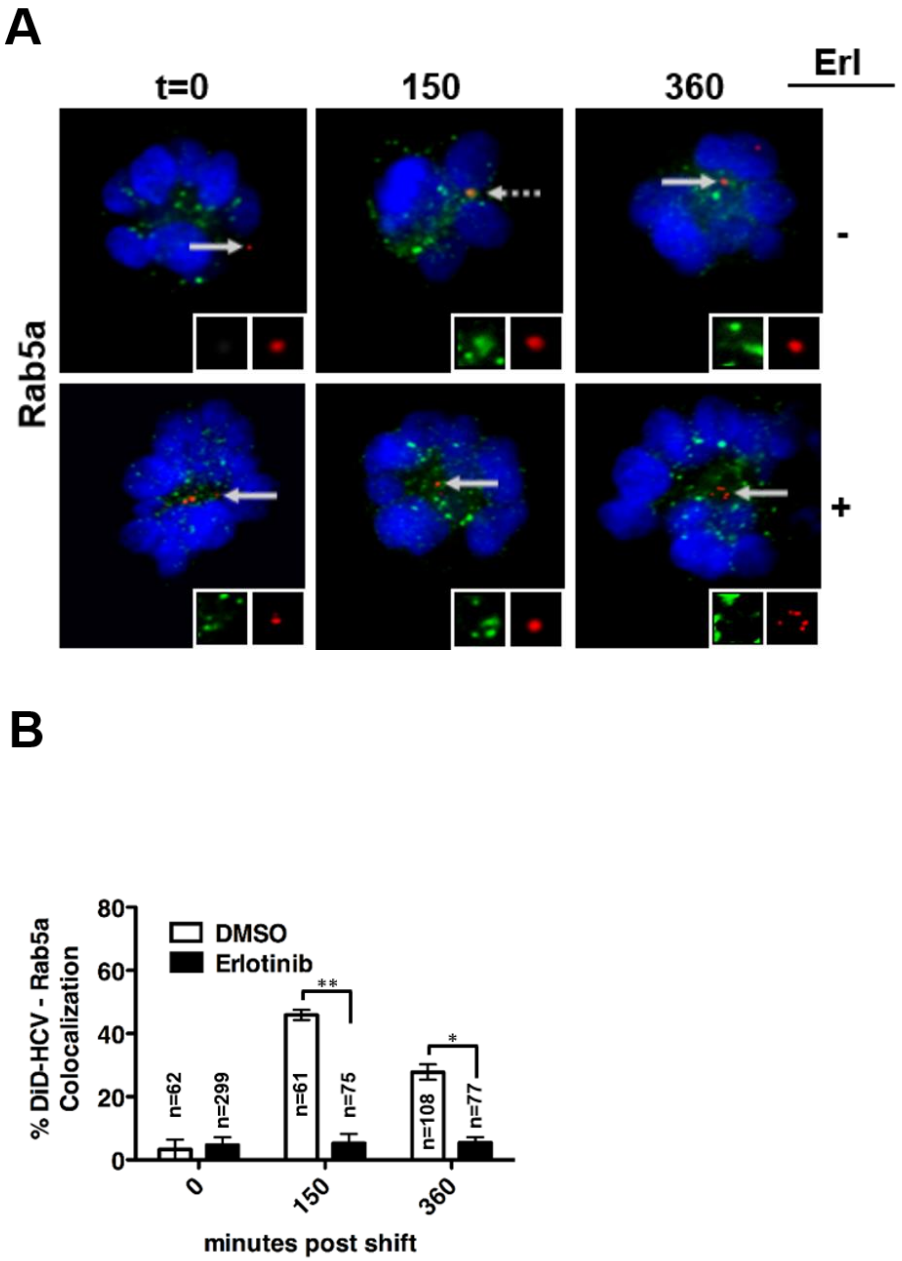

Figure 27. HCV traffics in Rab5a-positive endosomes. Huh-7.5 organoids were incubated with either erlotinib or vehicle control (VC) for 1 hour, infected with DiD-HCV for 1 hour at 4°C, shifted to 37°C for stated times, fixed, and probed for Rab5a, in green. Arrows mark areas enlarged in insets; dashed arrows and arrowheads denote colocalization with labeled host factor. (B) Quantitation of (A). n=total DiD signal, error bars=SD. *p<0.05, **p<0.01

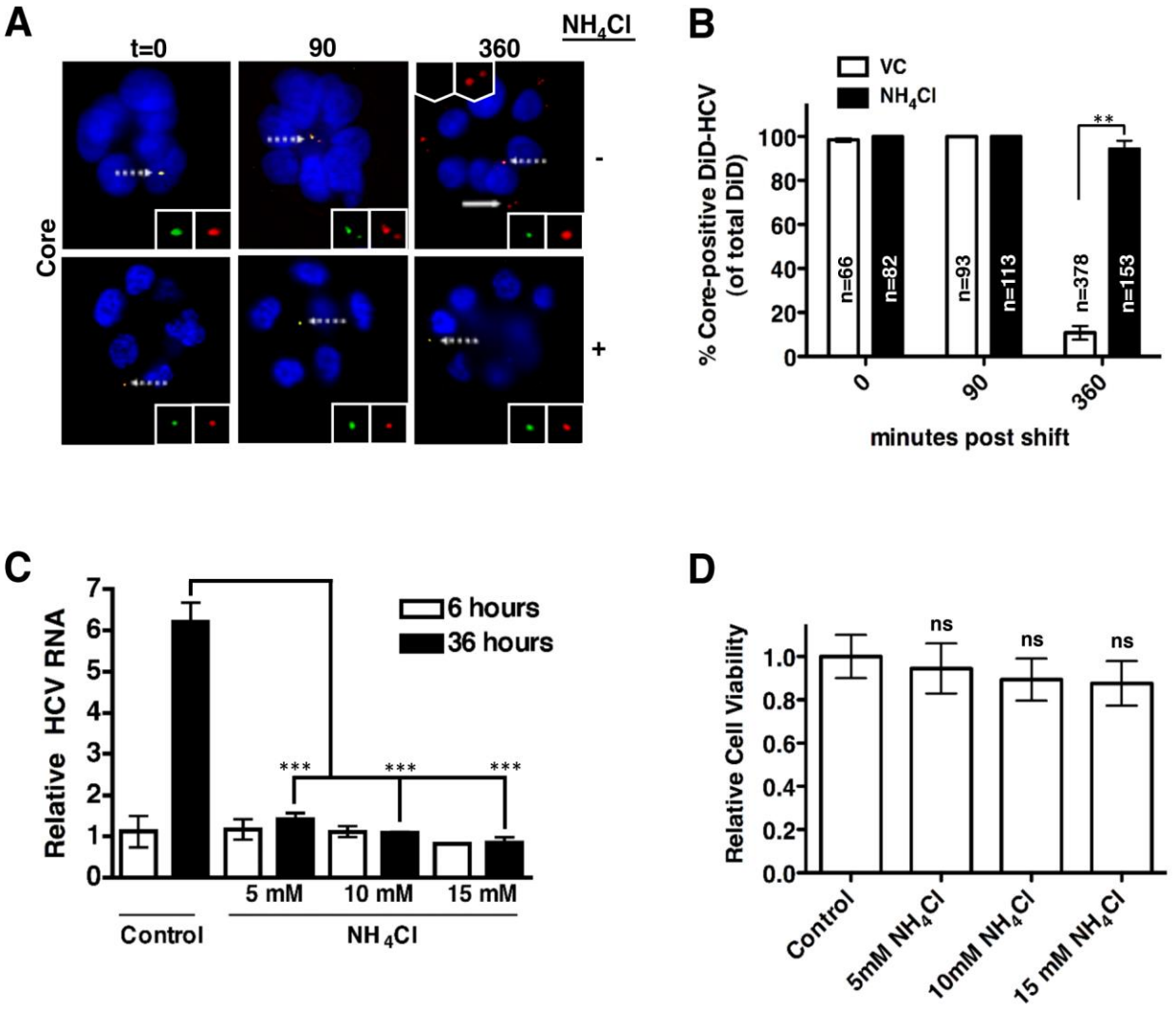

Figure 28. DID-HCV requires endosomal acidification for capsid release. (A, B) Huh-7.5 organoids were incubated with NH_4Cl, or vehicle control (VC) for 1 hour, then infected with DiD-HCV for 1 hour at 4°C, shifted to 37°C for the indicated times, fixed, and (A) probed for Core and (B) Quantified. Arrows denote area enlarged in inset. Lower square insets, indicated by dashed arrows, display core-positive particles, with core staining in green. Upper inset is indicated by solid arrow and shows uncoated particles. (C, D) Huh-7.5 organoids were pretreated for 2 hours with the indicated concentration of NH_4Cl, then infected with HCVcc. Using Matrigel cell recovery media, cells were harvested at 6 and 36 hpi and (C) relative HCV RNA levels and (D) cell viability were quantified. n=total DiD signal, error bars=SD. **p<0.01. ***p<0.001.

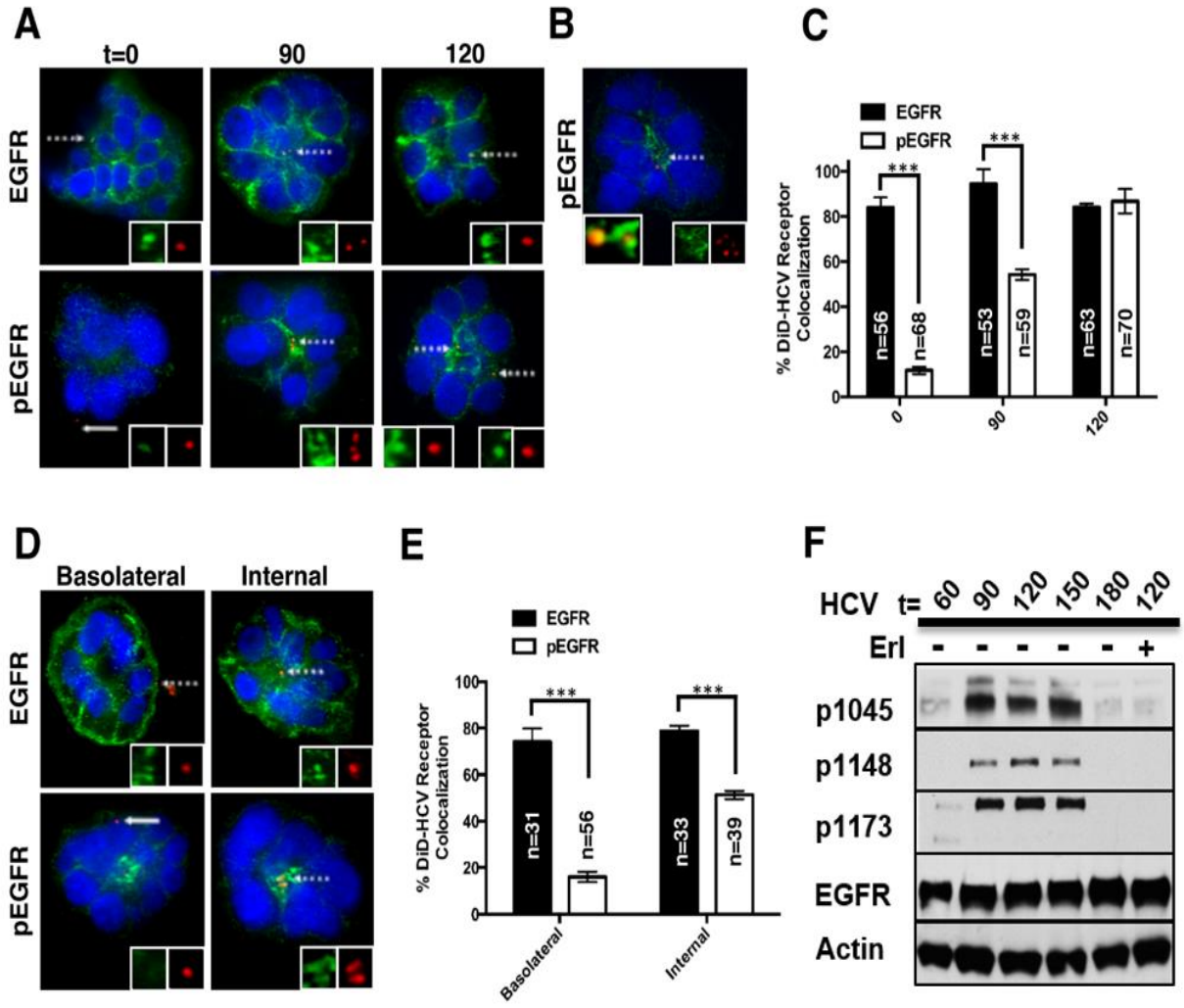

Figure 29. Activated EGFR is associated with DID-HCV at the tight junction prior to internalization. (A-E) Huh-7.5 organoids were infected with DiD-HCV for 1 hour at 4^{o}C, shifted to 37^{o}C for the indicated times, fixed, and probed for either total EGFR or phospho-EGFR 1045. (A, B, D) Arrows indicate area enlarged in insets; dashed arrows indicate DiD colocalization. (A) DiD-HCV colocalization over a time course of infection. (B) DiD-HCV colocalization with phospho-EGFR at 120 minutes post shift. Lower inset is merged and enlarged in upper inset. (D) DiD-HCV colocalization at 0 minutes post shift, analyzed for localization of DiD-HCV particles. (C,E) Quantification of (A) and (C), respectively. (F) Huh-7.5 organoids were serum starved, infected with concentrated HCV for 1 hour at 4^{o}C, shifted to 37^{o}C, then processed with Matrigel cell recovery solution and lysed at the indicated times. Lysate samples were immunoblotted for the specified proteins. n=total DiD signal, mean +/- SD. ***p<0.001.

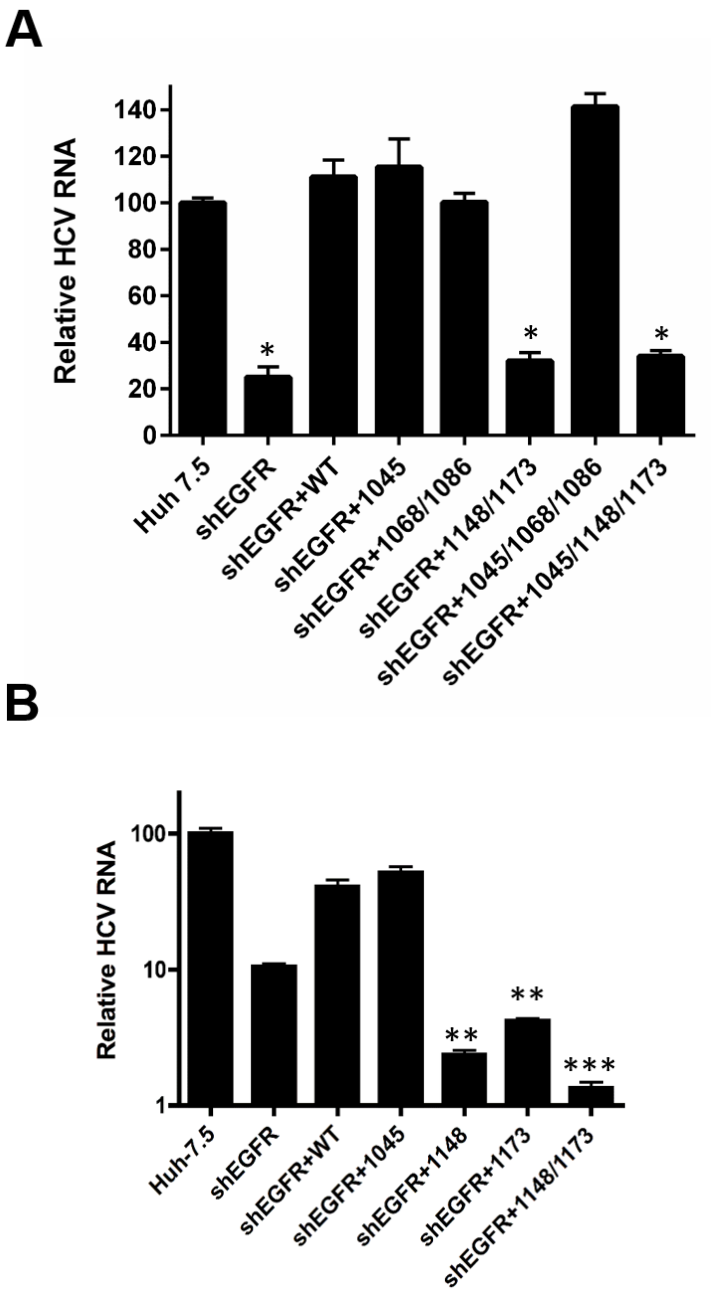

Figure 30. EGFR tyrosine residues are required for HCV infection. Wild type, shEGFR, or complemented cells were seeded onto 96 well plates, infected with HCVcc for 48 hours then analyzed for relative HCV RNA levels. (A) Complementation with double and triple mutants. (B) Complementation with single and double mutants. error bars=SD. *p<0.01. **p<0.01. ***p<0.001.

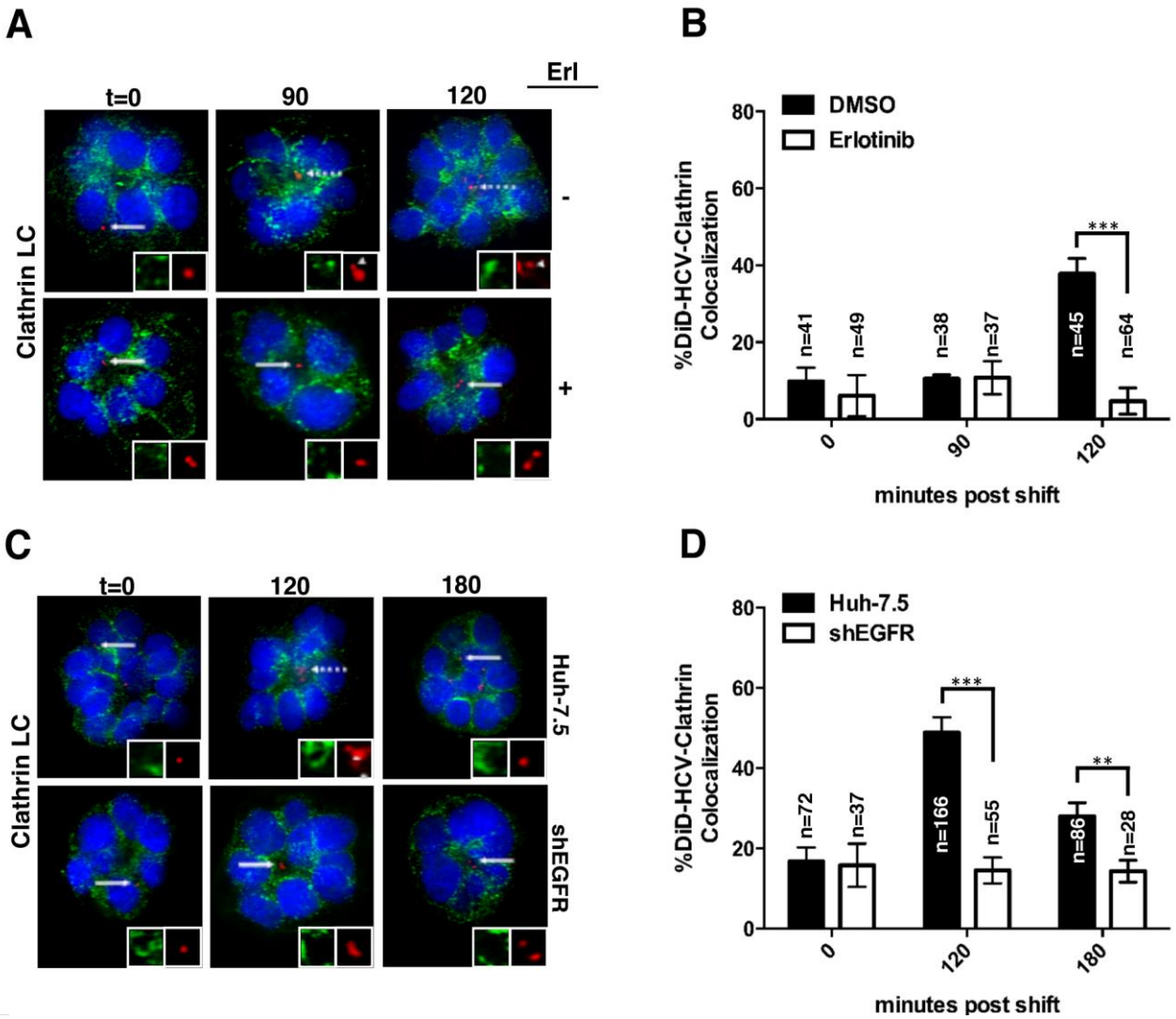

Figure 31. HCV requires EGFR for colocalization with clathrin. (A, B) Huh-7.5 organoids were incubated with either erlotinib or vehicle control (DMSO) for 1 hour, if indicated, infected with DiD-HCV for 1 hour at 4^{o}C, shifted to 37^{o}C for stated times, fixed, and probed for Clathrin light chain (Clathrin LC) (A,C) in green. Arrows mark areas enlarged in insets; dashed arrows and arrowheads denote colocalization with labeled host factor. (C) Organoids seeded with Huh-7.5 or Huh-7.5_shEGFR cells were infected with DiD-HCV as above, then fixed and stained for Clathrin LC. (B, D) Quantitation of A and E respectively. n=total DiD signal, error bars=SD. *p<0.05, **p<0.01, ***p<0.001.

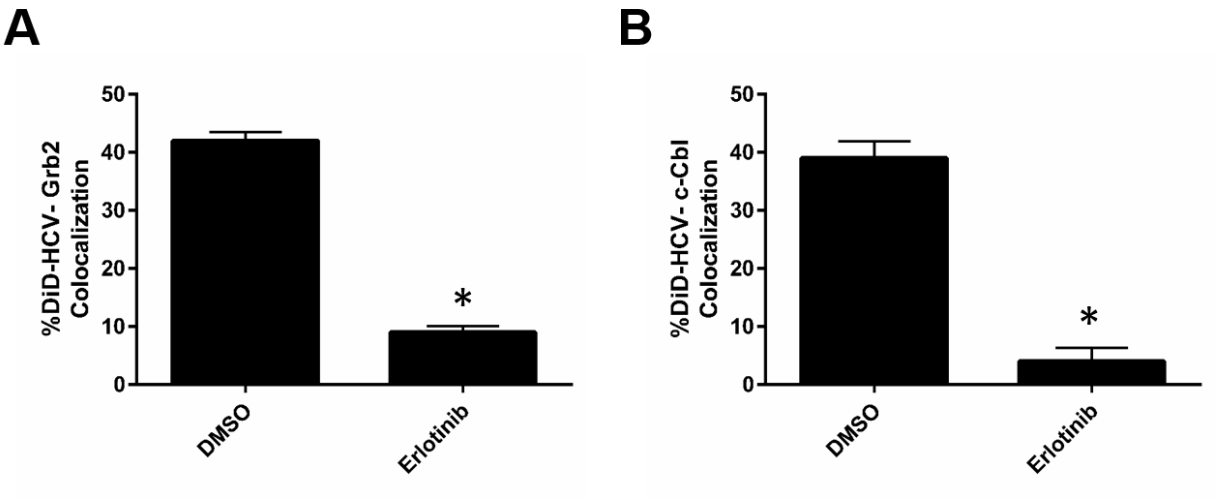

Figure 32. EGFR signaling is required for colocalization with components of the clathrin endocytic machinery. Huh-7.5 organoids were incubated with either erlotinib or vehicle control (DMSO) for 1 hour, infected with DiD-HCV for 1 hour at 4ºC, shifted to 37ºC for 2 hours, fixed, and probed for Grb2 (A) or c-Cbl (B) and quantified for colocalization with the indicated adaptor. error bars=SD. *$p<0.05$.

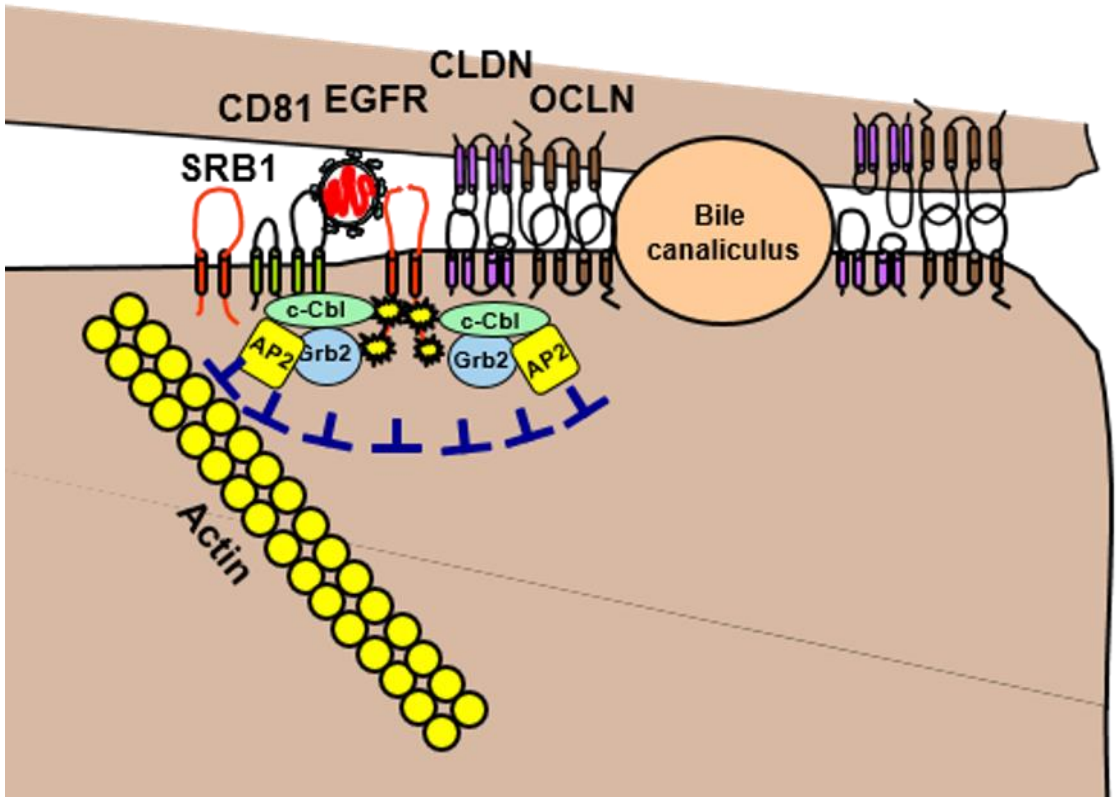

Figure 33. Model of EGFR Internalization. Once at the tight junction, EGFR activation leads to phosphorylation of residues on its cytoplasmic tail (notably 1148 and 1173). Phosphorylation leads to recruitment of various components of the clathrin machinery and eventual internalization via clathrin-mediated endocytosis.

BIBLIOGRAPHY

Ader, M., and Tanaka, E.M. (2014). Modeling human development in 3D culture. Curr Opin Cell Biol *31*, 23-28.

Afdhal, N., Zeuzem, S., Kwo, P., Chojkier, M., Gitlin, N., Puoti, M., Romero-Gomez, M., Zarski, J.P., Agarwal, K., Buggisch, P., *et al.* (2014). Ledipasvir and sofosbuvir for untreated HCV genotype 1 infection. N Engl J Med *370*, 1889-1898.

Agnello, V., Abel, G., Elfahal, M., Knight, G.B., and Zhang, Q.X. (1999). Hepatitis C virus and other Flaviviridae viruses enter cells via low density lipoprotein receptor. Proc Natl Acad Sci U S A *96*, 12766-12771.

Albecka, A., Belouzard, S., Op de Beeck, A., Descamps, V., Goueslain, L., Bertrand-Michel, J., Terce, F., Duverlie, G., Rouille, Y., and Dubuisson, J. (2012). Role of low-density lipoprotein receptor in the hepatitis C virus life cycle. Hepatology *55*, 998-1007.

Andre, P., Komurian-Pradel, F., Deforges, S., Perret, M., Berland, J.L., Sodoyer, M., Pol, S., Brechot, C., Paranhos-Baccala, G., and Lotteau, V. (2002). Characterization of Low- and Very-Low-Density Hepatitis C Virus RNA-Containing Particles. Journal of Virology *76*, 6919-6928.

Bankwitz, D., Steinmann, E., Bitzegeio, J., Ciesek, S., Friesland, M., Herrmann, E., Zeisel, M.B., Baumert, T.F., Keck, Z.Y., Foung, S.K., *et al.* (2010). Hepatitis C virus hypervariable region 1 modulates receptor interactions, conceals the CD81 binding site, and protects conserved neutralizing epitopes. J Virol *84*, 5751-5763.

Bartenschlager, R., Penin, F., Lohmann, V., and Andre, P. (2011). Assembly of infectious hepatitis C virus particles. Trends Microbiol *19*, 95-103.

Bartfeld, S., Bayram, T., van de Wetering, M., Huch, M., Begthel, H., Kujala, P., Vries, R., Peters, P.J., and Clevers, H. (2015). In vitro expansion of human gastric epithelial stem cells and their responses to bacterial infection. Gastroenterology *148*, 126-136 e126.

Barth, H., Schafer, C., Adah, M.I., Zhang, F., Linhardt, R.J., Toyoda, H., Kinoshita-Toyoda, A., Toida, T., Van Kuppevelt, T.H., Depla, E., *et al.* (2003). Cellular binding of hepatitis C virus envelope glycoprotein E2 requires cell surface heparan sulfate. The Journal of biological chemistry *278*, 41003-41012.

Barth, H., Schnober, E.K., Zhang, F., Linhardt, R.J., Depla, E., Boson, B., Cosset, F.L., Patel, A.H., Blum, H.E., and Baumert, T.F. (2006). Viral and cellular determinants of the hepatitis C virus envelope-heparan sulfate interaction. J Virol *80*, 10579-10590.

Bartosch, B., and Cosset, F.L. (2009). Studying HCV cell entry with HCV pseudoparticles (HCVpp). Methods Mol Biol *510*, 279-293.

Bartosch, B., Dubuisson, J., and Cosset, F.-L. (2003a). Infectious Hepatitis C Virus Pseudo-particles Containing Functional E1–E2 Envelope Protein Complexes. The Journal of Experimental Medicine *197*, 633-642.

Bartosch, B., Verney, G., Dreux, M., Donot, P., Morice, Y., Penin, F., Pawlotsky, J.M., Lavillette, D., and Cosset, F.L. (2005). An interplay between hypervariable region 1 of the hepatitis C virus E2 glycoprotein, the scavenger receptor BI, and high-density lipoprotein promotes both enhancement of infection and protection against neutralizing antibodies. J Virol *79*, 8217-8229.

Bartosch, B., Vitelli, A., Granier, C., Goujon, C., Dubuisson, J., Pascale, S., Scarselli, E., Cortese, R., Nicosia, A., and Cosset, F.L. (2003b). Cell entry of hepatitis C virus requires a set of co-receptors that include the CD81 tetraspanin and the SR-B1 scavenger receptor. The Journal of biological chemistry *278*, 41624-41630.

Batzer, A.G., Rotin, D., Urena, J.M., Skolnik, E.Y., and Schlessinger, J. (1994). Hierarchy of binding sites for Grb2 and Shc on the epidermal growth factor receptor. Mol Cell Biol *14*, 5192-5201.

Baumert, T.F., Ito, S., Wong, D.T., and Liang, T.J. (1998). Hepatitis C Virus Structural Proteins Assemble into Viruslike Particles in Insect Cells. Journal of Virology *72*, 3827-3836.

Baumert, T.F., Juhling, F., Ono, A., and Hoshida, Y. (2017). Hepatitis C-related hepatocellular carcinoma in the era of new generation antivirals. BMC Med *15*, 52.

Berger, E.A., Murphy, P.M., and Farber, J.M. (1999). Chemokine receptors as HIV-1 coreceptors: roles in viral entry, tropism, and disease. Annu Rev Immunol *17*, 657-700.

Berger, K.L., Cooper, J.D., Heaton, N.S., Yoon, R., Oakland, T.E., Jordan, T.X., Mateu, G., Grakoui, A., and Randall, G. (2009). Roles for endocytic trafficking and phosphatidylinositol 4-kinase III alpha in hepatitis C virus replication. Proc Natl Acad Sci U S A *106*, 7577-7582.

Bertaux, C., and Dragic, T. (2006). Different domains of CD81 mediate distinct stages of hepatitis C virus pseudoparticle entry. J Virol *80*, 4940-4948.

Bitzegeio, J., Bankwitz, D., Hueging, K., Haid, S., Brohm, C., Zeisel, M.B., Herrmann, E., Iken, M., Ott, M., Baumert, T.F., *et al.* (2010). Adaptation of hepatitis C virus to mouse CD81 permits infection of mouse cells in the absence of human entry factors. PLoS Pathog *6*, e1000978.

Blanchard, E., Belouzard, S., Goueslain, L., Wakita, T., Dubuisson, J., Wychowski, C., and Rouille, Y. (2006). Hepatitis C virus entry depends on clathrin-mediated endocytosis. J Virol *80*, 6964-6972.

Blight, K.J., McKeating, J.A., and Rice, C.M. (2002). Highly Permissive Cell Lines for Subgenomic and Genomic Hepatitis C Virus RNA Replication. Journal of Virology *76*, 13001-13014.

Brimacombe, C.L., Grove, J., Meredith, L.W., Hu, K., Syder, A.J., Flores, M.V., Timpe, J.M., Krieger, S.E., Baumert, T.F., Tellinghuisen, T.L., *et al.* (2011). Neutralizing antibody-resistant hepatitis C virus cell-to-cell transmission. J Virol *85*, 596-605.

Burbelo, P.D., Dubovi, E.J., Simmonds, P., Medina, J.L., Henriquez, J.A., Mishra, N., Wagner, J., Tokarz, R., Cullen, J.M., Iadarola, M.J., *et al.* (2012). Serology-enabled discovery of genetically diverse hepaciviruses in a new host. J Virol *86*, 6171-6178.

Burckhardt, C.J., Suomalainen, M., Schoenenberger, P., Boucke, K., Hemmi, S., and Greber, U.F. (2011). Drifting motions of the adenovirus receptor CAR and immobile integrins initiate virus uncoating and membrane lytic protein exposure. Cell host & microbe *10*, 105-117.

Burgos, P.V., Klattenhoff, C., de la Fuente, E., Rigotti, A., and Gonzalez, A. (2004). Cholesterol depletion induces PKA-mediated basolateral-to-apical transcytosis of the scavenger receptor class B type I in MDCK cells. Proc Natl Acad Sci U S A *101*, 3845-3850.

Catanese, M.T., Ansuini, H., Graziani, R., Huby, T., Moreau, M., Ball, J.K., Paonessa, G., Rice, C.M., Cortese, R., Vitelli, A., *et al.* (2010). Role of scavenger receptor class B type I in hepatitis C virus entry: kinetics and molecular determinants. J Virol *84*, 34-43.

Catanese, M.T., Uryu, K., Kopp, M., Edwards, T.J., Andrus, L., Rice, W.J., Silvestry, M., Kuhn, R.J., and Rice, C.M. (2013). Ultrastructural analysis of hepatitis C virus particles. Proc Natl Acad Sci U S A *110*, 9505-9510.

Chang, K.S., Jiang, J., Cai, Z., and Luo, G. (2007). Human apolipoprotein e is required for infectivity and production of hepatitis C virus in cell culture. J Virol *81*, 13783-13793.

Cheng, J.J., Li, J.R., Huang, M.H., Ma, L.L., Wu, Z.Y., Jiang, C.C., Li, W.J., Li, Y.H., Han, Y.X., Li, H., *et al.* (2016). CD36 is a co-receptor for hepatitis C virus E1 protein attachment. Sci Rep *6*, 21808.

Choe, H., Farzan, M., Sun, Y., Sullivan, N., Rollins, B., Ponath, P.D., Wu, L., Mackay, C.R., LaRosa, G., Newman, W., *et al.* (1996). The β-Chemokine Receptors CCR3 and CCR5 Facilitate Infection by Primary HIV-1 Isolates. Cell *85*, 1135-1148.

Chung, R.T., and Baumert, T.F. (2014). Curing chronic hepatitis C--the arc of a medical triumph. N Engl J Med *370*, 1576-1578.

Codran, A., Royer, C., Jaeck, D., Bastien-Valle, M., Baumert, T.F., Kieny, M.P., Pereira, C.A., and Martin, J.P. (2006). Entry of hepatitis C virus pseudotypes into primary human hepatocytes by clathrin-dependent endocytosis. The Journal of general virology *87*, 2583-2593.

Cohen, C.J., Shieh, J.T., Pickles, R.J., Okegawa, T., Hsieh, J.T., and Bergelson, J.M. (2001). The coxsackievirus and adenovirus receptor is a transmembrane component of the tight junction. Proc Natl Acad Sci U S A *98*, 15191-15196.

Coller, K.E., Berger, K.L., Heaton, N.S., Cooper, J.D., Yoon, R., and Randall, G. (2009). RNA interference and single particle tracking analysis of hepatitis C virus endocytosis. PLoS Pathog *5*, e1000702.

Coller, K.E., Heaton, N.S., Berger, K.L., Cooper, J.D., Saunders, J.L., and Randall, G. (2012). Molecular determinants and dynamics of hepatitis C virus secretion. PLoS Pathog *8*, e1002466.

Cormier, E.G., Tsamis, F., Kajumo, F., Durso, R.J., Gardner, J.P., and Dragic, T. (2004). CD81 is an entry coreceptor for hepatitis C virus. Proc Natl Acad Sci U S A *101*, 7270-7274.

Coyne, C.B., and Bergelson, J.M. (2005). CAR: a virus receptor within the tight junction. Advanced drug delivery reviews *57*, 869-882.

Coyne, C.B., and Bergelson, J.M. (2006). Virus-induced Abl and Fyn kinase signals permit coxsackievirus entry through epithelial tight junctions. Cell *124*, 119-131.

Coyne, C.B., Shen, L., Turner, J.R., and Bergelson, J.M. (2007). Coxsackievirus entry across epithelial tight junctions requires occludin and the small GTPases Rab34 and Rab5. Cell host & microbe *2*, 181-192.

Cukierman, L., Meertens, L., Bertaux, C., Kajumo, F., and Dragic, T. (2009). Residues in a highly conserved claudin-1 motif are required for hepatitis C virus entry and mediate the formation of cell-cell contacts. J Virol *83*, 5477-5484.

Dalgleish, A.G., Beverley, P.C.L., Clapham, P.R., Crawford, D.H., Greaves, M.F., and Weiss, R.A. (1984). The CD4 (T4) antigen is an essential component of the receptor for the AIDS retrovirus. Nature *312*, 763-767.

Dao Thi, V.L., Granier, C., Zeisel, M.B., Guerin, M., Mancip, J., Granio, O., Penin, F., Lavillette, D., Bartenschlager, R., Baumert, T.F., *et al.* (2012). Characterization of hepatitis C virus particle subpopulations reveals multiple usage of the scavenger receptor BI for entry steps. The Journal of biological chemistry *287*, 31242-31257.

Davis, C., Harris, H.J., Hu, K., Drummer, H.E., McKeating, J.A., Mullins, J.G., and Balfe, P. (2012). In silico directed mutagenesis identifies the CD81/claudin-1 hepatitis C virus receptor interface. Cellular microbiology *14*, 1892-1903.

de Haan, C.A., Li, Z., te Lintelo, E., Bosch, B.J., Haijema, B.J., and Rottier, P.J. (2005). Murine coronavirus with an extended host range uses heparan sulfate as an entry receptor. J Virol *79*, 14451-14456.

Deng, H., Liu, R., Ellmeier, W., Choe, S., Unutmaz, D., Burkhart, M., Di Marzio, P., Marmon, S., Sutton, R.E., Hill, C.M., *et al.* (1996). Identification of a major co-receptor for primary isolates of HIV-1. Nature *381*, 661-666.

Diao, J., Pantua, H., Ngu, H., Komuves, L., Diehl, L., Schaefer, G., and Kapadia, S.B. (2012). Hepatitis C Virus Induces Epidermal Growth Factor Receptor Activation via CD81 Binding for Viral Internalization and Entry. J Virol *86*, 10935-10949.

Dorner, M., Horwitz, J.A., Robbins, J.B., Barry, W.T., Feng, Q., Mu, K., Jones, C.T., Schoggins, J.W., Catanese, M.T., Burton, D.R., *et al.* (2011). A genetically humanized mouse model for hepatitis C virus infection. Nature *474*, 208-211.

Douam, F., Dao Thi, V.L., Maurin, G., Fresquet, J., Mompelat, D., Zeisel, M.B., Baumert, T.F., Cosset, F.L., and Lavillette, D. (2014). Critical interaction between E1 and E2 glycoproteins determines binding and fusion properties of hepatitis C virus during cell entry. Hepatology *59*, 776-788.

Dragic, T., Litwin, V., Allaway, G.P., Martin, S.R., Huang, Y., Nagashima, K.A., Cayanan, C., Maddon, P.J., Koup, R.A., Moore, J.P., *et al.* (1996). HIV-1 entry into CD4+ cells is mediated by the chemokine receptor CC-CKR-5. Nature *381*, 667-673.

Dreux, M., Dao Thi, V.L., Fresquet, J., Guerin, M., Julia, Z., Verney, G., Durantel, D., Zoulim, F., Lavillette, D., Cosset, F.L., *et al.* (2009). Receptor complementation and mutagenesis reveal SR-BI as an essential HCV entry factor and functionally imply its intra- and extra-cellular domains. PLoS Pathog *5*, e1000310.

Drost, J., van Jaarsveld, R.H., Ponsioen, B., Zimberlin, C., van Boxtel, R., Buijs, A., Sachs, N., Overmeer, R.M., Offerhaus, G.J., Begthel, H., *et al.* (2015). Sequential cancer mutations in cultured human intestinal stem cells. Nature *521*, 43-47.

Drummer, H.E., Boo, I., and Poumbourios, P. (2007). Mutagenesis of a conserved fusion peptide-like motif and membrane-proximal heptad-repeat region of hepatitis C virus glycoprotein E1. The Journal of general virology *88*, 1144-1148.

Drummer, H.E., Wilson, K.A., and Poumbourios, P. (2002). Identification of the Hepatitis C Virus E2 Glycoprotein Binding Site on the Large Extracellular Loop of CD81. Journal of Virology *76*, 11143-11147.

Easter, D.W., Wade, J.B., and Boyer, J.L. (1983). Structural integrity of hepatocyte tight junctions. The Journal of cell biology *96*, 745-749.

Eierhoff, T., Hrincius, E.R., Rescher, U., Ludwig, S., and Ehrhardt, C. (2010). The epidermal growth factor receptor (EGFR) promotes uptake of influenza A viruses (IAV) into host cells. PLoS Pathog *6*, e1001099.

Evans, M.J., von Hahn, T., Tscherne, D.M., Syder, A.J., Panis, M., Wolk, B., Hatziioannou, T., McKeating, J.A., Bieniasz, P.D., and Rice, C.M. (2007). Claudin-1 is a hepatitis C virus co-receptor required for a late step in entry. Nature *446*, 801-805.

Eyre, N.S., Drummer, H.E., and Beard, M.R. (2010). The SR-BI partner PDZK1 facilitates hepatitis C virus entry. PLoS Pathog *6*, e1001130.

Farquhar, M.J., Hu, K., Harris, H.J., Davis, C., Brimacombe, C.L., Fletcher, S.J., Baumert, T.F., Rappoport, J.Z., Balfe, P., and McKeating, J.A. (2012). Hepatitis C virus induces CD81 and claudin-1 endocytosis. J Virol *86*, 4305-4316.

Fauvelle, C., Colpitts, C.C., Keck, Z.Y., Pierce, B.G., Foung, S.K., and Baumert, T.F. (2016). Hepatitis C virus vaccine candidates inducing protective neutralizing antibodies. Expert Rev Vaccines *15*, 1535-1544.

Fehon, R.G., McClatchey, A.I., and Bretscher, A. (2010). Organizing the cell cortex: the role of ERM proteins. Nature reviews Molecular cell biology *11*, 276-287.

Feng, Y., Broder, C.C., Kennedy, P.E., and Berger, E.A. (1996). HIV-1 Entry Cofactor: Functional cDNA Cloning of a Seven-Transmembrane, G Protein-Coupled Receptor. Science *272*, 872-877.

Fofana, I., Zona, L., Thumann, C., Heydmann, L., Durand, S.C., Lupberger, J., Blum, H.E., Pessaux, P., Gondeau, C., Reynolds, G.M., *et al.* (2013). Functional analysis of claudin-6 and claudin-9 as entry factors for hepatitis C virus infection of human hepatocytes by using monoclonal antibodies. J Virol *87*, 10405-10410.

Freed, E.O. (2015). HIV-1 assembly, release and maturation. Nat Rev Microbiol *13*, 484-496.

Gastaminza, P., Cheng, G., Wieland, S., Zhong, J., Liao, W., and Chisari, F.V. (2008). Cellular determinants of hepatitis C virus assembly, maturation, degradation, and secretion. J Virol *82*, 2120-2129.

Gastaminza, P., Dryden, K.A., Boyd, B., Wood, M.R., Law, M., Yeager, M., and Chisari, F.V. (2010). Ultrastructural and biophysical characterization of hepatitis C virus particles produced in cell culture. J Virol *84*, 10999-11009.

Gastaminza, P., Kapadia, S.B., and Chisari, F.V. (2006). Differential biophysical properties of infectious intracellular and secreted hepatitis C virus particles. J Virol *80*, 11074-11081.

Gerold, G., Meissner, F., Bruening, J., Welsch, K., Perin, P.M., Baumert, T.F., Vondran, F.W., Kaderali, L., Marcotrigiano, J., Khan, A.G., *et al.* (2015). Quantitative Proteomics Identifies Serum Response Factor Binding Protein 1 as a Host Factor for Hepatitis C Virus Entry. Cell Rep *12*, 864-878.

Glomb-Reinmund, S., and Kielian, M. (1998). The role of low pH and disulfide shuffling in the entry and fusion of Semliki Forest virus and Sindbis virus. Virology *248*, 372-381.

Gower, E., Estes, C., Blach, S., Razavi-Shearer, K., and Razavi, H. (2014). Global epidemiology and genotype distribution of the hepatitis C virus infection. J Hepatol *61*, S45-57.

Greggio, C., De Franceschi, F., Figueiredo-Larsen, M., Gobaa, S., Ranga, A., Semb, H., Lutolf, M., and Grapin-Botton, A. (2013). Artificial three-dimensional niches deconstruct pancreas development in vitro. Development *140*, 4452-4462.

Greulich, H., Chen, T.H., Feng, W., Janne, P.A., Alvarez, J.V., Zappaterra, M., Bulmer, S.E., Frank, D.A., Hahn, W.C., Sellers, W.R., *et al.* (2005). Oncogenic transformation by inhibitor-sensitive and -resistant EGFR mutants. PLoS Med *2*, e313.

Grove, J., and Marsh, M. (2011). The cell biology of receptor-mediated virus entry. The Journal of cell biology *195*, 1071-1082.

Hagios, C., Lochter, A., and Bissell, M.J. (1998). Tissue architecture: the ultimate regulator of epithelial function? Philos Trans R Soc Lond B Biol Sci *353*, 857-870.

Haid, S., Pietschmann, T., and Pecheur, E.I. (2009). Low pH-dependent hepatitis C virus membrane fusion depends on E2 integrity, target lipid composition, and density of virus particles. The Journal of biological chemistry *284*, 17657-17667.

Harris, H.J., Davis, C., Mullins, J.G., Hu, K., Goodall, M., Farquhar, M.J., Mee, C.J., McCaffrey, K., Young, S., Drummer, H., *et al.* (2010). Claudin association with CD81 defines hepatitis C virus entry. The Journal of biological chemistry *285*, 21092-21102.

Harris, H.J., Farquhar, M.J., Mee, C.J., Davis, C., Reynolds, G.M., Jennings, A., Hu, K., Yuan, F., Deng, H., Hubscher, S.G., *et al.* (2008). CD81 and claudin 1 coreceptor association: role in hepatitis C virus entry. J Virol *82*, 5007-5020.

Harrison, S.C. (2005). Mechanism of Membrane Fusion by Viral Envelope Proteins. *64*, 231-261.

Helenius, A. (1980). On the entry of semliki forest virus into BHK-21 cells. The Journal of cell biology *84*, 404-420.

Herbst, R.S. (2004). Review of epidermal growth factor receptor biology. Int J Radiat Oncol Biol Phys *59*, 21-26.

Hewlett, L.J. (1994). The coated pit and macropinocytic pathways serve distinct endosome populations. The Journal of cell biology *124*, 689-703.

Higginbottom, A., Quinn, E.R., Kuo, C.C., Flint, M., Wilson, L.H., Bianchi, E., Nicosia, A., Monk, P.N., McKeating, J.A., and Levy, S. (2000). Identification of Amino Acid Residues in CD81 Critical for Interaction with Hepatitis C Virus Envelope Glycoprotein E2. Journal of Virology *74*, 3642-3649.

Hijikata, M., Shimizu, Y.K., Kato, H., Iwamoto, A., Shih, J.W., Alter, H.J., Purcell, R.H., and Yoshikura, H. (1993). Equilibrium centrifugation studies of hepatitis C virus: evidence for circulating immune complexes. J Virol *67*, 1953-1958.

Hishiki, T., Shimizu, Y., Tobita, R., Sugiyama, K., Ogawa, K., Funami, K., Ohsaki, Y., Fujimoto, T., Takaku, H., Wakita, T., *et al.* (2010). Infectivity of hepatitis C virus is influenced by association with apolipoprotein E isoforms. J Virol *84*, 12048-12057.

Hofer, F., Gruenberger, M., Kowalski, H., Machat, H., Huettinger, M., Kuechler, E., and Blass, D. (1994). Members of the low density lipoprotein receptor family mediate cell entry of a minor-group common cold virus. Proceedings of the National Academy of Sciences *91*, 1839-1842.

Hogle, J.M. (2002). Poliovirus cell entry: common structural themes in viral cell entry pathways. Annu Rev Microbiol *56*, 677-702.

Honda, M., Beard, M.R., Ping, L., and Lemon, S.M. (1999). A phylogenetically conserved stem-loop structure at the 5' border of the internal ribosome entry site of hepatitis C virus is required for cap-independent viral translation. Journal of Virology *73*, 1165-1174.

Hopcraft, S.E., and Evans, M.J. (2015). Selection of a hepatitis C virus with altered entry factor requirements reveals a genetic interaction between the E1 glycoprotein and claudins. Hepatology *62*, 1059-1069.

Hoshida, Y., Fuchs, B.C., Bardeesy, N., Baumert, T.F., and Chung, R.T. (2014). Pathogenesis and prevention of hepatitis C virus-induced hepatocellular carcinoma. J Hepatol *61*, S79-90.

Hsu, M., Zhang, J., Flint, M., Logvinoff, C., Cheng-Mayer, C., Rice, C.M., and McKeating, J.A. (2003). Hepatitis C virus glycoproteins mediate pH-dependent cell entry of pseudotyped retroviral particles. Proc Natl Acad Sci U S A *100*, 7271-7276.

Huang, H., Sun, F., Owen, D.M., Li, W., Chen, Y., Gale, M., Jr., and Ye, J. (2007). Hepatitis C virus production by human hepatocytes dependent on assembly and secretion of very low-density lipoproteins. Proc Natl Acad Sci U S A *104*, 5848-5853.

Huch, M., Dorrell, C., Boj, S.F., van Es, J.H., Li, V.S., van de Wetering, M., Sato, T., Hamer, K., Sasaki, N., Finegold, M.J., *et al.* (2013). In vitro expansion of single Lgr5+ liver stem cells induced by Wnt-driven regeneration. Nature *494*, 247-250.

Jamil, H., Chu, C.-H., Dickson Jr., J.K., Chen, T., Yan, M., Biller, S.A., Gregg, R.E., Wetterau, J.R., and Gordon, D.A. (1998). Evidence that microsomal triglyceride transfer protein is limiting in the production of apolipoprotein B-containing lipoproteins in hepatic cells. Journal of lipid research *39*, 1448-1454.

Jiang, J., Cun, W., Wu, X., Shi, Q., Tang, H., and Luo, G. (2012). Hepatitis C virus attachment mediated by apolipoprotein E binding to cell surface heparan sulfate. J Virol *86*, 7256-7267.

Jiang, J., and Luo, G. (2009). Apolipoprotein E but not B is required for the formation of infectious hepatitis C virus particles. J Virol *83*, 12680-12691.

Jiang, J., Wu, X., Tang, H., and Luo, G. (2013). Apolipoprotein E mediates attachment of clinical hepatitis C virus to hepatocytes by binding to cell surface heparan sulfate proteoglycan receptors. PloS one *8*, e67982.

Johannsdottir, H.K., Mancini, R., Kartenbeck, J., Amato, L., and Helenius, A. (2009). Host cell factors and functions involved in vesicular stomatitis virus entry. J Virol *83*, 440-453.

Kapoor, A., Simmonds, P., Gerold, G., Qaisar, N., Jain, K., Henriquez, J.A., Firth, C., Hirschberg, D.L., Rice, C.M., Shields, S., *et al.* (2011). Characterization of a canine homolog of hepatitis C virus. Proc Natl Acad Sci U S A *108*, 11608-11613.

Kapoor, A., Simmonds, P., Scheel, T.K., Hjelle, B., Cullen, J.M., Burbelo, P.D., Chauhan, L.V., Duraisamy, R., Sanchez Leon, M., Jain, K., *et al.* (2013). Identification of rodent homologs of hepatitis C virus and pegiviruses. MBio *4*, e00216-00213.

Klatzmann, D., Champagne, E., Chamaret, S., Gruest, J., Guetard, D., Hercend, T., Gluckman, J.-C., and Montagnier, L. (1984). T-lymphocyte T4 molecule behaves as the receptor for human retrovirus LAV. Nature *312*, 767-768.

Kobayashi, M., Bennett, M.C., Bercot, T., and Singh, I.R. (2006). Functional analysis of hepatitis C virus envelope proteins, using a cell-cell fusion assay. J Virol *80*, 1817-1825.

Kocher, O., and Krieger, M. (2009). Role of the adaptor protein PDZK1 in controlling the HDL receptor SR-BI. Current opinion in lipidology *20*, 236-241.

Koutsoudakis, G., Kaul, A., Steinmann, E., Kallis, S., Lohmann, V., Pietschmann, T., and Bartenschlager, R. (2006). Characterization of the early steps of hepatitis C virus infection by using luciferase reporter viruses. J Virol *80*, 5308-5320.

Krieger, S.E., Zeisel, M.B., Davis, C., Thumann, C., Harris, H.J., Schnober, E.K., Mee, C., Soulier, E., Royer, C., Lambotin, M., *et al.* (2010). Inhibition of hepatitis C virus infection by anti-claudin-1 antibodies is mediated by neutralization of E2-CD81-claudin-1 associations. Hepatology *51*, 1144-1157.

Krzyzaniak, M.A., Zumstein, M.T., Gerez, J.A., Picotti, P., and Helenius, A. (2013). Host cell entry of respiratory syncytial virus involves macropinocytosis followed by proteolytic activation of the F protein. PLoS Pathog *9*, e1003309.

Lakadamyali, M., Rust, M.J., Babcock, H.P., and Zhuang, X. (2003). Visualizing infection of individual influenza viruses. Proc Natl Acad Sci U S A *100*, 9280-9285.

Lancaster, M.A., Renner, M., Martin, C.A., Wenzel, D., Bicknell, L.S., Hurles, M.E., Homfray, T., Penninger, J.M., Jackson, A.P., and Knoblich, J.A. (2013). Cerebral organoids model human brain development and microcephaly. Nature *501*, 373-379.

Lavillette, D., Bartosch, B., Nourrisson, D., Verney, G., Cosset, F.L., Penin, F., and Pecheur, E.I. (2006). Hepatitis C virus glycoproteins mediate low pH-dependent membrane fusion with liposomes. The Journal of biological chemistry *281*, 3909-3917.

Lefevre, M., Felmlee, D.J., Parnot, M., Baumert, T.F., and Schuster, C. (2014). Syndecan 4 is involved in mediating HCV entry through interaction with lipoviral particle-associated apolipoprotein E. PloS one *9*, e95550.

Li, M.L., Aggeler, J., Farson, D.A., Hatier, C., Hassell, J., and Bissell, M.J. (1987). Influence of a reconstituted basement membrane and its components on casein gene expression and secretion in mouse mammary epithelial cells. Proceedings of the National Academy of Sciences *84*, 136-140.

Li, Q., Sodroski, C., Lowey, B., Schweitzer, C.J., Cha, H., Zhang, F., and Liang, T.J. (2016). Hepatitis C virus depends on E-cadherin as an entry factor and regulates its expression in epithelial-to-mesenchymal transition. Proc Natl Acad Sci U S A *113*, 7620-7625.

Liang, T.J., and Ghany, M.G. (2013). Current and future therapies for hepatitis C virus infection. N Engl J Med *368*, 1907-1917.

Lindenbach, B.D. (2013). Virion assembly and release. Curr Top Microbiol Immunol *369*, 199-218.

Lindenbach, B.D., Evans, M.J., Syder, A.J., Wolk, B., Tellinghuisen, T.L., Liu, C.C., Maruyama, T., Hynes, R.O., Burton, D.R., McKeating, J.A., *et al.* (2005). Complete replication of hepatitis C virus in cell culture. Science *309*, 623-626.

Lindenbach, B.D., Meuleman, P., Ploss, A., Vanwolleghem, T., Syder, A.J., McKeating, J.A., Lanford, R.E., Feinstone, S.M., Major, M.E., Leroux-Roels, G., *et al.* (2006). Cell culture-grown hepatitis C virus is infectious in vivo and can be recultured in vitro. Proc Natl Acad Sci U S A *103*, 3805-3809.

Liu, S., Yang, W., Shen, L., Turner, J.R., Coyne, C.B., and Wang, T. (2009). Tight junction proteins claudin-1 and occludin control hepatitis C virus entry and are downregulated during infection to prevent superinfection. J Virol *83*, 2011-2014.

Lopez, S., and Arias, C.F. (2004). Multistep entry of rotavirus into cells: a Versaillesque dance. Trends Microbiol *12*, 271-278.

Lupberger, J., Zeisel, M.B., Xiao, F., Thumann, C., Fofana, I., Zona, L., Davis, C., Mee, C.J., Turek, M., Gorke, S., *et al.* (2011). EGFR and EphA2 are host factors for hepatitis C virus entry and possible targets for antiviral therapy. Nat Med *17*, 589-595.

Lyons, S., Kapoor, A., Sharp, C., Schneider, B.S., Wolfe, N.D., Culshaw, G., Corcoran, B., McGorum, B.C., and Simmonds, P. (2012). Nonprimate hepaciviruses in domestic horses, United kingdom. Emerg Infect Dis *18*, 1976-1982.

Madshus, I.H., and Stang, E. (2009). Internalization and intracellular sorting of the EGF receptor: a model for understanding the mechanisms of receptor trafficking. Journal of cell science *122*, 3433-3439.

Maheshwari, A., and Thuluvath, P.J. (2010). Management of acute hepatitis C. Clin Liver Dis *14*, 169-176; x.

Maillard, P., Huby, T., Andreo, U., Moreau, M., Chapman, J., and Budkowska, A. (2006). The interaction of natural hepatitis C virus with human scavenger receptor SR-BI/Cla1 is mediated by ApoB-containing lipoproteins. FASEB journal : official publication of the Federation of American Societies for Experimental Biology *20*, 735-737.

Mariani, J., Coppola, G., Zhang, P., Abyzov, A., Provini, L., Tomasini, L., Amenduni, M., Szekely, A., Palejev, D., Wilson, M., *et al.* (2015). FOXG1-Dependent Dysregulation of GABA/Glutamate Neuron Differentiation in Autism Spectrum Disorders. Cell *162*, 375-390.

Marsh, M., and Helenius, A. (1989). Virus Entry into Animal Cells. *36*, 107-151.

Marsh, M., and Helenius, A. (2006). Virus entry: open sesame. Cell *124*, 729-740.

Martin, D.N., and Uprichard, S.L. (2013). Identification of transferrin receptor 1 as a hepatitis C virus entry factor. Proc Natl Acad Sci U S A *110*, 10777-10782.

Mateu, G., Donis, R.O., Wakita, T., Bukh, J., and Grakoui, A. (2008). Intragenotypic JFH1 based recombinant hepatitis C virus produces high levels of infectious particles but causes increased cell death. Virology *376*, 397-407.

McKeating, J.A., Zhang, L.Q., Logvinoff, C., Flint, M., Zhang, J., Yu, J., Butera, D., Ho, D.D., Dustin, L.B., Rice, C.M., *et al.* (2004). Diverse hepatitis C virus glycoproteins mediate viral infection in a CD81-dependent manner. J Virol *78*, 8496-8505.

McMahon, H.T., and Boucrot, E. (2011). Molecular mechanism and physiological functions of clathrin-mediated endocytosis. Nature reviews Molecular cell biology *12*, 517-533.

Medigeshi, G.R., Hirsch, A.J., Brien, J.D., Uhrlaub, J.L., Mason, P.W., Wiley, C., Nikolich-Zugich, J., and Nelson, J.A. (2009). West nile virus capsid degradation of claudin proteins disrupts epithelial barrier function. J Virol *83*, 6125-6134.

Mee, C.J., Grove, J., Harris, H.J., Hu, K., Balfe, P., and McKeating, J.A. (2008). Effect of cell polarization on hepatitis C virus entry. J Virol *82*, 461-470.

Mee, C.J., Harris, H.J., Farquhar, M.J., Wilson, G., Reynolds, G., Davis, C., van, I.S.C., Balfe, P., and McKeating, J.A. (2009). Polarization restricts hepatitis C virus entry into HepG2 hepatoma cells. J Virol *83*, 6211-6221.

Meertens, L., Bertaux, C., Cukierman, L., Cormier, E., Lavillette, D., Cosset, F.L., and Dragic, T. (2008). The tight junction proteins claudin-1, -6, and -9 are entry cofactors for hepatitis C virus. J Virol *82*, 3555-3560.

Meertens, L., Bertaux, C., and Dragic, T. (2006). Hepatitis C virus entry requires a critical postinternalization step and delivery to early endosomes via clathrin-coated vesicles. J Virol *80*, 11571-11578.

Mendelsohn, C.L., Wimmer, E., and Racaniello, V.R. (1989). Cellular receptor for poliovirus: Molecular cloning, nucleotide sequence, and expression of a new member of the immunoglobulin superfamily. Cell *56*, 855-865.

Mercer, J., and Helenius, A. (2008). Vaccinia virus uses macropinocytosis and apoptotic mimicry to enter host cells. Science *320*, 531-535.

Mercer, J., Knebel, S., Schmidt, F.I., Crouse, J., Burkard, C., and Helenius, A. (2010a). Vaccinia virus strains use distinct forms of macropinocytosis for host-cell entry. Proc Natl Acad Sci U S A *107*, 9346-9351.

Mercer, J., Schelhaas, M., and Helenius, A. (2010b). Virus entry by endocytosis. Annual review of biochemistry *79*, 803-833.

Merz, A., Long, G., Hiet, M.S., Brugger, B., Chlanda, P., Andre, P., Wieland, F., Krijnse-Locker, J., and Bartenschlager, R. (2011). Biochemical and morphological properties of hepatitis C virus particles and determination of their lipidome. The Journal of biological chemistry *286*, 3018-3032.

Mohd Hanafiah, K., Groeger, J., Flaxman, A.D., and Wiersma, S.T. (2013). Global epidemiology of hepatitis C virus infection: new estimates of age-specific antibody to HCV seroprevalence. Hepatology *57*, 1333-1342.

Molina-Jimenez, F., Benedicto, I., Dao Thi, V.L., Gondar, V., Lavillette, D., Marin, J.J., Briz, O., Moreno-Otero, R., Aldabe, R., Baumert, T.F., *et al.* (2012). Matrigel-embedded 3D culture of Huh-7 cells as a hepatocyte-like polarized system to study hepatitis C virus cycle. Virology *425*, 31-39.

Molleken, K., Becker, E., and Hegemann, J.H. (2013). The Chlamydia pneumoniae invasin protein Pmp21 recruits the EGF receptor for host cell entry. PLoS Pathog *9*, e1003325.

Monazahian, M., Böhme, I., Bonk, S., Koch, A., Scholz, C., Grethe, S., and Thomssen, R. (1999). Low density lipoprotein receptor as a candidate receptor for hepatitis C virus. Journal of Medical Virology *57*, 223-229.

Mondrinos, M.J., Koutzaki, S., Jiwanmall, E., Li, M., Dechadarevian, J.P., Lelkes, P.I., and Finck, C.M. (2006). Engineering three-dimensional pulmonary tissue constructs. Tissue Eng *12*, 717-728.

Montesano, R., Schaller, G., and Orci, L. (1991). Induction of epithelial tubular morphogenesis in vitro by fibroblast-derived soluble factors. Cell *66*, 697-711.

Moradpour, D., and Penin, F. (2013). Hepatitis C virus proteins: from structure to function. Curr Top Microbiol Immunol *369*, 113-142.

Narbus, C.M., Israelow, B., Sourisseau, M., Michta, M.L., Hopcraft, S.E., Zeiner, G.M., and Evans, M.J. (2011). HepG2 cells expressing microRNA miR-122 support the entire hepatitis C virus life cycle. J Virol *85*, 12087-12092.

Negro, F., Forton, D., Craxi, A., Sulkowski, M.S., Feld, J.J., and Manns, M.P. (2015). Extrahepatic morbidity and mortality of chronic hepatitis C. Gastroenterology *149*, 1345-1360.

Niepmann, M. (2013). Hepatitis C virus RNA translation. Curr Top Microbiol Immunol *369*, 143-166.

Ohba K, M.M., Ohno T, Suzuki K, Orito E, Ina Y, Lau JY, Gojobori T. (1995). Classification of hepatitis C virus into major types and subtypes based on molecular evolutionary analysis. Virus Research *36*, 201-214.

Ohno O, M.M., Wu R R, Saleh M G, Ohba K, Orito K, Mukaide M, Williams R, and Lau J Y (1997). New hepatitis C virus (HCV) genotyping system that allows for identification of HCV genotypes 1a, 1b, 2a, 2b, 3a, 3b, 4, 5a, and 6a. Journal of Clinical Microbiology *35*, 201-207.

Owen, D.M., Huang, H., Ye, J., and Gale, M., Jr. (2009). Apolipoprotein E on hepatitis C virion facilitates infection through interaction with low-density lipoprotein receptor. Virology *394*, 99-108.

Ozaras, R., and Tahan, V. (2009). Acute hepatitis C: prevention and treatment. Expert Rev Anti Infect Ther *7*, 351-361.

Pelkmans, L., Puntener, D., and Helenius, A. (2002). Local actin polymerization and dynamin recruitment in SV40-induced internalization of caveolae. Science *296*, 535-539.

Perrault, M., and Pecheur, E.I. (2009). The hepatitis C virus and its hepatic environment: a toxic but finely tuned partnership. The Biochemical journal *423*, 303-314.

Petracca, R., Falugi, F., Galli, G., Norais, N., Rosa, D., Campagnoli, S., Burgio, V., Di Stasio, E., Giardina, B., Houghton, M., *et al.* (2000). Structure-Function Analysis of Hepatitis C Virus Envelope-CD81 Binding. Journal of Virology *74*, 4824-4830.

Pileri, P., Uematsu, Y., Campagnoli, S., Galli, G., Falugi, F., Petracca, R., Weiner, A.J., Houghton, M., Rosa, D., Grandi, G., *et al.* (1998). Binding of hepatitis C virus to CD81. Science *282*, 938-941.

Ploss, A., Evans, M.J., Gaysinskaya, V.A., Panis, M., You, H., de Jong, Y.P., and Rice, C.M. (2009). Human occludin is a hepatitis C virus entry factor required for infection of mouse cells. Nature *457*, 882-886.

Prentoe, J., Serre, S.B., Ramirez, S., Nicosia, A., Gottwein, J.M., and Bukh, J. (2014). Hypervariable region 1 deletion and required adaptive envelope mutations confer decreased dependency on scavenger receptor class B type I and low-density lipoprotein receptor for hepatitis C virus. J Virol *88*, 1725-1739.

Racoosin, E.L. (1993). Macropinosome maturation and fusion with tubular lysosomes in macrophages. The Journal of cell biology *121*, 1011-1020.

Raghu, H., Sharma-Walia, N., Veettil, M.V., Sadagopan, S., and Chandran, B. (2009). Kaposi's sarcoma-associated herpesvirus utilizes an actin polymerization-dependent macropinocytic pathway to enter human dermal microvascular endothelial and human umbilical vein endothelial cells. J Virol *83*, 4895-4911.

Randall, G., Chen, L., Panis, M., Fischer, A.K., Lindenbach, B.D., Sun, J., Heathcote, J., Rice, C.M., Edwards, A.M., and McGilvray, I.D. (2006). Silencing of USP18 potentiates the antiviral activity of interferon against hepatitis C virus infection. Gastroenterology *131*, 1584-1591.

Randall, G., Panis, M., Cooper, J.D., Tellinghuisen, T.L., Sukhodolets, K.E., Pfeffer, S., Landthaler, M., Landgraf, P., Kan, S., Lindenbach, B.D., *et al.* (2007). Cellular cofactors affecting hepatitis C virus infection and replication. Proc Natl Acad Sci U S A *104*, 12884-12889.

Razavi, H., Waked, I., Sarrazin, C., Myers, R.P., Idilman, R., Calinas, F., Vogel, W., Mendes Correa, M.C., Hezode, C., Lazaro, P., *et al.* (2014). The present and future disease burden of hepatitis C virus (HCV) infection with today's treatment paradigm. Journal of viral hepatitis *21 Suppl 1*, 34-59.

Rees, J.S., Li, X.W., Perrett, S., Lilley, K.S., and Jackson, A.P. (2015). Protein Neighbors and Proximity Proteomics. Mol Cell Proteomics *14*, 2848-2856.

Rhainds, D., and Brissette, L. (2004). The role of scavenger receptor class B type I (SR-BI) in lipid trafficking. The International Journal of Biochemistry & Cell Biology *36*, 39-77.

Saeed, M.F., Kolokoltsov, A.A., Albrecht, T., and Davey, R.A. (2010). Cellular entry of ebola virus involves uptake by a macropinocytosis-like mechanism and subsequent trafficking through early and late endosomes. PLoS Pathog *6*, e1001110.

Sainz, B., Jr., Barretto, N., Martin, D.N., Hiraga, N., Imamura, M., Hussain, S., Marsh, K.A., Yu, X., Chayama, K., Alrefai, W.A., *et al.* (2012). Identification of the Niemann-Pick C1-like 1 cholesterol absorption receptor as a new hepatitis C virus entry factor. Nat Med *18*, 281-285.

Sainz, B., Jr., TenCate, V., and Uprichard, S.L. (2009). Three-dimensional Huh7 cell culture system for the study of Hepatitis C virus infection. Virol J *6*, 103.

Scarselli, E., Ansuini, H., Cerino, R., Roccasecca, R.M., Acali, S., Filocamo, G., Traboni, C., Nicosia, A., Cortese, R., and Vitelli, A. (2002). The human scavenger receptor class B type I is a novel candidate receptor for the hepatitis C virus. The EMBO journal *21*, 5017-5025.

Sharma, N.R., Mateu, G., Dreux, M., Grakoui, A., Cosset, F.L., and Melikyan, G.B. (2011). Hepatitis C virus is primed by CD81 protein for low pH-dependent fusion. The Journal of biological chemistry *286*, 30361-30376.

Shelness, G.S., and Sellers, J.A. (2001). Very-low-density lipoprotein assembly and secretion. Current opinion in lipidology *12*, 151-157.

Shi, Q., Jiang, J., and Luo, G. (2013). Syndecan-1 serves as the major receptor for attachment of hepatitis C virus to the surfaces of hepatocytes. J Virol *87*, 6866-6875.

Shin-I, T., Sugiyama, M., and Mizokami, M. (2016). Hepatitis C Virus Genotypes and Their Evolution. 15-29.

Smith, A.E., and Helenius, A. (2004). How viruses enter animal cells. Science *304*, 237-242.

Snyers, L., Zwickl, H., and Blaas, D. (2003). Human Rhinovirus Type 2 Is Internalized by Clathrin-Mediated Endocytosis. Journal of Virology *77*, 5360-5369.

Sourisseau, M., Michta, M.L., Zony, C., Israelow, B., Hopcraft, S.E., Narbus, C.M., Parra Martin, A., and Evans, M.J. (2013). Temporal analysis of hepatitis C virus cell entry with occludin directed blocking antibodies. PLoS Pathog *9*, e1003244.

Steinberg, M. (1964). The problem of adhesive selectivity in cellular interactions. . Cellular membranes in development, 321-366.

Steven, A.C., Heymann, J.B., Cheng, N., Trus, B.L., and Conway, J.F. (2005). Virus maturation: dynamics and mechanism of a stabilizing structural transition that leads to infectivity. Curr Opin Struct Biol *15*, 227-236.

Takebe, T., Sekine, K., Enomura, M., Koike, H., Kimura, M., Ogaeri, T., Zhang, R.R., Ueno, Y., Zheng, Y.W., Koike, N., *et al.* (2013). Vascularized and functional human liver from an iPSC-derived organ bud transplant. Nature *499*, 481-484.

Tao, W., Xu, C., Ding, Q., Li, R., Xiang, Y., Chung, J., and Zhong, J. (2009). A single point mutation in E2 enhances hepatitis C virus infectivity and alters lipoprotein association of viral particles. Virology *395*, 67-76.

Taylor, M.P., Koyuncu, O.O., and Enquist, L.W. (2011). Subversion of the actin cytoskeleton during viral infection. Nat Rev Microbiol *9*, 427-439.

Than, T.T., Tran, G.V., Son, K., Park, E.M., Kim, S., Lim, Y.S., and Hwang, S.B. (2016). Ankyrin Repeat Domain 1 is Up-regulated During Hepatitis C Virus Infection and Regulates Hepatitis C Virus Entry. Sci Rep *6*, 20819.

Thomssen R, B.S., Thiele A. (1993). Density heterogeneities of hepatitis C virus in human sera

due to the binding of beta-lipoproteins and immunoglobulins.

. Medical Microbiology and Immunology *182*, 329-334.

Triyatni, M., Saunier, B., Maruvada, P., Davis, A.R., Ulianich, L., Heller, T., Patel, A., Kohn, L.D., and Liang, T.J. (2002). Interaction of Hepatitis C Virus-Like Particles and Cells: a Model System for Studying Viral Binding and Entry. Journal of Virology *76*, 9335-9344.

Trotard, M., Lepere-Douard, C., Regeard, M., Piquet-Pellorce, C., Lavillette, D., Cosset, F.L., Gripon, P., and Le Seyec, J. (2009). Kinases required in hepatitis C virus entry and replication highlighted by small interference RNA screening. FASEB journal : official publication of the Federation of American Societies for Experimental Biology *23*, 3780-3789.

Tscherne, D.M., Jones, C.T., Evans, M.J., Lindenbach, B.D., McKeating, J.A., and Rice, C.M. (2006). Time- and temperature-dependent activation of hepatitis C virus for low-pH-triggered entry. J Virol *80*, 1734-1741.

Ujino, S., Nishitsuji, H., Hishiki, T., Sugiyama, K., Takaku, H., and Shimotohno, K. (2016). Hepatitis C virus utilizes VLDLR as a novel entry pathway. Proc Natl Acad Sci U S A *113*, 188-193.

Valiya Veettil, M., Sadagopan, S., Kerur, N., Chakraborty, S., and Chandran, B. (2010). Interaction of c-Cbl with myosin IIA regulates Bleb associated macropinocytosis of Kaposi's sarcoma-associated herpesvirus. PLoS Pathog *6*, e1001238.

van der Meer, A.J., Veldt, B.J., Feld, J.J., Wedemeyer, H., Dufour, J.F., Lammert, F., Duarte-Rojo, A., Heathcote, E.J., Manns, M.P., Kuske, L., *et al.* (2012). Association between sustained virological response and all-cause mortality among patients with chronic hepatitis C and advanced hepatic fibrosis. JAMA *308*, 2584-2593.

van der Schaar, H.M., Rust, M.J., Chen, C., van der Ende-Metselaar, H., Wilschut, J., Zhuang, X., and Smit, J.M. (2008). Dissecting the cell entry pathway of dengue virus by single-particle tracking in living cells. PLoS Pathog *4*, e1000244.

van der Schaar, H.M., Rust, M.J., Waarts, B.L., van der Ende-Metselaar, H., Kuhn, R.J., Wilschut, J., Zhuang, X., and Smit, J.M. (2007). Characterization of the early events in dengue virus cell entry by biochemical assays and single-virus tracking. J Virol *81*, 12019-12028.

Vlasak, M., Goesler, I., and Blaas, D. (2005). Human rhinovirus type 89 variants use heparan sulfate proteoglycan for cell attachment. J Virol *79*, 5963-5970.

Voisset, C., Callens, N., Blanchard, E., Op De Beeck, A., Dubuisson, J., and Vu-Dac, N. (2005). High density lipoproteins facilitate hepatitis C virus entry through the scavenger receptor class B type I. The Journal of biological chemistry *280*, 7793-7799.

von Hahn, T., Lindenbach, B.D., Boullier, A., Quehenberger, O., Paulson, M., Rice, C.M., and McKeating, J.A. (2006). Oxidized low-density lipoprotein inhibits hepatitis C virus cell entry in human hepatoma cells. Hepatology *43*, 932-942.

Wakita, T., Pietschmann, T., Kato, T., Date, T., Miyamoto, M., Zhao, Z., Murthy, K., Habermann, A., Krausslich, H.G., Mizokami, M., *et al.* (2005). Production of infectious hepatitis C virus in tissue culture from a cloned viral genome. Nat Med *11*, 791-796.

Wang, H., Gilham, D., and Lehner, R. (2007). Proteomic and lipid characterization of apolipoprotein B-free luminal lipid droplets from mouse liver microsomes: implications for very low density lipoprotein assembly. The Journal of biological chemistry *282*, 33218-33226.

Wang, X., Huang, D.Y., Huong, S.M., and Huang, E.S. (2005). Integrin alphavbeta3 is a coreceptor for human cytomegalovirus. Nat Med *11*, 515-521.

Webster, D.P., Klenerman, P., and Dusheiko, G.M. (2015). Hepatitis C. The Lancet *385*, 1124-1135.

Weiss, P., and Taylor, A.C. (1960). Reconstitution of Complete Organs from Single-Cell Suspensions of Chick Embryos in Advanced Stages of Differentiation. Proceedings of the National Academy of Sciences *46*, 1177-1185.

Westhaus, S., Bankwitz, D., Ernst, S., Rohrmann, K., Wappler, I., Agne, C., Luchtefeld, M., Schieffer, B., Sarrazin, C., Manns, M.P., *et al.* (2013). Characterization of the inhibition of hepatitis C virus entry by in vitro-generated and patient-derived oxidized low-density lipoprotein. Hepatology *57*, 1716-1724.

Wilkins T, M.J., Raina D, Schade RR (2010). Hepatitis C: diagnosis and treatment. American Family Physician *81*, 1351-1357.

Wroblewski, L.E., Piazuelo, M.B., Chaturvedi, R., Schumacher, M., Aihara, E., Feng, R., Noto, J.M., Delgado, A., Israel, D.A., Zavros, Y., *et al.* (2015). Helicobacter pylori targets cancer-associated apical-junctional constituents in gastroids and gastric epithelial cells. Gut *64*, 720-730.

Wunschmann, S., Medh, J.D., Klinzmann, D., Schmidt, W.N., and Stapleton, J.T. (2000). Characterization of Hepatitis C Virus (HCV) and HCV E2 Interactions with CD81 and the Low-Density Lipoprotein Receptor. Journal of Virology *74*, 10055-10062.

Xu, Z., Waeckerlin, R., Urbanowski, M.D., van Marle, G., and Hobman, T.C. (2012). West Nile virus infection causes endocytosis of a specific subset of tight junction membrane proteins. PloS one *7*, e37886.

Yoder, A., Yu, D., Dong, L., Iyer, S.R., Xu, X., Kelly, J., Liu, J., Wang, W., Vorster, P.J., Agulto, L., *et al.* (2008). HIV envelope-CXCR4 signaling activates cofilin to overcome cortical actin restriction in resting CD4 T cells. Cell *134*, 782-792.

Zahid, M.N., Turek, M., Xiao, F., Thi, V.L., Guerin, M., Fofana, I., Bachellier, P., Thompson, J., Delang, L., Neyts, J., *et al.* (2013). The postbinding activity of scavenger receptor class B type I mediates initiation of hepatitis C virus infection and viral dissemination. Hepatology *57*, 492-504.

Zeisel, M.B., Koutsoudakis, G., Schnober, E.K., Haberstroh, A., Blum, H.E., Cosset, F.L., Wakita, T., Jaeck, D., Doffoel, M., Royer, C., *et al.* (2007). Scavenger receptor class B type I is a key host factor for hepatitis C virus infection required for an entry step closely linked to CD81. Hepatology *46*, 1722-1731.

Zhang, J., Randall, G., Higginbottom, A., Monk, P., Rice, C.M., and McKeating, J.A. (2004). CD81 is required for hepatitis C virus glycoprotein-mediated viral infection. Journal of Virology *78*, 1448-1455.

Zheng, A., Yuan, F., Li, Y., Zhu, F., Hou, P., Li, J., Song, X., Ding, M., and Deng, H. (2007). Claudin-6 and claudin-9 function as additional coreceptors for hepatitis C virus. J Virol *81*, 12465-12471.

Zhong, J., Gastaminza, P., Cheng, G., Kapadia, S., Kato, T., Burton, D.R., Wieland, S.F., Uprichard, S.L., Wakita, T., and Chisari, F.V. (2005). Robust hepatitis C virus infection in vitro. Proc Natl Acad Sci U S A *102*, 9294-9299.

Zietek, T., Rath, E., Haller, D., and Daniel, H. (2015). Intestinal organoids for assessing nutrient transport, sensing and incretin secretion. Sci Rep *5*, 16831.

Zona, L., Lupberger, J., Sidahmed-Adrar, N., Thumann, C., Harris, H.J., Barnes, A., Florentin, J., Tawar, R.G., Xiao, F., Turek, M., *et al.* (2013). HRas signal transduction promotes hepatitis C virus cell entry by triggering assembly of the host tetraspanin receptor complex. Cell host & microbe *13*, 302-313.